



National Library
of Canada

Bibliothèque nationale
du Canada

Canadian Theses Service

Service des thèses canadiennes

Ottawa, Canada
K1A 0N4

NOTICE

The quality of this microform is heavily dependent upon the quality of the original thesis submitted for microfilming. Every effort has been made to ensure the highest quality of reproduction possible.

If pages are missing, contact the university which granted the degree.

Some pages may have indistinct print especially if the original pages were typed with a poor typewriter ribbon or if the university sent us an inferior photocopy.

Reproduction in full or in part of this microform is governed by the Canadian Copyright Act, R.S.C. 1970, c. C-30, and subsequent amendments.

AVIS

La qualité de cette microforme dépend grandement de la qualité de la thèse soumise au microfilmage. Nous avons tout fait pour assurer une qualité supérieure de reproduction.

S'il manque des pages, veuillez communiquer avec l'université qui a conféré le grade.

La qualité d'impression de certaines pages peut laisser à désirer, surtout si les pages originales ont été dactylographiées à l'aide d'un ruban usé ou si l'université nous a fait parvenir une photocopie de qualité inférieure.

La reproduction, même partielle, de cette microforme est soumise à la Loi canadienne sur le droit d'auteur, SRC 1970, c. C-30, et ses amendements subséquents.

UNIVERSITY OF ALBERTA

**TOWARD AN IMPLANTABLE GLUCOSE SENSOR
FOR THE ARTIFICIAL BETA CELL**

by

ROBIN F.B. TURNER

A THESIS SUBMITTED TO
THE FACULTY OF GRADUATE STUDIES AND RESEARCH
IN PARTIAL FULFILLMENT OF
THE REQUIREMENTS FOR THE DEGREE OF
DOCTOR OF PHILOSOPHY

DEPARTMENT OF ELECTRICAL ENGINEERING

EDMONTON, ALBERTA

SPRING, 1990



National Library
of Canada

Bibliothèque nationale
du Canada

Canadian Theses Service Service des thèses canadiennes

Ottawa, Canada
K1A 0N4

NOTICE

The quality of this microform is heavily dependent upon the quality of the original thesis submitted for microfilming. Every effort has been made to ensure the highest quality of reproduction possible.

If pages are missing, contact the university which granted the degree.

Some pages may have indistinct print especially if the original pages were typed with a poor typewriter ribbon or if the university sent us an inferior photocopy.

Reproduction in full or in part of this microform is governed by the Canadian Copyright Act, R.S.C. 1970, c. C-30, and subsequent amendments.

AVIS

La qualité de cette microforme dépend grandement de la qualité de la thèse soumise au microfilmage. Nous avons tout fait pour assurer une qualité supérieure de reproduction.

S'il manque des pages, veuillez communiquer avec l'université qui a conféré le grade.

La qualité d'impression de certaines pages peut laisser à désirer, surtout si les pages originales ont été dactylographiées à l'aide d'un ruban usé ou si l'université nous a fait parvenir une photocopie de qualité inférieure.

La reproduction, même partielle, de cette microforme est soumise à la Loi canadienne sur le droit d'auteur, SRC 1970, c. C-30, et ses amendements subséquents.

ISBN 0-315-60232-5

UNIVERSITY OF ALBERTA

RELEASE FORM

NAME OF AUTHOR: **Robin F.B. Turner**

TITLE OF THESIS: **Toward an Implantable Glucose Sensor
for the Artificial Beta Cell**

DEGREE FOR WHICH THESIS WAS PRESENTED: **Doctor of Philosophy**

YEAR THIS DEGREE GRANTED: **1990**

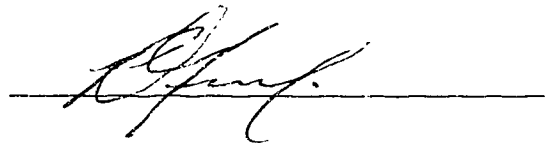
Permission is hereby granted to

THE UNIVERSITY OF ALBERTA LIBRARY

to reproduce single copies of this thesis, and to lend or sell such copies for private, scholarly or scientific research purposes only.

The author reserves other publication rights and neither the thesis, nor extensive extracts from it, may be printed or otherwise reproduced without the author's written permission.

AUTHOR'S SIGNATURE: _____



PERMANENT ADDRESS:

**Biotechnology Laboratory
University of British Columbia
237 - 6174 University Boulevard
Vancouver, B.C. V6T 1W5**

DATE: **February 26, 1990**

UNIVERSITY OF ALBERTA

FACULTY OF GRADUATE STUDIES AND RESEARCH

The undersigned certify that they have read, and recommend to the Faculty of Graduate Studies and Research for acceptance, a thesis entitled

**TOWARD AN IMPLANTABLE GLUCOSE SENSOR
FOR THE ARTIFICIAL BETA CELL**

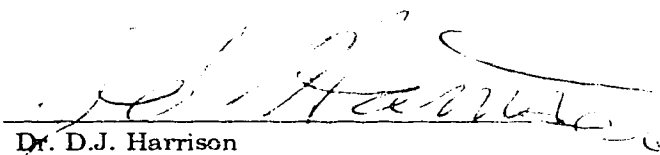
Submitted by

ROBIN F.B. TURNER

in partial fulfillment of the requirements for the degree of

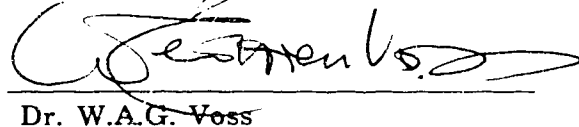
DOCTOR OF PHILOSOPHY

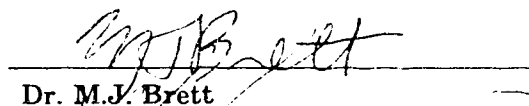
CO-SUPERVISOR:

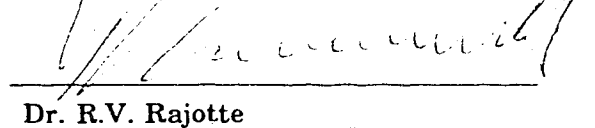

Dr. D.J. Harrison

CO-SUPERVISOR:

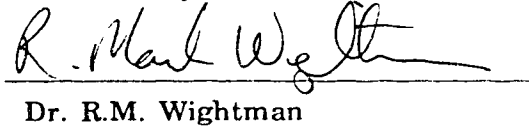

Dr. C.R. James


Dr. W.A.G. Voss


Dr. M.J. Brett


Dr. R.V. Rajotte

EXTERNAL EXAMINER:


Dr. R.M. Wightman

DATE: February 26, 1990

ABSTRACT

The research undertaken during the course of this program was directed toward the development of an implantable glucose sensor that could, ultimately, be incorporated into an Artificial Beta Cell for the treatment of Type I diabetes. Specifically, the two main objectives of this project were to develop improved instrumentation for implantable amperometric sensors, and to develop and characterize an electrode encapsulation technology with the potential for improved electrode stability and biocompatibility for continuous *in vivo* monitoring.

An integrated bi-potentiostat controller circuit for amperometric sensors is described and characterized. The amperometric approach, and the implementation entirely in CMOS technology, alleviates some of the problems associated with packaging implantable sensors, since the electronics can remain hermetically sealed and can be used in conjunction with remote reference and indicating electrodes. This design features a differential mode capability that provides a significant improvement in selectivity through nulling the effect of spurious background currents. The accuracy and precision of this instrument are comparable to a laboratory analytical potentiostat.

Experimental results characterizing the use of perfluorosulfonic acid polymer (Nafion[®]) as an encapsulating material for enzyme electrodes in whole blood are presented. Results show that Nafion effectively excludes blood cells, plasma proteins and other blood constituents that denature the enzyme and/or poison the catalytic activity of the platinum electrode. Nafion coated electrodes yielded highly reproducible and accurate single glucose assays in canine whole blood and plasma samples *in vitro* at room temperature, and at 37°C. The first results of biocompatibility testing of Nafion polymer implants are also presented which indicate excellent long-term tissue and blood compatibility in rats. Histological examination of tissues surrounding three and six month implants reveal a thin fibrous tissue capsule around the implant and little, if any, evidence of a chronic foreign body inflammatory response. An implantable version of the Nafion encapsulated glucose sensor electrode was designed, fabricated and tested

in whole blood *in vitro* and *in vivo*. Prototype electrodes performed satisfactorily *in vitro*, but intravenously implanted electrodes did not perform well and were short-lived. Subsequent diagnostic experiments identified flaws in the prototype design and fabrication. Corrective measures were proposed along with suggestions for proceeding with the next phase of this work.

ACKNOWLEDGMENTS

During the course of my graduate program, I was extremely fortunate to have the opportunity to interact with a number of scientists, engineers and technologists from widely different disciplines. All have contributed greatly to my education, and I would like to express my sincere appreciation to each of them, most notably to the following:

Dr. D.J. Harrison for welcoming me into his group and for providing encouragement, guidance and support throughout my program. Long before he had any obligation to do so, Dr. Harrison patiently taught me the skills and permitted me access to the facilities which I needed to carry out my work. I thank him for his leadership, and his friendship which I hope will continue long after the conclusion of my program.

Dr. C.R. James for stepping into the role of supervisor at a critical point in my program, and for his generous support since. I don't know where he found the time, but he did and I'm grateful.

Dr. W.A.G. Voss and Dr. R.V. Rajotte for giving me the opportunity and the confidence to pursue advanced studies. Unbeknownst to them (I think), they have greatly influenced my attitudes and ambitions toward a career in applied science. I am grateful for their friendship and their collaboration during several phases of my program.

Dr. H.P. Baltes for inviting me to join his group, for encouraging me to pursue a difficult project, and for providing the environment which made that pursuit possible. Dr. Baltes taught me a great deal about the art and science of research, and about big game hunting, and how they are related. I am proud to be one of his former students.

All of the other members of Dr. Harrison's research group for moral support and for invaluable (and numerous) philosophical and technical discussions.

The others I can only mention here, but I trust that my gratitude is not diminished by brevity:

Dr. D.F. Gerson (formerly) of the Alberta Research Council; Dr. R.W.M. Amy and Dr. N.A. Parfrey of the Department of Pathology; Dr. B.R. MacPherson of the Department of Anatomy and Cell Biology; Dr. I. Filanovsky, Mr. G. Fortier, Mr. I. McKay and Mr. E. Valk of the Department of Electrical Engineering; Dr. D. Finegood and Dr. P. Tobin of the Department of Endocrinology; Mr. G. Braybrook of the Department of Entomology and Mr. G. Olson, Ms. C. Long, Mr. T. Germain (and the other surgical technicians under his supervision) and Ms. E. Schwaldt of the Surgical-Medical Research Institute at the University of Alberta, for valuable discussions and technical assistance.

I would also like to acknowledge the support of the following organizations:

The Alberta Heritage Foundation for Medical Research; the Natural Sciences and Engineering Research Council of Canada; the Alberta Microelectronic Center; the Canadian Microelectronics Corporation; the Alberta Research Council; the departments of Electrical Engineering and Chemistry; the Surgical-Medical Research Institute and the Faculty of Graduate Studies and Research for providing financial support, equipment and facilities.

TABLE OF CONTENTS

CHAPTER	PAGE
1. Introduction	1
1.1 Diabetes and the Importance of Glucose Sensing.....	1
1.2 Problems and Progress	4
1.3 Objectives	8
1.4 Overview of the Sensor	10
1.4.1 Functional Components.....	10
1.4.2 Chemical and Electrochemical Considerations.....	12
1.4.3 Kinetic Considerations.....	16
1.5 Summary	18
1.6 References.....	20
2. A CMOS Potentiostat for Amperometric Chemical Sensors.....	29
2.1 Introduction	29
2.2 Circuit Description	31
2.2.1 Principles of Operation.....	31
2.2.2 Operational Amplifier.....	32
2.2.3 Output Stage	36
2.3 Experimental Results	37
2.3.1 Electrical Performance	37
2.3.2 Electrochemical Performance.....	41
2.4 Performance of Revised Versions	45
2.5 Conclusions.....	53
2.6 References	54
3. Characterization of Perfluorosulfonic Acid Polymer Coated Enzyme Electrodes for Glucose Analysis in Whole Blood	56
3.1 Introduction	56
3.2 Materials and Methods	60
3.2.1 Reagents	60
3.2.2 Electrode Preparation	60
3.2.3 Nafion Film Thickness.....	61

	3.2.4 Electrochemical Measurements.....	64
3.3	Results and Discussion.....	65
	3.3.1 Nafion Dialysis Membranes.....	65
	3.3.2 Quantitative Sensor Performance and Lifetime	76
3.4	Conclusions.....	78
3.6	References	79
4.	Preliminary <i>In Vivo</i> Biocompatibility Studies on Perfluorosulfonic Acid Polymer Membranes for Biosensor Applications.....	84
	4.1 Introduction	84
	4.2 Materials and Methods	86
	4.2.1 Biosensor Considerations	86
	4.2.2 Implant Preparation.....	87
	4.2.3 Implant Procedures and Treatment of Recovered Specimens.....	88
	4.3 Results and Discussion	89
	4.3.1 Short-Term Implants.....	89
	4.3.2 Long-Term Implants	96
	4.5 Conclusions.....	110
	4.7 References	111
5.	Design and <i>In Vivo</i> Testing of a Prototype Implantable Glucose Sensor for Continuous Monitoring in Whole Blood.....	114
	5.1 Introduction	114
	5.2 Materials and Methods	115
	5.2.1 Electrode Preparation	115
	5.2.2 <i>In Vitro</i> Characterization.....	118
	5.2.3 Implant Procedures and Instrumentation	120
	5.2.4 Experimental Glucose Challenge Protocols.....	123
	5.3 Results and Discussion.....	125
	5.3.1 <i>In Vivo</i> Performance ..	125
	5.3.2 Post-Operative Evaluation of Electrodes.....	130

5.4	Conclusions.....	135
5.6	References.....	138
6.	Conclusions.....	141
6.1	Summary of Contributions	141
6.2	Directions for Future Research.....	143
6.3	Other Applications	145
6.4	References.....	147

Appendix

Integrated Potentiostat Circuit Implementaion Data	149
Original Bonding Diagrams and Package Specifications.....	152

LIST OF TABLES

TABLE		PAGE
1.1	Normal concentrations of constituents of human arterial plasma (compiled from various sources).	13
2.1	Component values employed in realization of prototype potentiostat circuit.	35
3.1	Sample film thickness data obtained by cyclic voltammetry at Pt electrode coated with Ru(NH ₃) ₆ ³⁺ saturated Nafion membranes.	63
3.2	Comparison of response times of Nafion versus cellulose dialysis membranes.	75
4.1	Distribution of histology and scanning electron microscopy specimens (number of specimens x time <i>in situ</i>).	90
5.1	Blood gas, haematology and electrolyte data obtained from venous blood samples collected from Dogs K-118 and J-518 taken before and after each experiment.	124
6.1	Some other immobilized enzyme based biochemical assays that could be performed with the combined potentiostat/Nafion encapsulated electrode system presented here.	146
A.1	Typical CMOS 1B process parameters	149
A.2	Pin assignments for CMOS potentiostat integrated circuits.	150
A.3	Pin assignments for CMOS potentiostat integrated circuits.	151

LIST OF FIGURES

FIGURE		PAGE
1.1	Block diagram of a hypothetical Artificial Beta Cell system.	3
1.2	Schematic cross sectional view of the glucose sensitive.	11
2.1	Block diagram of amperometric measurement system.	33
2.2	Schematic Diagram of two-channel CMOS potentiostat.	34
2.3	Photomicrograph of prototype potentiostat circuit.	38
2.4	Measured output voltage as a function of simulated WE current.	39
2.5	Dependence of applied bias voltage on simulated WE Current.	40
2.6	Applied voltage as a function of ferrocyanide concentration in unstirred test solution.	42
2.7	Cottrell plot of time dependence of output voltage after the applied voltage is stepped to a potential at which ferrocyanide is oxidized.	44
2.8	Output voltage as a function of glucose concentration.	46
2.9	Time record of output voltage response to changes in interferent concentration.	47
2.10	Time record of differential output voltage response to changes in ascorbate interferent concentration.	48
2.11	Cross correlation between the two-electrode integrated potentiostat circuit and a commercial three-electrode analytical potentiostat (Pine Instrument Company model RDE-4).	50
2.12	Electrical response characteristics of an improved version of the integrated bi-potentiostat circuit.	52

3.1	Chemical structure of repeating unit (mer) of perfluorosulfonic acid (Nafion) polymer.	59
3.2	Typical sensor calibration curves in phosphate buffer showing the effect of Nafion membrane thickness on the response characteristic.	67
3.3	Typical glucose assay in whole blood by standard additions with a 1.7 μm thick Nafion dialysis membrane.	69
3.4	Typical glucose assay in whole blood by standard additions with a 12,000 MWCO cellulose dialysis membrane.	70
3.5	Typical glucose assay in blood plasma by standard additions with a 12,000 MWCO cellulose dialysis membrane.	71
3.6	Cyclic voltammograms at 100 mV/s in buffer and whole blood showing the effect of added glucose.	72
4.1	Scanning electron micrographs showing surface features of subcutaneous (L. thigh) disc shaped Nafion implant after 1 day <i>in situ</i> .	92
4.2	Scanning electron micrographs showing surface features of subcutaneous (L. thigh) disc shaped Nafion implant after 4 days <i>in situ</i> .	93
4.3	Scanning electron micrographs showing surface features of intravenous (inferior vena cava) cannula shaped Nafion implant after 1 day <i>in situ</i> .	94
4.4	Scanning electron micrographs showing surface features of intravenous (inferior vena cava) cannula shaped Nafion implant after 4 days <i>in situ</i> .	95
4.5	Partial transverse section of subcutaneous (L. thigh) disc shaped, plain (<i>i.e.</i> uncoated) Nafion implant and surrounding tissues after 105 days.	97

4.6	Partial transverse section of subcutaneous (L. thigh) disc shaped, solution cast Nafion coated (on solid Nafion) implant and surrounding tissues after 105 days.	98
4.7	Partial transverse section of subcutaneous (L. thigh) disc shaped, Silastic implant and surrounding tissues after 105 days.	100
4.8	Partial transverse section of disc shaped, plain (<i>i.e.</i> uncoated) Nafion implant and surrounding tissues after 105 days in abdominal cavity.	102
4.9	Partial transverse section of disc shaped, solution cast Nafion coated (on solid Nafion) implant and surrounding tissues after 105 days in abdominal cavity (omentum).	103
4.10	Partial transverse section of disc shaped, Silastic implant and surrounding tissues after 105 days in abdominal cavity (omentum).	104
4.11	Transverse section of intravenous (inferior vena cava) cannula shaped, plain (<i>i.e.</i> uncoated) Nafion implant after 105 days showing surrounding vessel wall.	107
4.12	Transverse section of intravenous (inferior vena cava) cannula shaped, solution cast Nafion coated (on solid Nafion) implant after 105 days showing surrounding vessel wall.	108
4.13	Transverse section of intravenous (inferior vena cava) cannula shaped, Silastic implant after 105 days showing surrounding vessel wall.	109
5.1	Cross sectional view of a prototype implantable electrode used for in vivo glucose monitoring in whole blood.	116
5.2	<i>In vitro</i> calibration curves for the prototype electrodes in phosphate buffer solution (pH 7.4).	119

5.3	Grans plot of standard additions data obtained <i>in vitro</i> using electrode B3 in canine whole blood at room temperature.	121
5.4	Electrode B1 response and Beckman plasma glucose profiles from dog K-118 (male, 22.4 kg) post pancreatectomy.	126
5.5	Smoothed electrode B2 response and Beckman plasma glucose profiles from dog J-518 (male, 30 kg).	128
5.6	Envelope of actual oscillatory response of electrode B2 obtained during IVGTT on dog J-518.	129
5.7	Cross correlation between the <i>in vivo</i> response of electrode B2 and (<i>in vitro</i>) plasma glucose readings obtained from sampled venous blood.	131
5.8	Response of dog J-518 to intravenous glucose challenge (833 mg/kg) as determined by Beckman analyses of sampled venous blood.	132
5.9	Cross correlation between the <i>in vitro</i> response of electrode B1 and (Beckman) plasma glucose readings obtained from sampled venous blood during subsequent IVGTT on dog J-518.	134
5.10	Scanning electron micrographs of electrode B2 following <i>in vivo</i> testing in dog J-518.	136

LIST OF SYMBOLS AND ABBREVIATIONS

A	Electrode area (millimeters ²)
APT	3-Aminopropyltriethoxysilane
BSA	Bovine Serum Albumin
C	Capacitance (farads)
C_a	Concentration of analyte species (moles/meter ³)
ChemFET	Chemically Sensitive Field Effect Transistor
CMOS	Complementary Metal Oxide Semiconductor
C_{red}, C_{ox}	Bulk concentrations of reduced and oxidized species respectively (moles/meter ³)
CSM	Chemically Selective (or Sensitive) Membrane
CSSD	Chemically Sensitive Semiconductor Device
δ	Thickness of Nernst diffusion layer (meters)
D_{red}, D_{ox}	Diffusion coefficients for reduced and oxidized species respectively (meters ² /s)
DM	Dialysis membrane
E	Enzyme
E_a	Bias potential applied to a working electrode measured with respect to the reference electrode (volts)
EDTA	Ethylenediaminetetraacetic acid
E·S	Enzyme-Substrate complex
E°	Electrode potential measured with respect to a standard hydrogen electrode at pH 0 (volts)
e^-	Electron
F	Faraday constant (96,487 Coulombs/mole)
FAD	Flavin Adenine Dinucleotide
ΔG	Gibbs free energy change (kilojoules/mole)
Glu	Glucose (Dextrose)
GO, GOx	Glucose Oxidase
GSM	Glucose Sensitive Membrane
GTT	Glucose Tolerance Test
Hct	Haematocrit
Hgb	Haemoglobin
HGlu	Gluconic Acid

I	Current (amperes)
i_a	Time dependent electrode current due to reduction/oxidation of analyte species (amperes)
I_a, I_k	Steady state anodic and cathodic electrode currents respectively (amperes)
IVC	Inferior vena cava
IC	Integrated Circuit
ISFET	Ion Sensitive Field Effect Transistor
I.M	Intramuscular
IP	Intraperitoneal
I/V	Current-to-Voltage Converter
IV	Intravenous
IVGTT	Intravenous Glucose Tolerance Test
k	Kinetic rate constant (units depend on order of reaction)
K	Chemical equilibrium constant (units depend on order of reaction)
K_m	Michaelis constant (units of concentration)
M	Molar concentration (moles of solute/liter of solution)
M	Current mirror gain (dimensionless)
MWCO	Molecular Weight Cut-Off (Daltons)
m.w.	Equivalent molecular weight (grams/mole)
n	Negative charge carrier, or concentration of same (meters ⁻³), contributed by donor impurities in semiconductor devices
OA	Operational Amplifier
p	Positive charge carrier, or concentration of same (meters ⁻³), contributed by acceptor impurities in semiconductor devices
P	Product
PG	Plasma glucose level (milligrams/100 milliliters)
R	Resistance (ohms)
R_o	Output resistance (ohms)
RBC	Red Blood Cell
RE	Reference Electrode
S	Substrate
SC	Subcutaneous
SCE	Saturated Calomel Electrode
SEM	Scanning Electron Microscopy

SHE	Standard Hydrogen Electrode
SPICE	Simulation Program with Integrated Circuit Emphasis
t	Time (seconds)
TTACl	N-Trimethoxysilylpropyl-N,N,N-Trimethylammonium Chloride
V	Voltage (volts)
V, V _{max}	Velocity and maximum velocity respectively of enzyme catalyzed reactions obeying Michaelis Menton kinetics (units of concentration/second)
V _a , V _{BIAS}	Applied bias voltage of a working electrode measured with respect to the reference electrode (volts)
V _{ds} , V _{gs}	Transistor drain and gate voltages respectively, measured with respect to the source (volts)
V _o	Output voltage (volts)
W	Window width (in terms of number of data points) used in moving average type smoothing algorithm
WBC	White Blood Cell
WE	Working Electrode
W/L	Geometric Width-to-Length ratio of integrated field effect transistors (dimensionless)
z	Number of moles of electrons transferred per mole of reactant electrochemically oxidized/reduced (dimensionless)

CHAPTER 1

Introduction

A sensor is an input transducer to an electronic system that converts a physical or chemical signal into an electrical signal. Advances in analytical chemistry, particularly those involving solid state devices, have opened up possibilities for the application of sensor technology to biomedical problems. New bionic devices can now be conceived which potentially offer major advancements in the treatment and management of certain diseases such as diabetes. The Artificial Beta Cell is one such device that could be realized if a sufficiently stable and accurate glucose sensor could be developed. The work presented here is directed toward this goal. A brief introduction to the problems and state-of-the-art of biomedical glucose sensing is given in this chapter, and the specific objectives and scope of the work described in subsequent chapters is defined. An overview of the glucose sensor configuration employed in this study is also presented, including a few theoretical considerations important to an understanding of the principals of operation. Finally, a summary is given which highlights the most important aspects of the work.

1.1 DIABETES AND THE IMPORTANCE OF GLUCOSE SENSING

Diabetes is now considered to be the third leading cause of death in first-world countries. The most severe form of the disease is called Idiopathic Diabetes Mellitus—Type I, or Insulin-Dependent Diabetes Mellitus (IDDM). It arises due to the failure of the pancreatic beta cells of afflicted individuals to produce and secrete sufficient levels of the hormone insulin, resulting in the deregulation of blood sugar levels [1]. The insulin producing beta cells are just one of the four cell types that comprise the so called Islets of Langerhans which, collectively, comprise the endocrine pancreas. The other three cell types—alpha, delta and pancreatic polypeptide cells—are also important in the regulation of blood glucose levels, but these cells together make up less than 30% of the Islet cells. It is the diminished beta cell activity that is primarily responsible for the symptoms of Type I diabetes [2].

Conventional treatment of Type I Diabetes usually involves a strict regimen of dietary management and daily prescribed doses of exogenous insulin. Current insulin therapies, however, are ineffective in maintaining normal blood glucose levels because of the intermittent nature of insulin delivery via discrete injections [3,4]. That is, blood glucose levels in diabetics fluctuate considerably in response to ingestion of foodstuffs, activity levels, *etc.*, and insulin requirements depend on the glucose concentration (and the rate of change of the glucose concentration) in the blood. Thus, without a means of sensing these instantaneous fluctuations, it is not possible to maintain a physiologically optimum concentration of insulin in bodily tissues. Excessive or depressed insulin levels, relative to glucose levels, can have severely adverse effects on many key cellular metabolic processes. Over the course of several years, poor blood glucose regulation can lead to blindness and other vision problems, impotence, infertility, circulatory and kidney disorders, heart disease, chronic infections, *etc.* [3,5].

It would of course be ideal if fundamental medical research could produce a cure for Diabetes by correcting the pathological conditions which cause the disease. However, in the meantime, it is essential to develop more physiologically optimal methods of delivering insulin, which more closely model the endocrine functions of the healthy pancreas [6-9]. In effect, what is required is the development of an Artificial Endocrine Pancreas, or at least an Artificial Beta Cell (ABC). The two main components of such a closed-loop blood glucose control system would have to be: (1) a glucose sensor, to continuously monitor the glucose levels in the blood; and (2) a servoactuated pump to administer controlled amounts of insulin and glucose (or glucagon), based on the feedback signal from the sensor. The latter component, and all of the associated electronic control circuitry, can already be implemented in a form suitable for implantation using presently available technology. Rather, it is the glucose sensor component that has been identified as the greatest challenge to be overcome in the quest to develop an implantable artificial beta cell [10,11]. A simplified block diagram of a hypothetical artificial beta cell is shown in Figure 1.1.

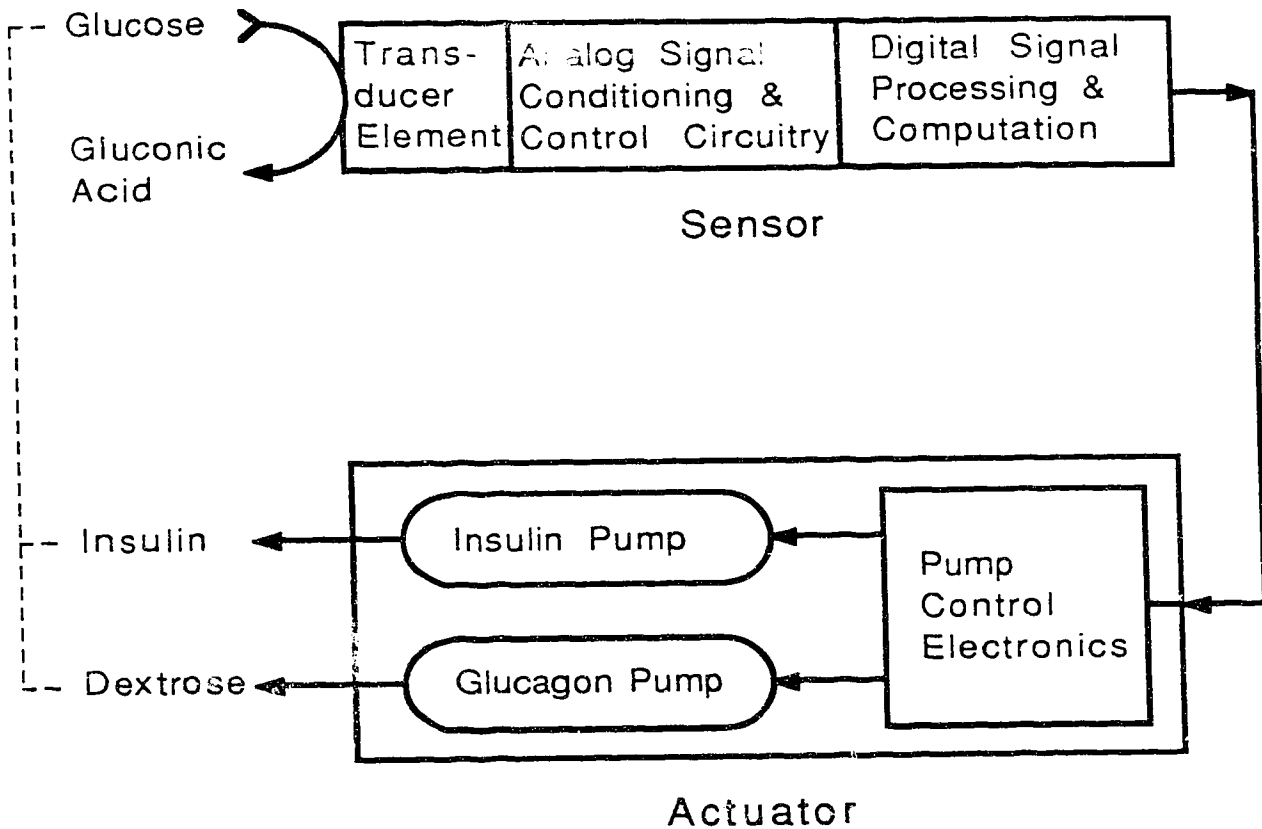


Figure 1.1 Block diagram of a hypothetical artificial beta cell system. In this system, the glucose sensor component is based on an enzymatic method. The digital signal processing and computational block is shown as part of the sensor since, in principle, this block could be integrated on the same chip as the sensor control circuitry.

1.2 PROBLEMS AND PROGRESS

The first successful implementation of closed-loop glycaemic control was reported by Albisser, *et al.* [12,13] in 1974. Albisser's group had developed a complex bedside system that included a commercial laboratory glucose analyzer, a powerful minicomputer and peripherals, peristaltic and pulsatile infusion pumps, and two intravenous catheters to interface with the patient. This experimental system was capable of maintaining normoglycaemia in hospitalized patients for extended periods of time, and demonstrated the feasibility of automatic blood glucose control by an artificial device. This work provided a major impetus for subsequent research and led to the development of the commercial Biostator® Glucose Controlled Insulin Infusion System (GCIIS), which is used in hospitals today [14,15]. The Biostator is certainly accurate and reliable, but it is not portable and patients are continuously subjected to the discomfort (and risk) of external intravenous catheters. Both of these problems could be alleviated if the machine could be miniaturized and implanted.

A partial solution has been made available to some patients in the form of portable open-loop insulin delivery systems. These are becoming increasingly more popular due to much work that has been done to optimize their performance [7,8]. Commercially available devices usually consist of a subcutaneous catheter and a control/pump unit, worn externally by the patient, which injects insulin continuously according to a preprogrammed algorithm [16,17]. More recently, clinical trials have been reported involving implantable (open-loop) insulin delivery systems [18,19]. However, surgical complications and stability problems have yet to be resolved for long-term applications (*e.g.* six months to two years). These devices are an improvement over discrete insulin injections for day-to-day diabetes management, but the same basic concerns persist regarding long-term complications of the disease. Still, this research has provided a foundation for developing algorithms which could be employed in closed-loop systems [20-22]. Portable versions of such closed-loop systems are, however, still in the experimental stage [23,24].

Glucose analysis is one of the most common clinical laboratory assays, and enzymatic methods for precise glucose determination are well developed [25]. The classical methods involving immobilized (as opposed to soluble) enzymes have been reviewed extensively by Guilbault [25,26] and others [27-29]. Enzymes are highly specific biological catalysts which, when activated, can accelerate biochemical reactions by factors of 10^6 or more. In fact, most reactions catalyzed by natural enzymes do not proceed at detectable rates in the absence of the particular enzyme involved. The detailed mechanisms of enzyme catalysis are still a topic of research, but a general description was given as early as 1948 by Linus Pauling which is still considered useful [30]:

"I think that enzymes are molecules that are complementary in structure to the activated complexes of the reactions that they catalyze, that is, to the molecular configuration that is intermediate between the reacting substances and the products of reaction for these catalyzed processes. The attraction of the enzyme molecule for the activated complex would thus lead to a decrease in the energy of activation of the reaction and to an increase in the rate of reaction."

Virtually all laboratory glucose analyzers, such as the Yellow Springs Instrument and Beckman models, are based on the oxidation of the beta anomer of D-glucose by the enzyme glucose oxidase, as first described by Clark and Lyons [31] in 1962. In the presence of dissolved oxygen, β -D-glucose is converted to D-gluconic acid and hydrogen peroxide; the rate of the reaction (and hence the concentration of the substrate glucose) are commonly determined spectrophotometrically or electrochemically [26]. These systems are difficult to miniaturize and require frequent recalibration and replacement of reagents.

The first miniature immobilized enzyme electrode for glucose sensing was reported by Updike and Hicks [32] in 1967. This sensor is based on the polarographic measurement of the rate of oxygen consumption in the glucose oxidase reaction described above. Several other authors have since described sensors based on oxygen uptake [33-36], but many of these

suffer from nonlinear effects due to oxygen transport limitations (depletion zones) or physiological variations in dissolved oxygen tension due to factors that are not necessarily related to glucose concentration. That is, if the dissolved oxygen tension falls too low, then the reaction rate will become limited by the oxygen concentration rather than glucose. A partial solution to these problems was proposed by Cleland and Enfors [37,38] who described an oxygen stabilized sensor. Most oxygen uptake type sensors, however, are difficult to miniaturize due to the need for both internal and external electrolytes, and more complicated membrane systems than other types.

Another electrochemical approach employing the same basic glucose oxidase mediated reaction, is to determine the rate of hydrogen peroxide production [39-44]. Presently, this is the least complicated and most commonly employed detection mechanism for miniaturized glucose sensors. Sensors of this type are also amperometric, but have a much broader dynamic range than oxygen uptake sensors. This arises because oxygen uptake sensors rely on differential measurements where both the signal and background level can change significantly, whereas hydrogen peroxide sensors measure a signal relative to a fairly constant background level. As a consequence, it is somewhat less complicated to reduce the sensitivity of a hydrogen peroxide electrode to dissolved oxygen. Glucose determination by the measurement of hydrogen peroxide production is the approach adopted in the present work, and further advantages and disadvantages of this technique will be discussed in later Chapters.

A few designs have also been reported which substitute an alternate electron acceptor such as quinone [45] or ferrocene [46] in place of oxygen, in an effort to realize an oxygen-independent sensor. The advantages of this approach are that dissolved oxygen tension is no longer critical, and the enzyme denaturing effect that occurs with hydrogen peroxide production over the long-term [28,29] is entirely avoided. This approach may ultimately lead to the technology of choice for miniaturized glucose sensors, but is still under development and many of these sensors incur problems as a result of reactions between the alternate acceptor and dissolved oxygen in the analyte solution [47]. Seeking to avoid the use of an electron transfer intermediate has led others to investigate sensors based

on the direct transfer of electrons from the enzyme-substrate complex to conducting electrodes [47-49]. However, these electrodes can be expected to be short-lived and to inherently exhibit poor sensitivity to glucose, since only a monolayer of enzyme adsorbed onto the electrode surface actually contributes to the electrode current.

Yet another method of detection based on the glucose oxidase reaction is that of measuring localized pH changes due to the production of gluconic acid. This is the method employed in the so called Enzyme Field Effect Transistor (ENFET) which is fabricated by immobilizing the enzyme in a membrane fixed or cast over the gate region of an H⁺ Ion Sensitive FET (ISFET) [50-53]. These devices represent one of the few truly integrated glucose sensors which have appeared in the literature thus far, and could potentially offer all of the touted advantages that accompany this technology. However, ENFET devices are very sensitive to variations in the reaction kinetics, interfering species and liquid junction potentials. In the words of one researcher[†]: "*unfortunately, [these devices] make better buffer capacity sensors than glucose sensors*". These devices also tend to be rather short-lived since the delicate gate oxide remains exposed and is therefore vulnerable to contamination by (for example) sodium or chloride ions which are also present in appreciable concentrations in all body fluids. Macroscopic potentiometric glucose sensors based on pH determination [54-56] are more robust in this respect, but suffer from the same sensitivity to buffer capacity, interfering species, etc. Furthermore, the sensitivity to glucose of all potentiometric sensors is limited in that the signal is logarithmic with respect to glucose concentration; whereas amperometric sensors yield a signal that is linear with glucose concentration (at least over some useful range).

There are several problems which plague all enzyme based glucose sensors and these are discussed at length elsewhere [57-62]. The most serious problem, with regard to implantable sensors, is the perpetual drift in calibration characteristics due (mostly) to decreasing enzyme activity

[†] Steven D. Caras in a private conversation with the author at the Transducers '87 conference in Tokyo (June 1987). Dr. Caras worked extensively with ENFET devices during the course of his doctoral studies and is the author of several publications dealing with ENFET development and characterization.

and electrode fouling over time. The working lifetime of the best enzyme based electrodes, operated in discrete assay systems, is typically a few months under carefully controlled storage conditions [26,62]. The lifetime of these electrodes operated continuously in blood at 37°C is seldom reported, but is certain to be considerably shorter. Much of the current research effort in this field is focused on developing methods of improving the stability of the immobilized enzyme in order to reduce drift [63,64], although progress in this area does not necessarily bear on the problems of electrode fouling or enzyme inhibition by interfering species.

Several nonenzymatic methods have also been proposed for *in vivo* measurements of glucose concentration. For example, several researchers have experimented with electrocatalytic glucose electrodes [65-68] which are based on the direct electrochemical detection of glucose. Also, Wingard [69] has described an immobilized flavin fuel cell electrode where the flavin cofactor (FAD) of glucose oxidase is covalently attached to a solid carbon electrode in order to facilitate direct electron transfer to the electrode during the oxidation of glucose. Schultz, *et al.* [70] have devised a so called "affinity sensor" based on techniques similar to those used in radioimmunoassays. Optical methods, such as the measurement of the Faraday rotation of polarized light [71] have also been applied to glucose sensing. Most of these "exotic" methods are highly experimental and many practical problems remain to be solved.

1.3 OBJECTIVES

The ultimate objective of research in this field is to realize a miniature, solid state glucose sensor, suitable for incorporation into an implantable closed-loop blood glucose control system. Over the past two decades, efforts worldwide have elucidated many of the obstacles that stand in the way of this goal, and it has become clear that no single project could realistically undertake to solve all of the problems at once. The research described here is directed toward this ultimate goal, but we have elected to focus on two main objectives as described below.

(1) Improved Instrumentation. Previous work in this field, involving amperometric sensors, was done mainly with benchtop analytical

instruments or custom circuits fabricated from discrete components. One of the objectives was to apply integrated circuit technology to the development of practical electronic instrumentation for implantable (or portable) glucose sensors. The main considerations were: miniature size, low power consumption, high sensitivity, voltage output, and differential measurement capability. Also a priority, was to design the circuit to be flexible enough to be useful as a research tool. An important, but secondary, consideration was to employ a minimum number of devices so as to minimize the chip area in order to facilitate later expansion of the design to incorporate further signal processing (and possibly computational) circuitry on the same chip. The provision for integrating micro-electrode structures on the same chip was also considered.

(2) Improved Electrode Stability and Biocompatibility. The interface between the body and an implanted sensor, and the role of biocompatibility in the performance and lifetime of the sensor, is poorly understood. Glucose sensor development has generally proceeded using conventional dialysis materials with the understanding that the problems of biocompatibility would, eventually, be solved by incorporating additional membrane layers comprised of biocompatible material. The second main objective of this work was to explore a novel membrane material with the potential for combined dialysis and biocompatibility functions. Conceptually, the project was divided into multiple phases with the following priorities: to learn about the requirements of biosensor dialysis membranes, in general, in biological media *in vitro*; to characterize the new material in the laboratory and characterize its effect on the operation and stability of glucose sensors of the amperometric type *in vitro*; to examine its biocompatibility and ascertain its suitability for *in vivo* studies. We then approached the design of an implantable sensor prototype, guided by the experience gained from the earlier *in vitro* studies. It is worth noting that, even if sensors based on an alternate electron transfer mediator (or direct electron transfer) are perfected, a dialysis membrane system would still be required for sensors intended to operate *in vivo*.

The scope of the work undertaken here includes design, fabrication and testing of integrated electronic devices; preparation and charact-

erization of polymer dialysis membranes; and the design, fabrication and testing of sensors incorporating the results of both instrumentation and membrane aspects. The work includes some elements of electrical engineering, chemistry, and biology. All data are empirical and no theoretical modelling was undertaken. Both instrumentation and membrane aspects are developed to the point of demonstrating the advantages (and disadvantages) of the approach, elucidating some of the problems in implementing this technology and proposing some solutions. Further development and optimization are left for future efforts, although some discussion as to the direction of future work is presented in Chapter 6.

1.4 OVERVIEW OF THE SENSOR

1.4.1 Functional Components

As mentioned previously, the approach adopted in this work involves the amperometric determination of hydrogen peroxide produced by the enzymatic oxidation of glucose. The physical embodiment of the sensor based on this approach is comprised of two main functional parts: a glucose sensitive membrane system, coupled to a platinum indicating electrode, which converts the glucose concentration signal into an electrical signal; and an integrated potentiostat circuit which applies a controlled bias potential to the electrode, and converts the input electrode current into a useful output voltage. A self-contained discussion of the function and characteristics of the integrated potentiostat circuit will be presented in the following chapter. The main focus of the rest of the thesis is, in fact, on the glucose sensitive membrane/electrode system. It would be useful here to introduce some of the complexities of this system in order to facilitate the discussion presented in later chapters.

A schematic diagram of the glucose sensitive membrane/electrode system is shown in Figure 1.2, which also depicts some of the important functional aspects. The outermost membrane layer is the dialysis component which also constitutes the critical interface between the body and the sensor. Briefly, the function of this membrane is to permit electrolytes, glucose and oxygen to diffuse into the reactive enzyme layer and to exclude blood cells, plasma proteins, and other blood constituents

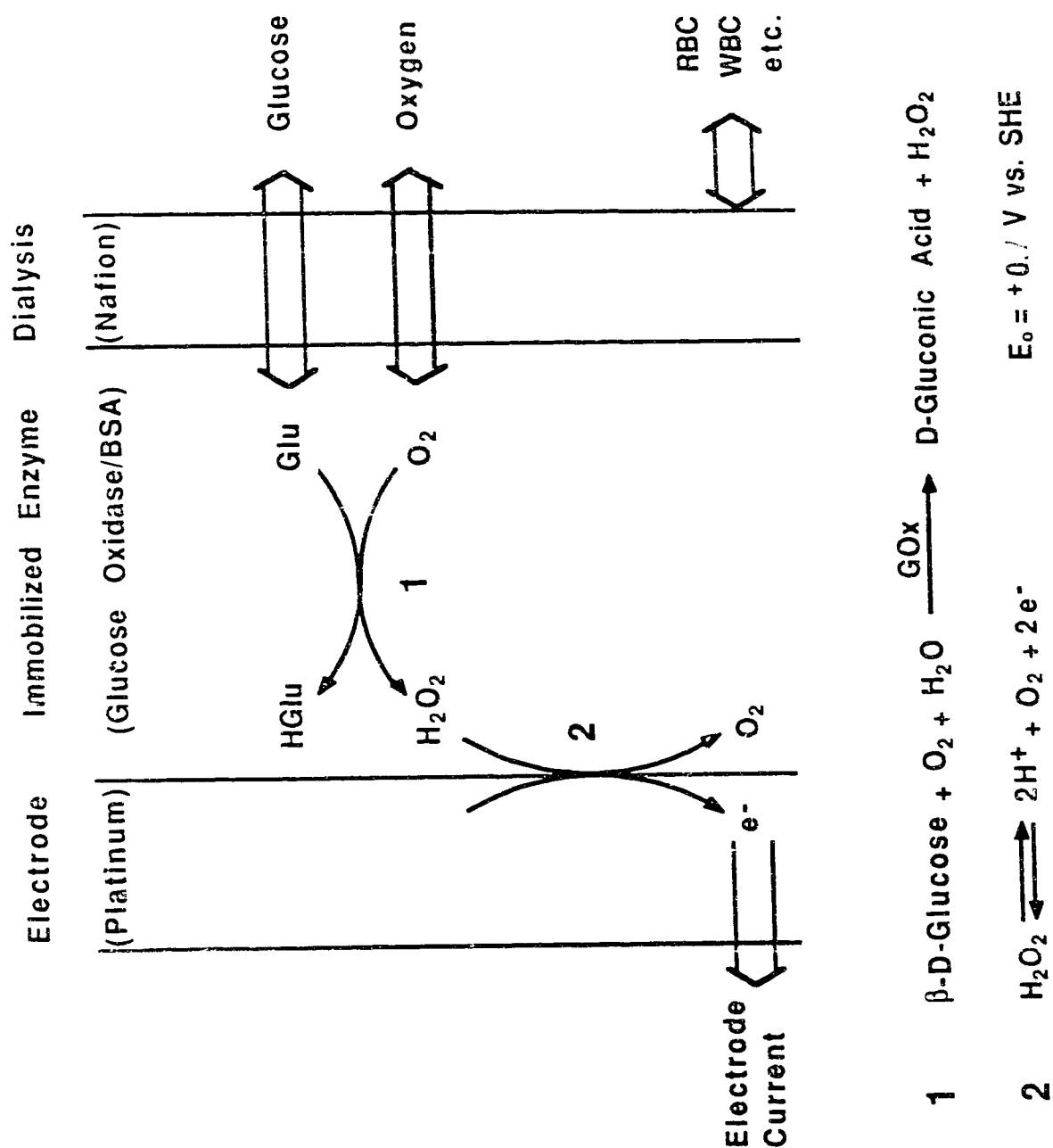


Figure 1.2 Schematic cross sectional view of the glucose sensitive membrane/electrode system. RBC, WBC, *etc.*, refer to red blood cells, white blood cells, platelets, plasma proteins and other blood constituents that have a detrimental effect on the function of the immobilized enzyme (GOx) or the platinum indicating electrode. Glu and HGlu refer to glucose and gluconic acid respectively.

that interfere with the chemical and electrochemical processes. Interference can take the form of generating a spurious signal, suppressing the signal for glucose, or poisoning the enzyme/electrode system. In the immobilized enzyme layer, glucose oxidase mediates the oxidation of glucose to gluconic acid, and the reduction of oxygen to hydrogen peroxide. The hydrogen peroxide then diffuses to the surface of the platinum electrode and undergoes electrochemical oxidation that liberates oxygen, protons and, most importantly, electrons which result in the measured electrode current.

The dialysis membrane component would not be required if the sensor were intended for glucose assays in aqueous buffer solutions. However, living whole blood is a far more complicated matrix as shown in Table 1.1 and many of the constituents of this matrix are detrimental to the operation of the sensor. For example, some plasma proteins can cause steric hindrances and disrupt or impede the access of glucose to the active site of the enzyme; also, electroactive species such as ascorbic acid and some waste products can interfere with electrochemical processes. Hence, in a blood or blood plasma matrix, the dialysis membrane component provides a crucial "screening function" to reduce or eliminate these species from the internal regions of the membrane system. In the configuration adopted here, the dialysis membrane component is also responsible for biocompatibility, which is important not only from the point of view of the host, but is also critical in maintaining a stable environment around the sensor. Finally, the dialysis membrane also provides the capability to control the mass transport of glucose relative to oxygen through the membrane, in order to increase the dynamic range of the sensor and linearize the response. The trade-off for these advantages is decreased sensitivity, although this can be compensated for by increasing the gain of the potentiostat circuit.

1.4.2 Chemical and Electrochemical Considerations

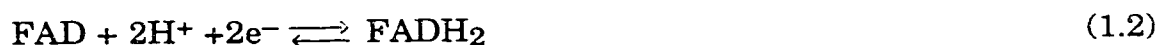
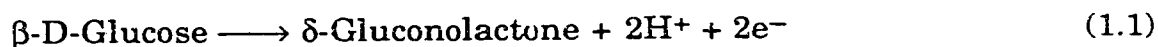
The reaction mechanisms involved in the conversion of a glucose concentration signal to an electrical signal are fundamental to an understanding of the operation of the sensor, and thus warrant at least a brief

TABLE 1.1 Normal concentrations of constituents of human arterial plasma (compiled from various sources).

COMPONENT	SPECIES	CONCENTRATION
SOLVENT:	Water	93% of plasma weight
ELECTROLYTES:	Na ⁺	142 mM
	K ⁺	4 mM
	Ca ₂ ⁺	2.5 mM
	Mg ₂ ⁺	1.5 mM
	Cl ⁻	103 mM
	HCO ₃ ⁻	27 mM
	(Total) Phosphates	1 mM
	SO ₄ ²⁻	0.5 mM
PROTEINS:	Albumins	4.5 g/100 ml
	Globulins	2.5 g/100 ml
	Fibrinogen	0.3 g/100 ml
	(Individual) Hormones	0.001-50 mg/100 ml
DISSOLVED GASES:	CO ₂	2 mmol/100 ml
	O ₂	0.2 mmol/100 ml
	N ₂	0.9 mmol/100 ml
NUTRIENTS:	Carbohydrates	100 mg/100 ml (5.6 mM)
	(Total) Amino Acids	40 mg/100 ml (2 mM)
	(Total) Lipids	500 mg/100 ml (7.5 mM)
	Cholesterol	150-250 mg/100 ml (4-7 mM)
	(Individual) Vitamins	0.0001-2.5 mg/100 ml
	Trace Elements	0.001-0.3 mg/100 ml
WASTE PRODUCTS:	Urea	34 mg/100 ml (5.7 mM)
	Uric Acid	5 mg/100 ml (0.3 mM)
	Creatinine	1 mg/100 ml (0.09 mM)
	Bilirubin	0.2-1.2 mg/100 ml (3-18 mM)

treatment here. These mechanisms have been well studied and comprehensive treatments can be found in standard texts in enzymology [72,73] and electrochemistry [74].

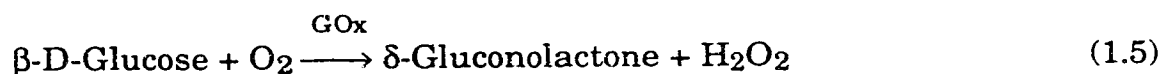
The glucose oxidase mediated reaction given in Figure 1.2 is actually a net reaction that proceeds via two redox steps and a hydrolysis step. The first redox step involves the oxidation of glucose and the reduction of the prosthetic group flavin adenine dinucleotide (FAD) according to



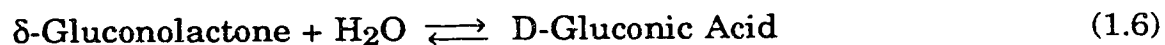
and the second redox step involves the reoxidation of FADH₂ and the reduction of oxygen, *viz.*



which sum to yield the net (redox) reaction



where GOx represents the involvement of the enzyme glucose oxidase. The hydrolysis of the lactone, *viz.*

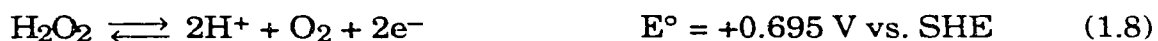


is spontaneous (*i.e.* does not depend on the involvement of the enzyme catalyst). The reactions (1.5) and (1.6) sum to give the overall net reaction



which has been referred to repeatedly in previous sections.

Some of the hydrogen peroxide produced in the above reaction diffuses to the surface of the platinum indicating electrode where it is oxidized electrochemically according to the half-cell reaction



where E° represents the electrode potential with respect to a standard hydrogen electrode (SHE) at pH 0. At an electrode potential that is positive of this value, reaction (1.8) is spontaneous (*i.e.* $\Delta G < 0$), although it may be kinetically limited. At pH 7, the standard potential is shifted cathodically (*i.e.* to a more negative potential) by approximately 410 mV. Generally, in order to overcome the kinetic barrier to oxidation and ensure that the rate of reaction is limited by mass transport effects, a voltage significantly more anodic (*i.e.* more positive than E°) is applied. A value of approximately +0.94 V versus SHE is typically found to provide sufficient driving force to ensure mass transport limitation. Under these conditions the current will be proportional to concentration.

The SHE is not a convenient reference electrode to use and so a saturated calomel electrode or a silver/silver chloride electrode is typically used. The appropriate half cell reactions are



where it is understood that the internal electrolyte of the calomel electrode is saturated KCl, and the silver/silver chloride cell is 1 M in chloride. In this work, both of these references were employed for studies in the laboratory, although the Ag/AgCl electrode was always used with the integrated potentiostat.

The charge transfer between the indicating and reference electrodes in solution is mediated by the supporting electrolyte. In blood, the supporting electrolyte is comprised primarily of sodium and chloride ions that are present in relatively large concentrations (see Table 1.1). The electrons liberated in reaction (1.8) are the charge carriers that constitute

the glucose dependent component of the electrode current. Additional (interference) components may also exist, and must be accounted for in the measurements.

1.4.3 Kinetic Considerations

The linearity (or nonlinearity rather) of the sensor response with respect to glucose concentration, depends on a number of kinetic factors. These factors are complicated and it is beyond the scope of this thesis to present a realistic theoretical analysis. However, as a first order approximation, the kinetic model of Michaelis and Menton [75] provides a reasonable qualitative description. This model is based on the generic (single substrate) reaction



where E=enzyme, S=substrate, E·S=enzyme-substrate complex, P=product, and k_1 , k_2 , k_3 are the rate constants associated with the pathways indicated. The concentration of the E·S complex is assumed to rapidly attain a steady state condition where

$$\frac{d[E \cdot S]}{dt} = k_1 [E] [S] - (k_2 + k_3) [E \cdot S] = 0 \quad (1.12)$$

and since, at any time, the total amount of free and bound enzyme must be conserved (*i.e.* $[E] + [E \cdot S] = \text{constant} = [E]_0$),

$$[E \cdot S] = \frac{k_1 [E]_0 [S]}{(k_2 + k_3) + k_1 [S]} \quad (1.13)$$

where $[E]_0$ represents the total concentration of the enzyme at $t=0$. Then the rate of formation V , of the product P, is

$$\frac{d[P]}{dt} = V = \frac{k_1 k_3 [E]_0 [S]}{(k_2 + k_3) + k_1 [S]} \quad (1.14)$$

or

$$V = \frac{V_{\max} [S]}{K_m + [S]} \quad (1.15)$$

where $V_{\max} = k_3[E]_0$ and $K_m = (k_2 + k_3)/k_1$ which is called the Michaelis constant and is characteristic of a given enzyme/substrate system obeying Michaelis Menton kinetics. In the present case, the substrate S refers to glucose and the product P refers to hydrogen peroxide. Note that equation (1.15) can be rearranged to obtain

$$\frac{1}{V} = \frac{K_m}{V_{\max}} \frac{1}{[S]} + \frac{1}{V_{\max}} \quad (1.16)$$

so that, if observed kinetic data are plotted as $1/V$ versus $1/[S]$, the value of K_m can be determined graphically from the slope and intercept. Such a plot is called a Lineweaver-Burke plot [75].

Assuming that the electrochemical oxidation of hydrogen peroxide described by reaction (1.8) proceeds at a much faster rate than V , then the dependence of the electrode current on glucose concentration can be approximated by

$$I \propto \frac{[S]}{K_m + [S]} \quad (1.17)$$

which is hyperbolic in $[S]$ (the concentration of glucose). Note that the value of K_m represents the glucose concentration at which the electrode current is one half of the maximum current; and for concentrations small compared to K_m , the current is approximately linear with glucose concentration. The value of K_m thus serves as a useful figure of merit describing the linear dynamic range of the sensor.

Equation (1.17) qualitatively describes the dependence of electrode current on glucose concentration. However, the glucose oxidase mechanism is considerably more complicated since two substrates are actually involved (i.e. glucose and oxygen), and a number of intermediate steps and alternate pathways exist [73,76]. Furthermore, this analysis

totally neglects all mass transport effects including the effects of immobilizing the enzyme and the effect of the presence of the dialysis membrane. Nevertheless, equation (1.16) does give a reasonable fit to the calibration data obtained for the sensors described in this thesis. And an apparent K_m value can be determined for a given membrane/electrode system from a graphical analysis (*i.e.* Lineweaver-Burke plot) of the calibration data.

1.4 SUMMARY

The research undertaken during the course of this program, and described herein, was directed toward the development of an implantable glucose sensor for the Artificial Beta Cell. Electrochemical methods for glucose analysis involving the highly specific enzyme glucose oxidase have long been employed in laboratory plasma glucose assays *in vitro*. However, efforts to miniaturize this technology and to develop a sufficiently stable sensor for long-term *in vivo* applications have failed, primarily due to electrode stability and biocompatibility problems. Both of these problems have been addressed in the scientific aspects of this project and, in the engineering aspects, advanced instrumentation for amperometric sensors was developed.

The overall body of work is divided into four independent studies which are reported here in a "paper format". That is, each independent study is presented in a format that follows closely the format of the published version of the study. Note that, as a result, some duplication of references and explicatory material exists. Each of the following paragraphs briefly summarizes the salient features of each of the four studies presented in Chapters 2 through 5, respectively.

A Complementary Metal Oxide Semiconductor (CMOS) integrated controller circuit that operates in an amperometric mode was developed which greatly alleviates problems associated with packaging the sensor as the chip can remain hermetically sealed, and be used in conjunction with remote reference and indicating electrodes. Compared to potentiometric systems, the amperometric approach offers enhanced precision and immunity to noise and electrochemical interference. This design also

provides a significant improvement in selectivity due to the differential mode capability which nulls the effect of spurious background currents. The output voltage is linearly related to anode current down to a detection limit of less than 10 nA, which is suitable for use with the small electrode areas desirable for *in vivo* assay systems. This device represents an essential step toward miniaturization and implantability.

A process was also developed for encapsulating glucose oxidase enzyme electrodes in a perfluorosulfonic acid polymer (Nafion®) membrane that functions as a protective dialysis layer and yields superior performance and reproducibility over conventional materials such as cellulose and cellulose acetates. Experiments *in vitro* showed that Nafion effectively excludes blood cells, plasma proteins and other blood constituents that denature the enzyme and/or poison the catalytic activity of the electrode surface. It was also shown that the mass transport of glucose relative to oxygen through the membrane can be controlled in order to obtain linear characteristics up to at least 540 mg/dl (>30 mM) glucose concentration and that Nafion membranes have a minimal effect on the response time of the electrode. This represents the first study demonstrating Nafion polymer as a suitable dialysis membrane material for use in whole blood samples and that it can be employed for preferential separation of neutral species such as glucose.

In order to realize a reliable implantable sensor, the encapsulating material must obviously invoke a minimal biological response, which has proven to be a major problem with conventional materials. In regard to this criterion, the first long-term biocompatibility studies on Nafion polymer were conducted, and results indicated excellent tissue and blood compatibility in rats. For example, histological examination of tissues surrounding 3 month and 6 month Nafion implants reveals a thin fibrous connective tissue capsule around the implant and little, if any, evidence of a foreign body inflammatory response. The fibrous capsule appears to be stable and permeable to glucose and electrolytes, thus preserving the microenvironment around the sensor. These findings may be applicable to a broad range of problems afflicting other implantable biosensors, artificial organs and prostheses.

An implantable version of the Nafion encapsulated glucose sensor electrode was designed, fabricated and tested in whole blood *in vitro* and *in vivo*. The implantable version incorporates modifications to the electrode surface treatment that substantially improve the adhesion of both the enzyme and Nafion polymer membranes. Prototype electrodes performed satisfactorily *in vitro*, but intravenously implanted electrodes did not perform well and were short-lived. Subsequent diagnostic testing suggested significant differences exist in the dialysis membrane requirements for *in vivo* versus *in vitro* glucose sensing in whole blood. Flaws in the prototype design and fabrication were identified, and corrective measures were suggested. These results represent the first step in the transfer of Nafion encapsulation technology from discrete *in vitro* glucose assays in the laboratory, to continuous *in vivo* monitoring.

1.5 REFERENCES

- [1] Guyton, *Textbook of Medical Physiology*, 7th Edition, W.B. Saunders Company, Philadelphia, 1986.
- [2] Connaught Laboratories Ltd., *Insulin in the Control of Diabetes*, Published jointly by the Clinical and Scientific Section of the Canadian Diabetes Association and Connaught Laboratories, 1983.
- [3] M. Brownlee, Ed., *Handbook of Diabetes Mellitus*, Volume 5: Current and Future Therapies, Garland STPM Press, New York, 1981.
- [4] P. Raskin, "Treatment of Type I Diabetes with Portable Insulin Infusion Devices", *Diabetes Care*, Vol. 5, Suppl. 1, pp. 48-52, 1982.
- [5] J.H. Fuller, J. Elford, P. Goldblatt and A.M. Adelstein, "Diabetes Mortality: New Light on an Underestimated Public Health Problem", *Diabetologia*, Vol. 24, pp. 336-341, 1983.
- [6] American Diabetes Association, "Indications for Use of Continuous Insulin Delivery Systems and Self-Measurement of Blood Glucose", *Diabetes Care*, Vol. 5, No. 2, pp. 140-141, 1982.

- [7] J.S. Skyler, D.E. Seigler and M.L. Reeves, "Optimizing Pumped Insulin Delivery", *Diabetes Care*, Vol. 5, No. 2, pp. 135-139, 1982.
- [8] C.M. Peterson, "[Introduction to] Symposium on Optimal Insulin Delivery", *Diabetes Care*, Vol. 5, Suppl. 1, pp. 1-5, 1982.
- [9] A.M. Albisser, "Insulin Delivery Systems: Do They Need a Glucose Sensor?", *Diabetes Care*, Vol. 5, No. 3, pp. 166-173, 1982.
- [10] J.S. Soeldner, "[Introduction to] Symposium on Potentially Implantable Glucose Sensors", *Diabetes Care*, Vol. 5, No. 3, p. 147, 1982.
- [11] B.J. Oberhardt, E.J. Fogt and A.H. Clemens, "Glucose Sensor Characteristics for Miniaturized Portable Closed-Loop Insulin Delivery: a Step Toward Implantation", *Diabetes Care*, Vol. 5, No. 3, pp. 213-217, 1982.
- [12] A.M. Albisser, B.S. Leibel, T.G. Ewart, Z. Davidovac, C.K. Botz and W. Zingg, "An Artificial Endocrine Pancreas", *Diabetes*, Vol. 23, pp. 389-396, 1974.
- [13] A.M. Albisser, B.S. Leibel, T.G. Ewart, Z. Davidovac, C.K. Botz, W. Zingg, H. Schipper and R. Gander, "Clinical Control of Diabetes by the Artificial Pancreas", *Diabetes*, Vol. 23, No. 3, pp. 397-404, 1974.
- [14] E.J. Fogt, L.M. Dodd, E.M. Jennings and A.H. Clemens, "Development and Evaluation of a Glucose Analyzer for a Glucose-Controlled Insulin Infusion System (Biostator)", *Clinical Chemistry*, Vol. 24, pp. 1366-1372, 1978.
- [15] A.H. Clemens, P.W. Chang and R.W. Myers, "The Development of Biostator, a Glucose-Controlled Insulin Infusion System (GCIIS)", *Horm. Metabol. Research*, Vol. 7, Suppl., pp. 23-33, 1977.
- [16] S. Genuth and P. Martin, "Control of Hyperglycemia in Adult Diabetes by Pulsed Insulin Delivery", *Diabetes*, Vol. 26, pp. 571-581, 1977.

- [17] Y. Gloriya, A. Bahoric, E.B. Marliss, B. Zinman, B.S. Leibel and A.M. Albisser, "Glycemic Regulation Using a Programmed Insulin Delivery Device. III.", *Diabetes*, Vol. 28, pp. 558-564, 1979.
- [18] K.D. Hepp and R. Renner, Eds., *Continuous Insulin Infusion Therapy: Experience from One Decade*, Symposium Proceedings, Munich, May 1984, Schattauer, Stuttgart, 1985.
- [19] H. Regal, "Implanted Versus External Pump", Presented at meeting of the International Study Group on Diabetes Treatment with Implantable Insulin Delivery Devices (ISGIID), Cohasset, Mass., September 28-October 1, 1986.
- [20] C.K. Botz, "An Improved Control Algorithm for an Artificial B-Cell", *IEEE Trans. Biomed. Eng.*, Vol. 23, pp. 252-255, 1976.
- [21] U. Fischer, E. Jutzi, E-J. Freyse and E. Salzsieder, "Derivation and Experimental Proof of a New Algorithm for the Artificial B-Cell Based on the Individual Analysis of the Physiological Insulin/Glucose Relationship", *Endokrinologie*, Vol. 71, pp. 65-75, 1978.
- [22] A.H. Clemens and P.W. Chang, "Continuous Blood Glucose Analysis and Feedback Control Dynamics for Glucose Controlled Insulin Infusion (Artificial B-Cell)", Proceedings of the 14th International Congress on Therapeutics, Montpellier, France, September 8-10, 1979, *L'Expansion Scientifique*, pp. 45-58, 1979.
- [23] M. Shichiri, R. Kawamori, N. Hakui, Y. Yamasaki and H. Abe, "Closed-Loop Glycemic Control with a Wearable Artificial Endocrine Pancreas: Variations in Daily Insulin Requirements to Glycemic Response", *Diabetes*, Vol. 33, pp. 1200-1202, 1984.
- [24] M. Shichiri, R. Kawamori, Y. Goriya, Y. Yamasaki, M. Nomura, N. Hakui and H. Abe, "Glycaemic Control in Pancreatectomized Dogs with a Wearable Artificial Endocrine Pancreas", *Diabetologia*, Vol. 24, pp. 179-184, 1983.

- [25] G.G. Guilbault, *Handbook of Enzymatic Methods of Analysis*, Marcel Dekker, New York, 1976.
- [26] G.G. Guilbault, *Analytical Uses of Immobilized Enzymes*, Marcel Dekker, New York, 1984.
- [27] S.J. Gutcho, *Immobilized Enzymes—Preparation and Engineering Techniques*, Noyes Data Corporation, New Jersey, 1974.
- [28] L.B. Wingard, Jr., E. Katchalski-Katzir and L. Goldstein, *Immobilized Enzyme Principles*, Applied Biochemistry and Bioengineering, Vol. 1, Academic Press, New York, 1976.
- [29] P.W. Carr and L.D. Bowers, *Immobilized Enzymes in Analytical and Clinical Chemistry*, John Wiley & Sons, New York, 1980.
- [30] L. Stryer, *Biochemistry*, W.H. Freeman and Co., San Francisco, Ch. 7, pp. 167, 1975.
- [31] L.C. Clark and C. Lyons, "Electrode Systems for Continuous Monitoring in Cardiovascular Surgery", *Ann. New York Acad. Sci.*, Vol. 102, pp. 29-35, 1962.
- [32] S.J. Updike and G.P. Hicks, "The Enzyme Electrode", *Nature*, Vol. 214, pp. 986-988, 1967.
- [33] T. Kondo, K. Ito, K. Ohkura, K. Ito and S. Ikeda, "A Miniature Glucose Sensor, Implantable in the Blood Stream", *Diabetes Care*, Vol. 5, No. 3, pp. 218-221, 1982.
- [34] D.A. Gough, J.K. Leyboldt and J.C. Armour, "Progress Toward a Potentially Implantable, Enzyme-Based Glucose Sensor", *Diabetes Care*, Vol. 5, No. 3, pp. 190-198, 1982.
- [35] Y. Miyahara, F. Matsu, T. Moriizumi, H. Matsuoka, I. Karube and S. Suzuki, "Micro Enzyme Sensors Using Semiconductor and Enzyme Immobilization Techniques", Proceedings of the International Meeting on Chemical Sensors, Fukuoka, Japan,

- Sept. 19-22, 1983, Analytical Chemistry Symposia Series, Vol. 17, pp. 501-506, Elsevier, Amsterdam, 1983.
- [36] S. Ikeda, K. Ito, T. Kondo, K. Ichikawa, T. Yukawa and H. Ichihashi, "Prolongation of Life-Time of Enzyme Electrode Type Glucose Sensor for Artificial Pancreas", Proceedings of the International Meeting on Chemical Sensors, Fukuoka, Japan, Sept. 19-22, 1983, Analytical Chemistry Symposia Series, Vol. 17, pp. 620-625, Elsevier, Amsterdam, 1983.
- [37] S-O. Enfors, "Oxygen Stabilized Electrode for D-Glucose Analysis in Fermentation Broths", *Enz. Microb. Technol.*, Vol. 3, pp. 29-32, 1981.
- [38] N. Cleland and S-O. Enfors, "Control of Glucose-Fed Batch Cultivations of *E. coli* by Means of an Oxygen Stabilized Enzyme Electrode", *European J. Appl. Microbiol. Biotechnol.*, Vol. 18, pp. 141-147, 1983.
- [39] G.G. Guilbault and G.J. Lubrano, "Enzyme Electrode for Glucose", *Analytica Chimica Acta*, Vol. 60, pp. 254-255, 1972.
- [40] G.G. Guilbault and G.J. Lubrano, "An Enzyme Electrode for the Amperometric Determination of Glucose", *Analytica Chimica Acta*, Vol. 64, pp. 439-455, 1973.
- [41] L.C. Clark, Jr. and C.A. Duggan, "Implanted Electroenzymatic Glucose Sensors", *Diabetes Care*, Vol. 5, No. 3, pp. 174-180, 1982.
- [42] T. Yao, "A Chemically Modified Enzyme Membrane Electrode as an Amperometric Glucose Sensor", *Analytica Chimica Acta*, Vol. 148, pp. 27-33, 1983.
- [43] G. Nagy, L.H. Von Storp and G.G. Guilbault, "Enzyme Electrode for Glucose Based on an Iodide Membrane Sensor", *Analytica Chimica Acta*, Vol. 66, pp. 443-455, 1973.
- [44] M.A. Greshaw, and J.E. Jones, "Whole Blood Glucose Enzyme Electrode", *J. Electrochem. Soc.* Vol. 136, pp. 414-417, 1989.

- [45] D.L. Williams, A.R. Doig, Jr. and A. Karosi, "Electrochemical-Enzymatic Analysis of Blood Glucose and Lactate, *Analytical Chemistry*, Vol. 42, No. 1, pp. 118-121, 1970
- [46] A.E.G. Cass, G. Davis, G.D. Francis, H.A.O. Hill, W.J. Aston, I.J. Higgins, E.V. Potkin, L.D.L. Scott and A.P.F. Turner, "Ferrocene-Mediated Enzyme Electrode for Amperometric Determination of Glucose", *Analytical Chemistry*, Vol. 56, No. 4, pp. 667-671, 1984.
- [47] A.P.F. Turner, "Applications of Direct Electron Transfer Bioelectrochemistry in Sensors and Fuel Cells", *Biotech '83*, Proceedings of the first International Conference on the Commercial Applications and Implications of Biotechnology, London, England, pp. 643-654, 1983.
- [48] R.M. Ianniello, T.J. Lindsay and A.M. Yacynych, "Differential Pulse Voltammetric Study of Direct Electron Transfer in Glucose Oxidase Chemically Modified Graphite Electrodes", *Analytical Chemistry*, Vol. 54, No. 7, pp. 1098-1101, 1982.
- [49] J.J. Kulys, V-S.A. Laurinavičius, M.V. Pesliakiene and V.V. Gurevičiene, "The Determination of Glucose, Hypoxanthine and Uric Acid with the Use of Bi-Enzyme Amperometric Electrodes", *Analytica Chimica Acta*, Vol. 148, pp. 13-18, 1983.
- [50] S.D. Caras, J. Janata, D. Saupe and K. Schmitt, "pH-Based Enzyme Potentiometric Sensors", Part I, *Anal. Chem.*, Vol. 57, pp. 1917-1920, 1985. See also: Part II, *Ibid.*, pp. 1920-1923; and Part III, *Ibid.*, pp. 1924-1925.
- [51] B. Danielsson, F. Winquist and K. Mosbach, "Enzyme Transistors", *Biotech '83*, Proceedings of the first International Conference on the Commercial Applications and Implications of Biotechnology, London, England, pp. 679-688, 1983.

- [52] J. Janata, "Chemically Sensitive Field Effect Transistor as a Potentially Implantable Glucose Sensor", *Diabetes Care*, Vol. 5, No. 3, p. 271, 1982.
- [53] T. Moriizumi and Y. Miyahara, "Monolithic Multi-Function ENFET Biosensors", *Transducers '85*, International Conference on Solid State Sensors and Actuators, Philadelphia, Pennsylvania, June 10-14, 1985, Digest of Technical Papers, pp. 148-151, 1985.
- [54] L.B. Wingard, Jr., C.C. Liu, S.K. Wolfson, Jr., S.J. Yao and A.L. Drash, "Potentiometric Measurement of Glucose Concentration with an Immobilized Glucose Oxidase/Catalase Electrode", *Diabetes Care*, Vol. 5, No. 3, pp. 199-202, 1982.
- [55] L. Gorton and K.M. Bhatti, "Potentiometric Determination of Glucose by Enzymatic Oxidation in a Flow System", *Analytica Chimica Acta*, Vol. 105, pp. 43-52, 1979.
- [56] D.A. Gough and L. Leyboldt, *Applied Biochemistry and Bioengineering*, pp. 175-207, Academic Press, New York, 1981.
- [57] S.J. Updike, M. Shults and B. Ekman, "Implanting the Glucose Enzyme Electrode: Problems, Progress and Alternative Solutions", *Diabetes Care*, Vol. 5, No. 3, pp. 207-212, 1982.
- [58] L.B. Wingard, Jr., "Immobilized Enzyme Electrodes for Glucose Determination for the Artificial Pancreas", *Federation Proceedings*, Vol. 42, pp. 288-291, 1983.
- [59] D.R. Thévenot, R. Sternberg and P.R. Coulet, "A Glucose Electrode Using High-Stability Glucose Oxidase-Collagen Membranes", *Diabetes Care*, Vol. 5, No. 3, pp. 203-206, 1982.
- [60] G.G. Guilbault, "Enzymatic Glucose Electrodes", *Diabetes Care*, Vol. 5, No. 3, pp. 181-183, 1982.
- [61] P.R. Coulet and D.C. Gautheron, "Resistance to Deactivation of Enzyme-Collagen Membranes", *Biochimie*, Vol. 62, pp. 543-547, 1980.

- [62] D.R. Thévenot, "Problems in Adapting a Glucose-Oxidase Electrochemical Sensor Into an Implantable Glucose-Sensing Device", *Diabetes Care*, Vol. 5, No. 3, pp. 184-189, 1982.
- [63] K. Mosbach, Ed., *Immobilized Enzymes and Cells*, included in the series *Methods in Enzymology*, Colowick and Kaplan, Eds., Vol. 135, Part B, Academic Press, London, 1987.
- [64] K. Mosbach, Ed., *Immobilized Enzymes and Cells, Ibid.*, Vol. 137, Part D, Academic Press, London, 1988.
- [65] G.J. Richter, G. Luft and U. Gebhardt, "Development and Present Status of an Electrocatalytic Glucose Sensor", *Diabetes Care*, Vol. 5, No. 3, pp. 224-228, 1982.
- [66] H. Lerner, J. Giner, J.S. Soeldner and C.K. Colton, "An Implantable Electrochemical Glucose Sensor", *Annals New York Academy of Sciences*, Vol. 428, pp. 263-278, 1984.
- [67] H. Lerner, J.S. Soeldner, C.K. Colton and J. Giner, "Measurement of Glucose Concentration in the Presence of Coreactants with a Platinum Electrode", *Diabetes Care*, Vol. 5, No. 3, pp. 229-237, 1982.
- [68] J.J. Lewandowski, E. Szczepańska-Sadowska, J. Krzymień and M. Nałecz, "Amperometric Glucose Sensor: Short-Term, *In Vivo* Test", *Diabetes Care*, Vol. 5, No. 3, pp. 238-244, 1982.
- [69] L.B. Wingard, Jr., "Possibility for an Immobilized Flavin Fuel Cell Electrode for Glucose Measurements", *Diabetes Care*, Vol. 5, No. 3, pp. 222-223, 1982.
- [70] J.S. Schultz, S. Mansouri and I.J. Goldstein, "Affinity Sensor: A New Technique for Developing Implantable Sensors for Glucose and Other Metabolites", *Diabetes Care*, Vol. 5, No. 3, pp. 245-253, 1982.
- [71] B. Rabinovitch, W.F. March and R.L. Adams, "Noninvasive Glucose Monitoring of the Aqueous Humor of the Eye: Part I. Measurement

of Very Small Optical Rotations", *Diabetes Care*, Vol. 5, No. 3, pp. 254-258, 1982.

- [72] R. Bently, "Glucose Oxidase" in *The Enzymes*, Second Edition, P.D. Boyer, H. Lardy and K. Myrbäck, Eds., Vol. 7, Part A, Chapter 24, pp. 567-586, Academic Press, New York, 1963. See also: Third Edition, P.D. Boyer, Ed., Vols. 1-3, 1970.
- [73] M. Dixon and E.C. Webb, *Enzymes*, Academic Press, New York, 1964.
- [74] A.J. Bard and L.R. Faulkner, *Electrochemical Methods: Fundamentals and Applications*, John Wiley & Sons, New York, 1980.
- [75] K.M. Plowman, *Enzyme Kinetics*, McGraw-Hill, New York, 1972.
- [76] M.K. Weibel and H.J. Bright, "The Glucose Oxidase Mechanism: Interpretation of the pH Dependence", *J. Biological Chemistry*, Vol. 246, No. 9, pp. 2734-2744, 1971.

CHAPTER 2

A CMOS Potentiostat for Amperometric Chemical Sensors[†]

A simple CMOS integrated potentiostatic electrode control circuit is described. The circuit maintains a constant bias potential between the reference and indicating electrodes of an electrochemical measurement cell. Chemical concentration signals are converted amperometrically to an output voltage with a sensitivity (slope) of approximately 60 mV/ μ A. The lower detection limit is less than 2 nA, and redox currents from 0.1 to 3.5 μ A can be measured with a maximum nonlinearity of $\pm 2\%$ over this range. The total power consumption is less than 2 mW with power supply voltages of ± 6 V. This design also provides the capability of performing differential measurements which null the effect of spurious background currents in order to enhance analyte selectivity. Experimental results are reported showing the performance of the circuit as a chemical sensor control system.

2.1 INTRODUCTION

Research in the field of solid state electronics has expanded in recent years to include the development of data acquisition systems which incorporate transducer elements as part of the integrated circuit. A variety of new integrated chemical sensors realized using chemically selective membrane technology have yielded the capability of performing electrochemical analyses in real time, in remote applications, at reasonable cost [1]. Biochemical sensors in particular have received a great deal of attention due to interest in biomedical applications such as glucose determination [2,3]. In general, the advantages of integrating biomedical transducers include miniaturization for the purposes of implantation and the capability of including additional "on-chip" circuitry for *in situ* signal conditioning and control. Also, the application of integrated circuit design strategies permits the optimization of application specific designs.

[†] A version of this chapter has been published as:

R.F.B. Turner, D.J. Harrison and H.P. Baltes, "A CMOS Potentiostat for Amperometric Chemical Sensors", *I.E.E.E. J. Solid-State Circuits*, Vol. SC-22, No. 3, pp. 473-478, June 1987.

Most of the effort thus far in this area has been focused on chemically sensitive semiconductor devices (CSSD's) [1,4], such as the ion-selective field effect transistor (ISFET) which operates in a potentiometric mode [5]. That is, the input signal is an open-circuit electrochemical potential that arises directly from concentration changes of the analyte species, or a derivative of the analyte, in the test solution. Potentiometric systems can be subject to difficulties arising from liquid junction potentials, electrochemical noise due to high electrode impedances [6], and sensitivity to buffer capacity [7] and interfering species in the test solution. Furthermore, the best sensitivity obtainable in a potentiometric mode is 59 mV/decade concentration change (logarithmic response), which also limits the precision [6] of the technique.

The response of a number of membrane/electrode systems, for example those using immobilized enzymes, can be determined either potentiometrically, or amperometrically where a current is allowed to flow in the cell. The current arises from the oxidation or reduction of the analyte (or a derivative thereof) at an inert electrode and the signal is linear, rather than logarithmic, with concentration. For a number of systems, many of the aforementioned difficulties cited for potentiometric systems can be avoided by operating in an amperometric mode. The present paper describes a simple CMOS integrated circuit that facilitates this type of electrochemical measurement.

An amperometric assay of a particular analyte consists essentially of monitoring electrode current in order to obtain a quantitative measurement of the rate of electrolysis of the analyte in the test solution. If a sufficiently large potential difference is applied between the anode and cathode of an electrolytic cell, and a steady state flux of analyte has been attained, then a mass transport limited current will flow in the external circuit. Assuming a linear (*i.e.* Nernst) diffusion layer of fixed thickness δ , the current is given by

$$I_k = -zFAD_{Ox}C_{Ox}/\delta \quad (2.1)$$

for cathodic processes, and

$$I_a = zFAD_{red}C_{red}/\delta \quad (2.2)$$

for anodic processes [8]. Here z is the number of moles of electrons transferred per mole of reactant, F is the Faraday constant (96,487 C/mole); A is the electrode area (m^2); D_{ox} , D_{red} are the diffusion coefficients for the oxidized and reduced species respectively (m^2/s); and C_{ox} , C_{red} are the bulk concentrations of the oxidized and reduced species respectively (moles/ m^3), in the test solution. The magnitude of the applied potential difference depends on the theoretical half-cell potential for the particular redox process under study, and on the type of reference electrode used. If the test solution contains additional electroactive species that are capable of undergoing oxidation/reduction at the same applied potential as the analyte, then a suitable chemically selective membrane must be employed in order to isolate the species of interest.

Commercial instruments such as the Princeton Applied Research Model 273 analytical potentiostat or the Yellow Springs Instruments Model 53 Oxygen Monitor have provided standard means of performing amperometric assays in the laboratory. Our approach has therefore been to design an integrated circuit which emulates certain essential functions of a laboratory potentiostat, tailored for a specific assay determined by the design of the chemically selective electrodes. The advantage of this circuit over previous designs [9] lies in its ability to accurately sense very small currents (less than a few microamperes) with a minimal number of devices, low power consumption, and without introducing excessive noise. This design also utilizes a two-electrode measurement technique, rather than the conventional three-electrode technique, which further simplifies the implementation of the transducer elements by reducing the number of electrodes (in addition to the reference) required for differential measurements from three to two.

2.2 CIRCUIT DESCRIPTION

2.2.1 Principles of Operation

The function of the potentiostatic control circuit is to provide the required constant bias potential between anode and cathode, and to make a

nonperturbing measurement of the resulting redox current. A block diagram of the system designed for this purpose is shown in Figure 2.1. The working electrode (WE), or indicating electrode, is presumed to be the site where the current limiting process described by (2.1) or (2.2) occurs. The same current flows through the reference electrode (RE), where a complementary (albeit nonlimiting) process occurs. That is, if an oxidation process occurs at the WE, then a reduction occurs at the RE, and *vice versa*. The WE has been shown as the anode and the RE as the cathode, however this polarity may be reversed depending on the application.

Under conditions where (2.1) or (2.2) is valid and the process at the RE is nonlimiting, the WE behaves essentially as a concentration-dependent current source which determines the drain current of transistor M14. In equilibrium, the operational amplifier (OA) controls the value of V_{gs} of M14. If the concentration (and hence the current) changes, the finite output resistance of M14 is sufficient to initiate a corresponding change in the differential input voltage to the OA which, in turn, moves V_{gs} to a new equilibrium value.

A practical implementation of the network depicted in Figure 2.1 is shown in the schematic of Figure 2.2. The component values employed in the fabrication of the prototype integrated circuit are given in Table 2.1. The current-to-voltage conversion (I/V) is accomplished simply by mirroring the electrode current through a resistance R_o . The cathode has been connected to the ground in the output stage so that V_a can be obtained from the same subcircuitry as was used to establish the bias current of the OA. The circuit of channel 2 is identical to channel 1 and shares the same power supplies and ground. Differential measurements are performed by comparing the outputs of channels 1 and 2.

2.2.2 Operational Amplifier

Since the operational amplifier is not required to source any current, a simple two-stage design was used. The configuration shown has a dc open loop gain of approximately 90 dB, and a unity gain bandwidth of approximately 4 MHz with a differential stage bias current of $3.5 \mu\text{A}$. A right-hand plane zero occurs at approximately 0.5 MHz and hence the

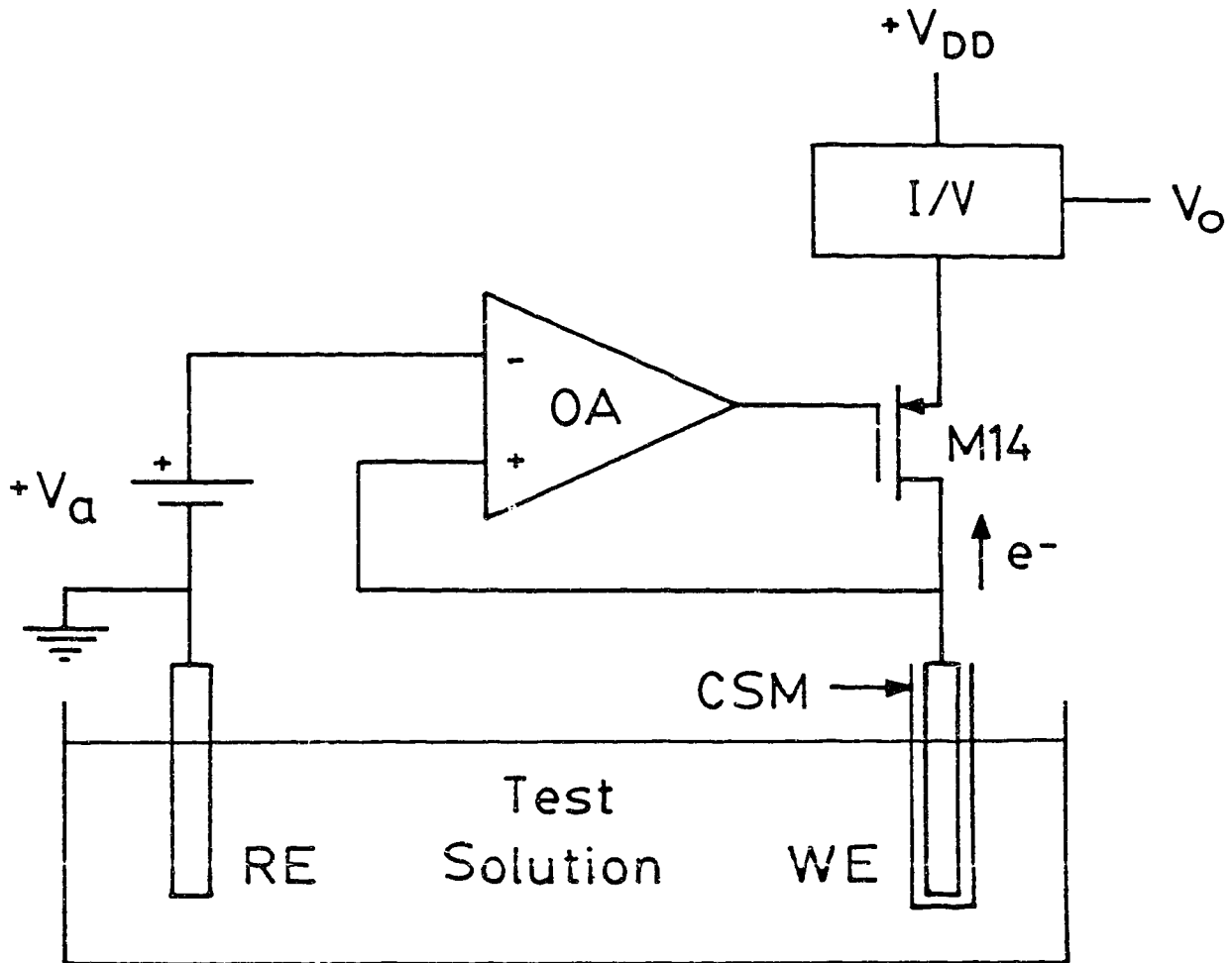


Figure 2.1 Block diagram of amperometric measurement system. V_a is the applied bias voltage between the WE and RE. The WE is shown with a chemically selective membrane (CSM) which determines the specificity of the assay for a particular analyte.

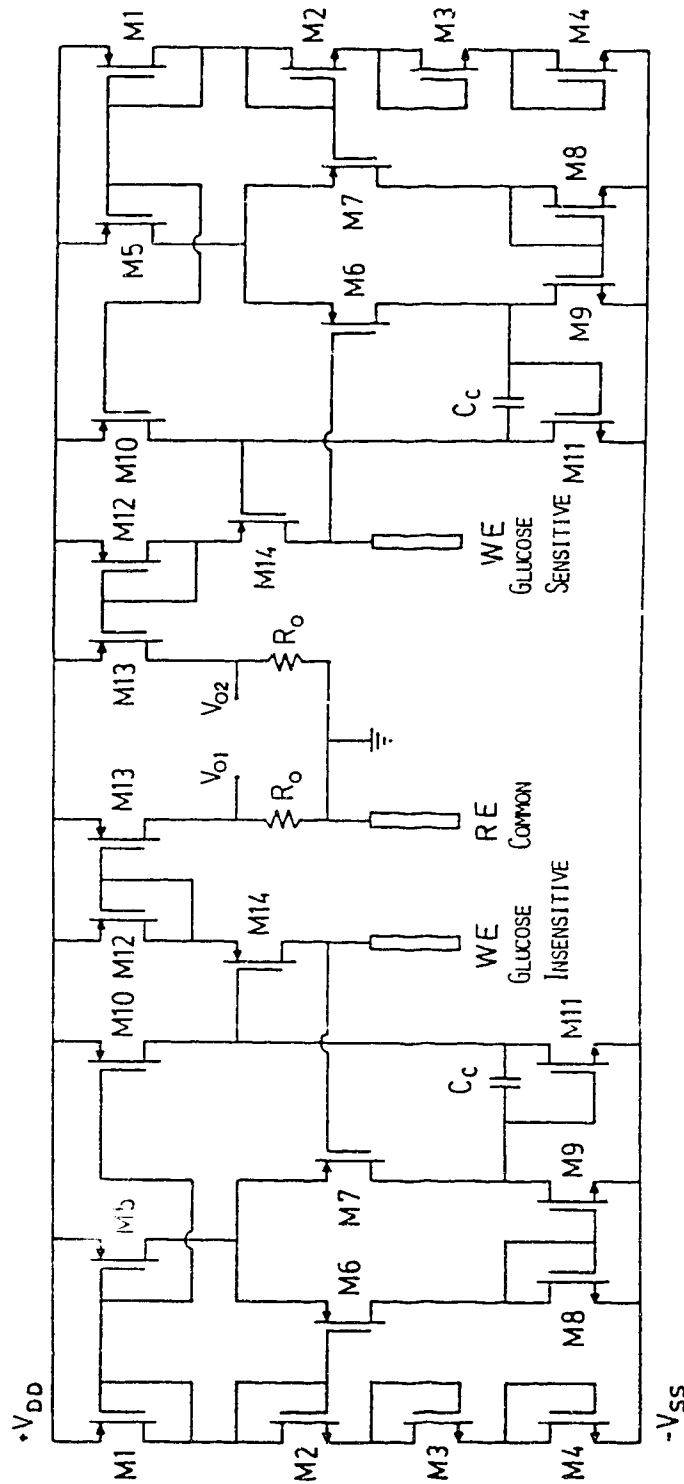


Figure 2.2 Schematic diagram of two-channel CMOS potentiostat. Both channels share a common RE but each has a unique WE in order to facilitate differential measurements.

TABLE 2.1 Component Values employed in realization of prototype potentiostat circuit. The dimensionless ratios refer to the geometric channel width (μm) vs. channel length (μm) of each transistor.

Component	Value	Component	Value
M1	5/60	M9	35/15
M2	5/15	M10	5/120
M3	5/15	M11	35/15
M4	5/15	M12	5/120
M5	5/60	M13	15/15
M6	230/5	M14	140/5
M7	230/5	C_c	2.6 pF
M8	35/15	R_o	2.5 k Ω

stability of the closed-loop system depends on the position of the low-frequency pole contributed by the output stage which, in turn, depends on the impedance characteristics of the electrodes.

2.2.3 Output Stage

The characteristics of the output stage determine the sensitivity of the output voltage with respect to the concentration-dependent current from the WE. In the present configuration, the current through the output resistor R_o is M times the WE current I_a due to electrons (e^- in Figure 2.1) liberated by the electrochemical process occurring at the WE. This results in an output voltage of MI_aR_o and gives a sensitivity of

$$\frac{\partial V_o}{\partial I_a} = MR_o + R_o I_a \frac{\partial M}{\partial I_a} \quad (2.3)$$

assuming the WE is the anode. For small currents (but not small enough that M14 enters the triode region), the second term is negligible and V_o is approximately linear with I_a as long as M14 remains in the saturation region. For power supply voltages of ± 5 V, the linear range of operation is approximately 0.1 – $2 \mu\text{A}$, over which the output sensitivity is approximately $60 \text{ mV}/\mu\text{A}$. The upper end of this range can be extended to approximately $3.5 \mu\text{A}$ with a power supply of ± 6 V.

Substituting (2.2) for the WE current I_a , the sensitivity with respect to changes in the concentration of the analyte C_a is

$$\frac{\partial V_o}{\partial C_a} = MR_o z F A D_a / \delta \quad (2.4)$$

over the linear range of operation. Note that the parameters A , D_a and δ depend on the design of the transducing membrane/electrode, which is therefore an integral part of the design.

Full integration of the transducing electrodes, including the reference, with the controlling circuitry cannot be accomplished with a standard CMOS process since the usual aluminum metallization layer does not provide an electrochemically active electrode surface. Some

additional processing is therefore required in order to make use of this or any integrated circuit as an amperometric chemical sensor. However, the inherent noise immunity of the amperometric technique allows this circuit to be used to control externally connected electrodes. In some applications (for example, *in vivo* biochemical assays) this approach can be advantageous in that the electronic part of the sensor can be hermetically sealed against the chemically harsh environment in which the electrodes must function, thus alleviating many of the packaging problems associated with ISFET devices [2,7]. All experimental results reported here were obtained using externally connected electrodes.

2.3 EXPERIMENTAL RESULTS

2.3.1 Electrical Performance

The circuit of Figure 2.2 was fabricated using a standard polysilicon-gate CMOS process (Northern Telecom CMOS-1B). The minimum feature size is 5 μm and the total die area occupied by both channels of the sensor circuit, excluding bonding pads, is 0.53 mm^2 . A photomicrograph of the implemented circuit is shown in Figure 2.3. Additional implementation data are provided in the Appendix.

The output voltage linearity and control system performance were tested using an HP 4145A Semiconductor Parameter Analyzer. For the purpose of electronic testing, the actual WE was simulated by a swept current source which varied the magnitude of the input current from 0 to 3 μA . The output voltage response characteristics of channels 1 and 2 are superimposed on Figure 2.4, and the corresponding WE electrode bias voltages are superimposed on Figure 2.5. These results are in reasonable agreement with digital simulations of the same circuit using a version of the commercially available SPICE simulation program.

The mask layouts used for each channel were identical, as were the measurement conditions; the differences in characteristics between the two channels are thus attributed to process variations across the die. The difference in the slopes of the output voltages of the two channels has the most detrimental effect on the results of differential measurements. The

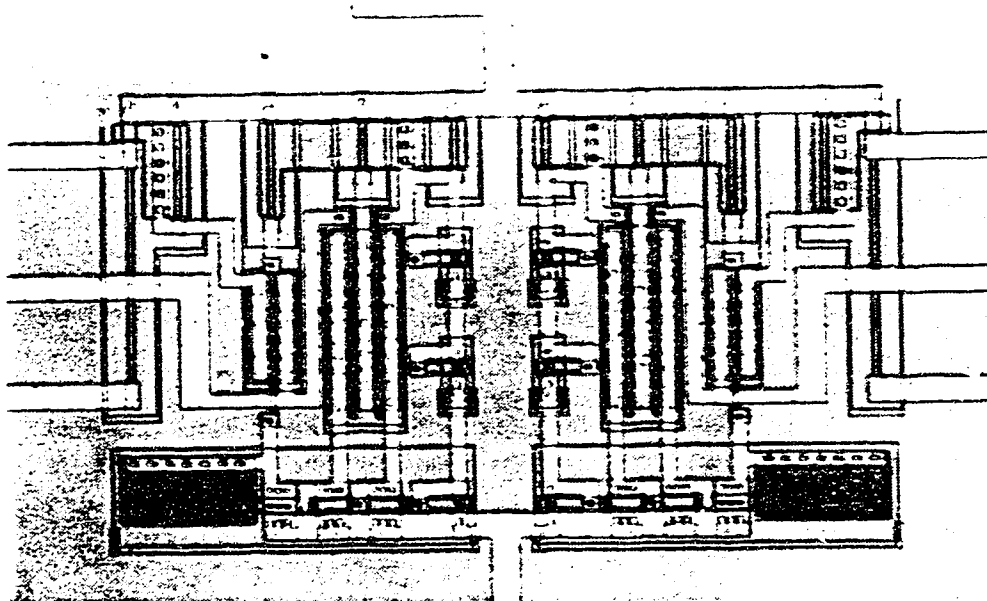


Figure 2.3 Photomicrograph of prototype potentiostat circuit. The bonding pads (not shown) are connected via the eight broad metal lines leading away from the circuit; these lines are 25 μm wide.

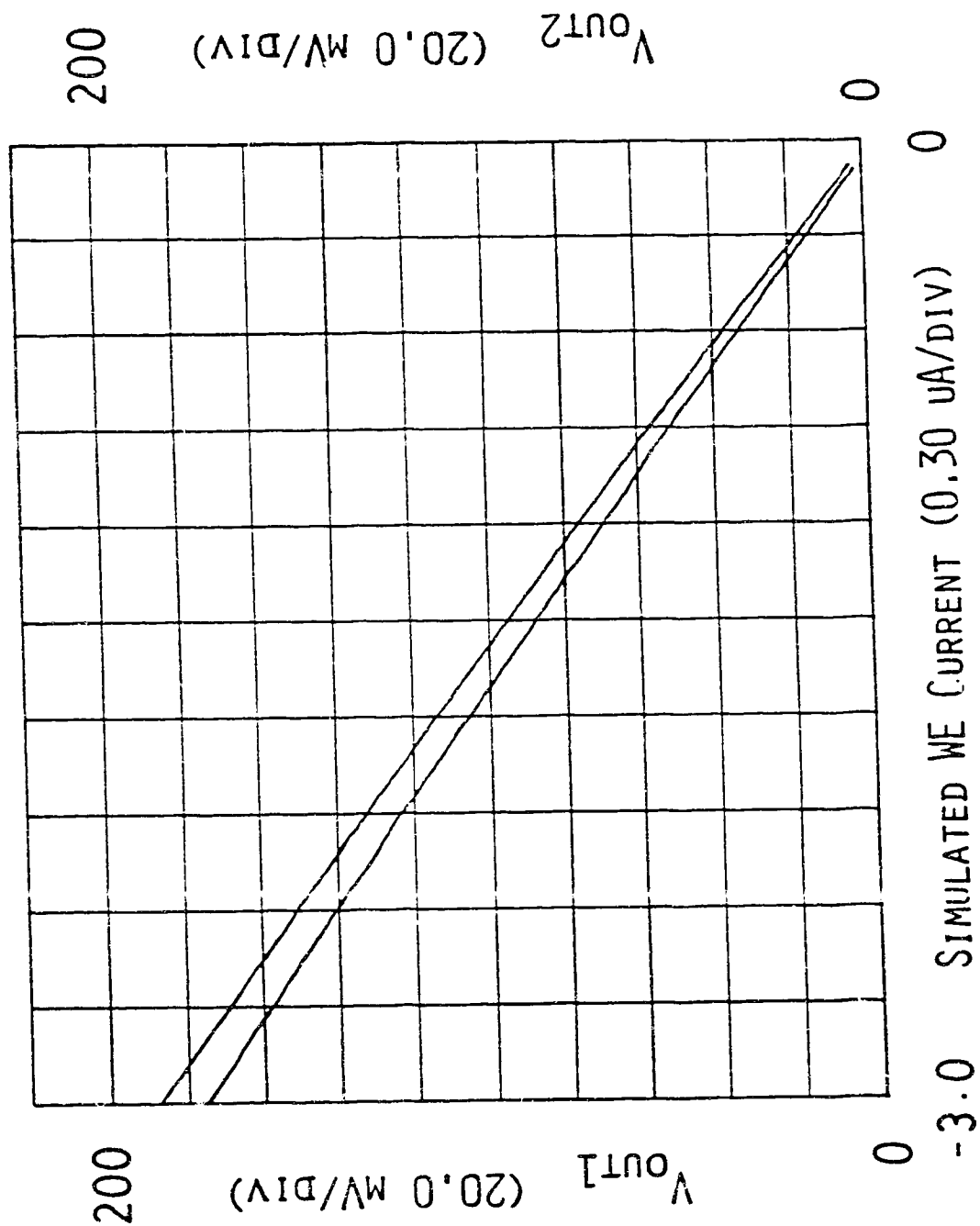


Figure 2.4 Measured output voltage as a function of simulated WE current. The upper curve pertains to channel 1 and the lower curve pertains to channel 2.

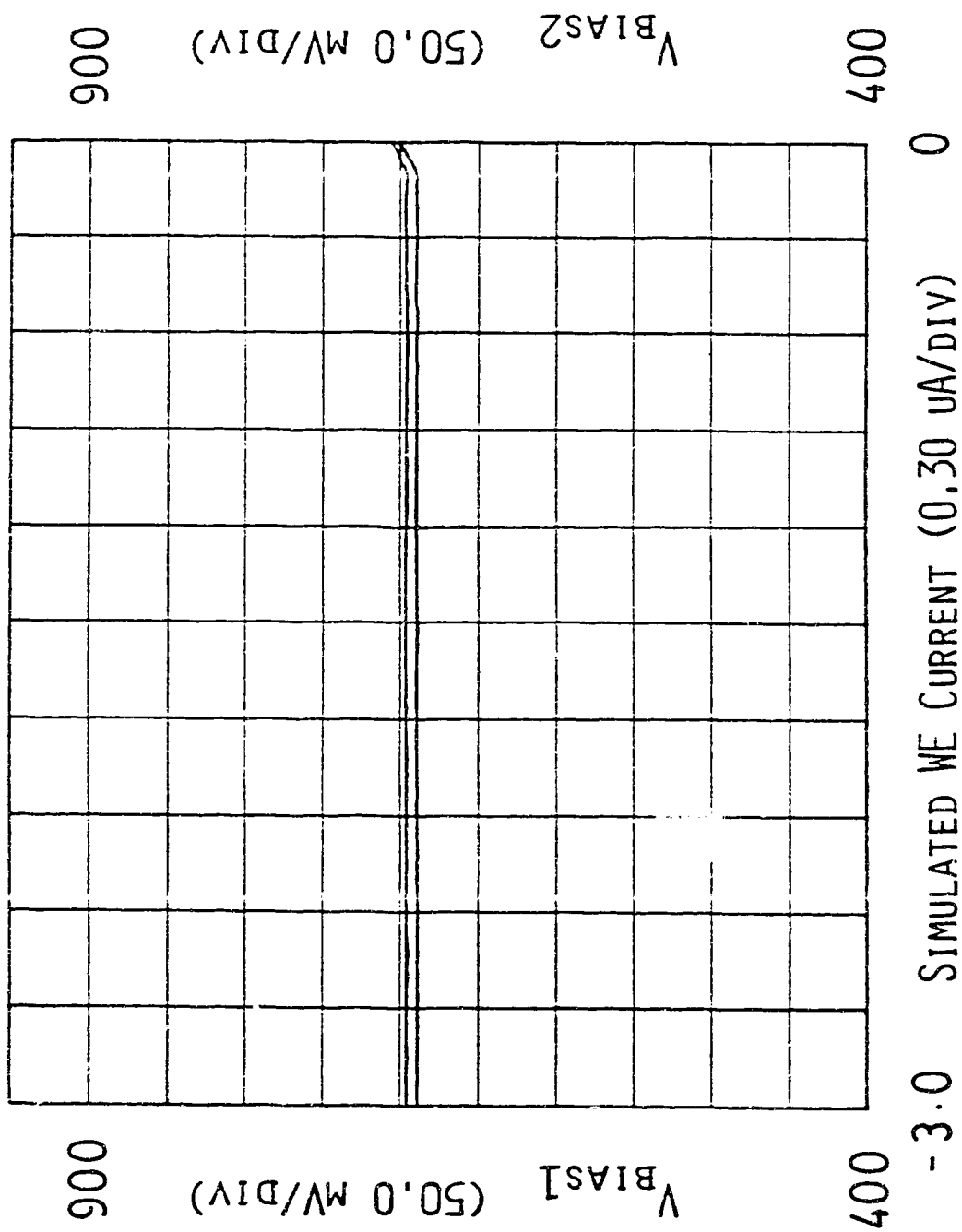


Figure 2.5 Dependence of applied bias voltage on simulated WE current. The upper curve pertains to channel 1 and the lower curve pertains to channel 2.

main component of this difference is likely due to slight variations in the values of R_c for each channel, which were implemented as p^+ diffusion resistors. The difference in the WE bias voltages is less than 10 mV, which is negligible in most applications. The output voltages of both channels are linear to within $\pm 2\%$ and the WE bias voltages are maintained constant to within 1% over the range of electrode currents from 0.1 to 3.5 μA . Note that the WE bias voltage reference levels were taken from the internal OA bias network and could be adjusted over a substantial range (approximately $\pm 0.5\text{ V}$) by adjusting the power supply voltages without degrading the linearity or control function.

In CMOS technology, it is common practice to use a resistor in series with the compensation capacitor C_c in order to eliminate the right half plane zero. Omission of this resistor in this prototype design did not lead to oscillation problems because the feedback magnitude is relatively small. However, a series resistor was included in a later redesigned version of the circuit.

2.3.2 Electrochemical Performance

In order to evaluate the performance of the circuit as an amperometric sensor, an external (planar) platinum working electrode was connected to the drain of M14, and an external Ag/AgCl reference electrode was connected to the common circuit ground. The bias potential between WE and RE was adjusted to +0.7 V and the steady state output voltage was recorded (allowing approximately 1 min. for the transient response to decay) as aliquots of $\text{K}_4\text{Fe}(\text{CN})_6$ in 0.1 M KCl were added to a quiescent 0.1 M KCl solution. The results for one channel are plotted in Figure 2.6; similar results were obtained for both channels. The scatter present in the data of Figure 2.6 is due to variations in the mass transport of $\text{Fe}(\text{CN})_6^{4-}$ ions to the electrode surface caused by convection currents [8] in the test solution. Data from a laboratory analytical potentiostat exhibit the same degree of scatter under the same experimental conditions. The concentration axis offset in Figure 2.6 is apparently an artifact from the chip fabrication process; other chips from the same run do not exhibit such an offset.

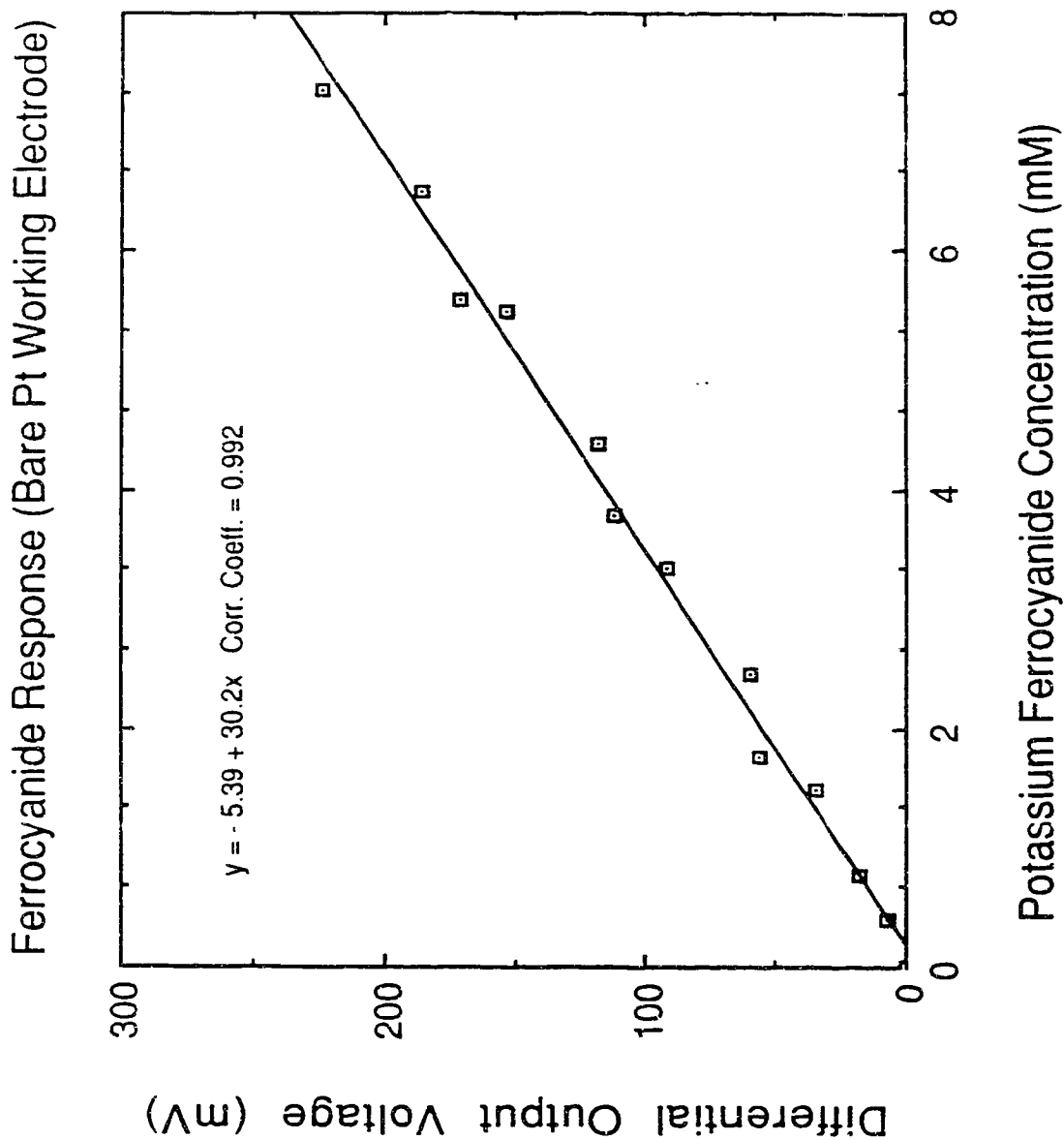


Figure 2.6 Output voltage as a function of ferrocyanide concentration in unstirred test solution. Data were obtained using a bare platinum WE (1.65 mm diameter) attached to channel 1.

The electrochemical transient response was also investigated. As noted previously, equations (2.1) and (2.2) describe the steady state mass transport limited current. Current during the transient period prior to the establishment of a constant thickness Nernst diffusion layer is described by the Cottrell equation [8], *viz.*

$$i_a(t) = zFAC_aD^{1/2}\pi^{-1/2}t^{-1/2} \quad (2.5)$$

which applies to linear diffusion to a horizontal planar electrode. The WE and RE were disconnected from the circuit and placed in a quiescent solution of $K_4Fe(CN)_6$ (in 0.1 M KCl). At $t=0$, the electrodes were switched into the circuit, driving the WE to +0.7 V vs. Ag/AgCl, corresponding to a thermodynamic potential at which $Fe(CN)_6^{4-}$ is oxidized under mass transport control. This essentially simulates a step increase in the $Fe(CN)_6^{4-}$ concentration at the electrode surface. The output voltage was recorded for 1 s from $t=0$ and several points were taken from the current response trace and plotted against $t^{-1/2}$ as shown in Figure 2.7. The slope of the data in Figure 2.7 was used to compute the concentration of ferrocyanide in the test solution, which agreed to within 5% of the known concentration. This result demonstrates that the response time of the circuit is sufficiently low to be able to follow abrupt changes in the analyte concentration (provided, of course, that the electrodes used also respond rapidly).

In order to evaluate the differential measurement capability of the sensor in a biochemical assay, a pair of working electrodes was prepared; one WE was sensitive to glucose (connected to channel 1), and the other WE was insensitive to glucose (connected to channel 2). The glucose sensitive membrane was cast directly over a platinum electrode surface and had an approximate composition (by weight) of 20% glucose oxidase, 75% bovine serum albumin and 5% glutaraldehyde [10]. The non-glucose sensitive membrane composition was 95% albumin and 5% glutaraldehyde and hence could not oxidize glucose, yet presented a similar matrix for diffusion of electrochemically active species in the vicinity of the electrode surface. The enzyme glucose oxidase reacts only with β -D-glucose and, in the presence of dissolved oxygen, produces gluconic acid and H_2O_2 [11]. It is

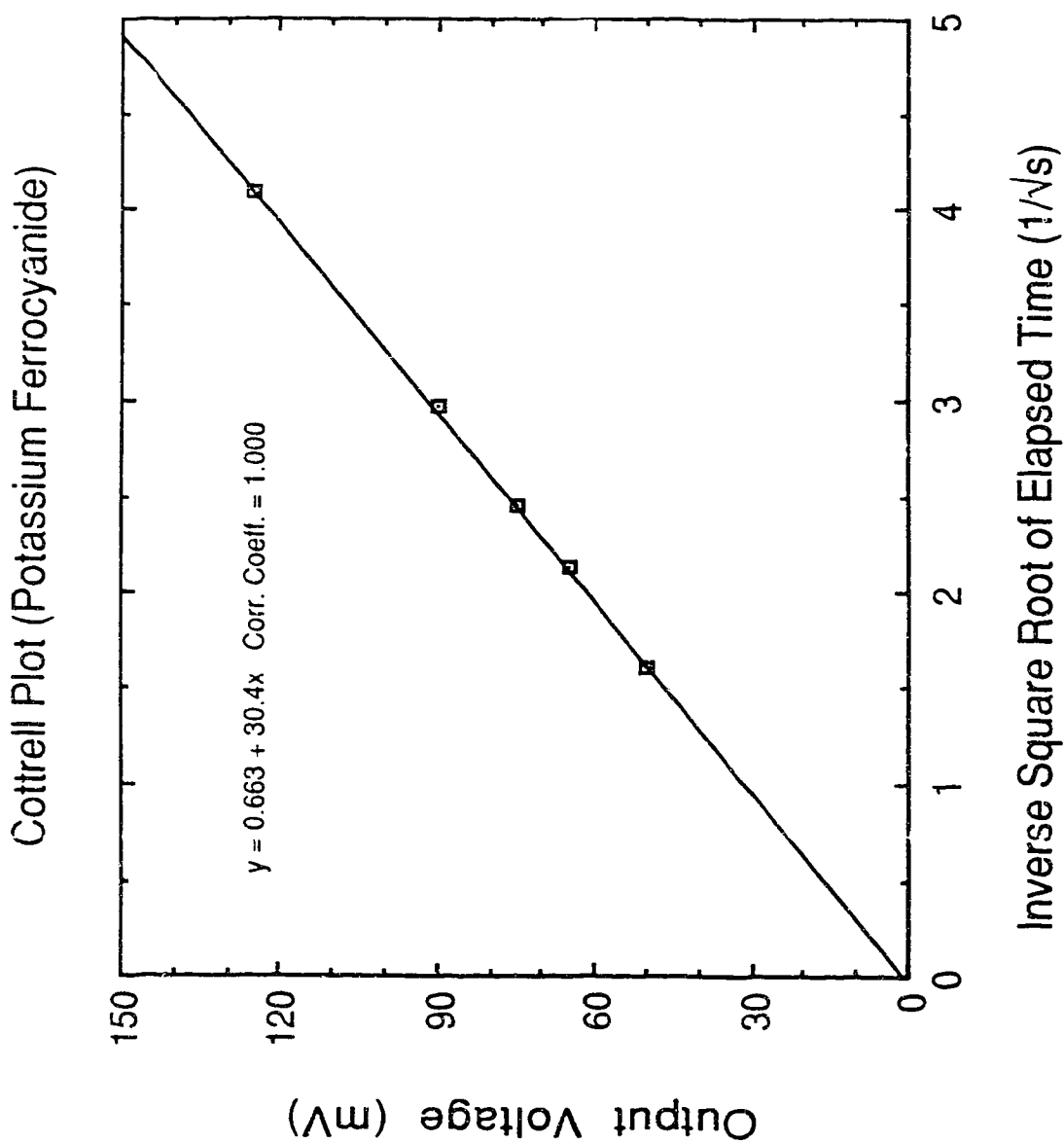


Figure 2.7 Cottrell plot of time dependence of output voltage after the applied voltage is stepped to a potential at which ferrocyanide is oxidized. Data were obtained using a bare (planar disc) platinum WE (2.65 mm diameter) attached to channel 1.

the H_2O_2 derived from this reaction that is the actual analyte that is sensed amperometrically, and the resulting output voltage depends on glucose concentration as shown in Figure 2.8. Note that the nonlinearity of the response to glucose is not a result of any characteristics of the integrated potentiostat circuit, but rather is due to the chemical and mass transport kinetics relating to the enzyme reaction itself [11].

Figure 2.9 shows the effect on the output voltage of each channel when an interfering species is present that will react at both working electrodes. An aliquot of H_2O_2 is introduced (at point 'A') into a solution initially containing only 5 mM glucose in buffered 0.1 M NaCl (pH 7.4) and the solution is subsequently diluted (at point 'B') by adding more buffered 5 mM glucose solution. Note that the difference between the two output voltages (*i.e.* $V_{o1}-V_{o2}$) remains constant throughout the experiment, reflecting the true concentration of glucose even in the presence of a background concentration of H_2O_2 in the bulk test solution. The momentary increase in V_{o1} at point 'B' on the trace is apparently a mass transport effect due to mixing (*i.e.* an electrochemical transient), and is not an artifact due to the integrated circuit.

Figure 2.10 shows the result of a similar differential mode measurement where the interfering species is ascorbic acid, rather than H_2O_2 . In this case, a series of aliquots of ascorbic acid were introduced into a cell that initially contained only 5 mM glucose in buffered 0.1 M NaCl (pH 7.4). Again, note that the differential signal (*i.e.* $V_{o1}-V_{o2}$) remains essentially constant, reflecting the true concentration of glucose even in the presence of a background concentration of ascorbate in the bulk test solution. The differential signal does, however, exhibit a downward drift toward the end of the experiment, which is likely due to ascorbate poisoning of the platinum electrode surface.

2.4 PERFORMANCE OF REVISED VERSIONS

The original prototype potentiostat circuit, as described in the preceding sections, had a sensitivity of approximately 60 mV/ μA and could accurately measure redox currents over the range of 0.1 to 3.5 μA . Two

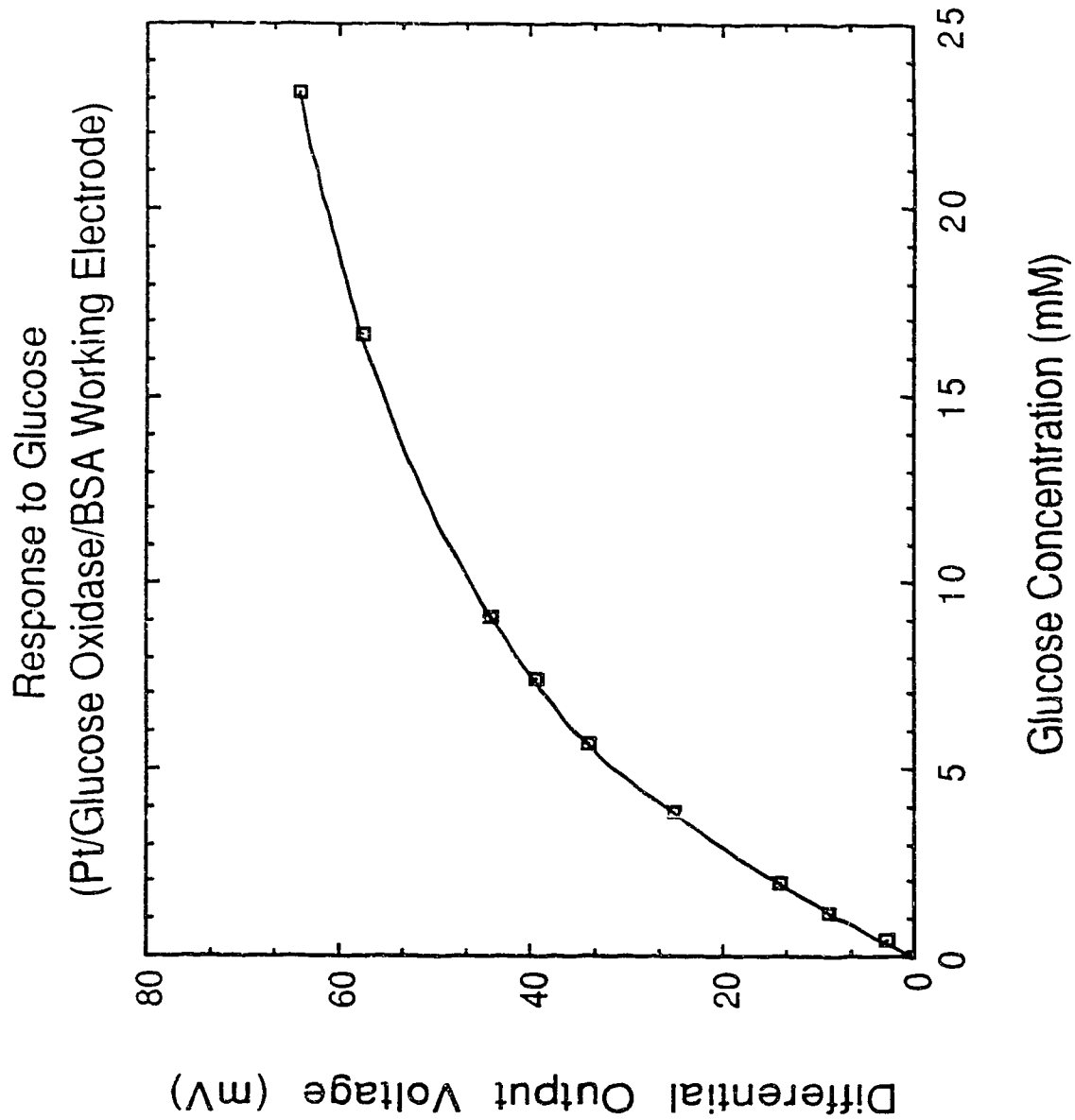


Figure 2.8 Output voltage as a function of glucose concentration. An enzymatic glucose-sensitive membrane was applied to a platinum WE (0.643 mm diameter) attached to channel 1.

HYDROGEN PEROXIDE INTERFERENCE

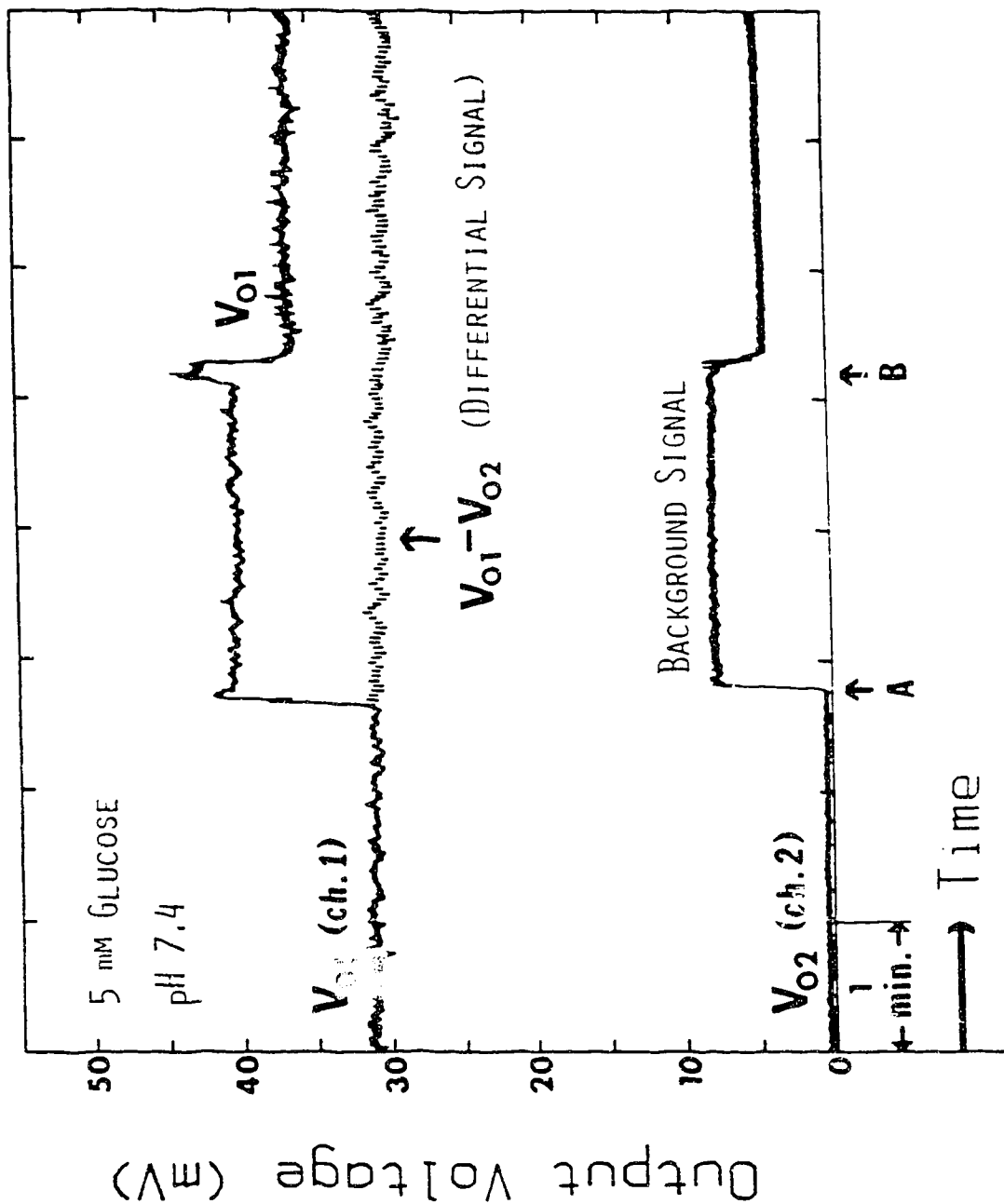


Figure 2.9 Time record of output voltage response to changes in H_2O_2 interferent concentration. Prior to point 'A', the (buffered) test solution contained 5 mM glucose and 0.1 M NaCl only. At point 'A', an aliquot of non-enzymatically produced H_2O_2 was added. At point 'B', the H_2O_2 was diluted by adding more 5 mM glucose (in buffered 0.1 M NaCl).

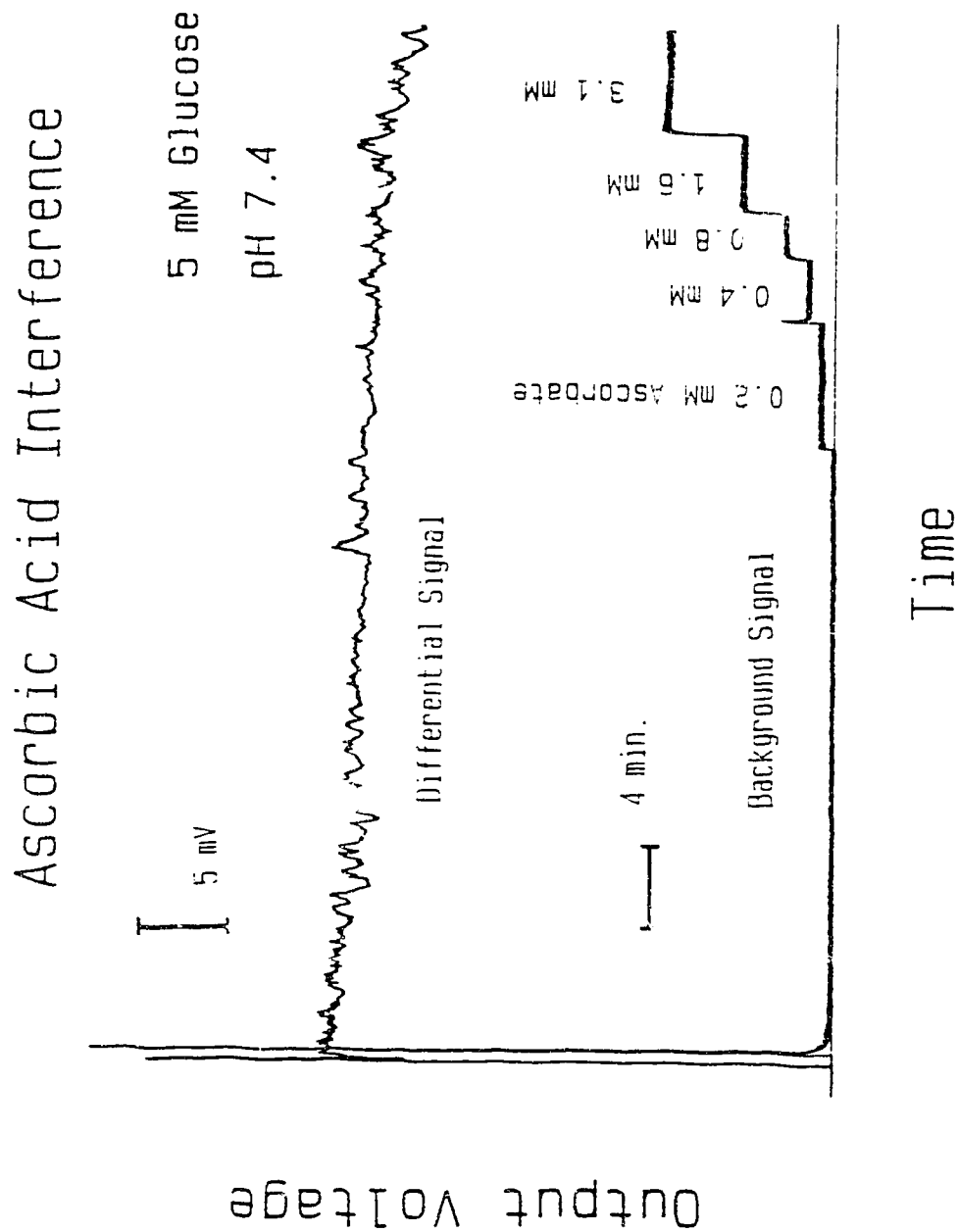


Figure 2.10 Time record of differential output voltage response to changes in ascorbate interferent concentration. Initially, the (buffered) test solution contained 5 mM glucose and 0.1 M NaCl only. Aliquots of ascorbic acid were added, which equally contribute to the WE current measured by both channels of the integrated potentiostat.

improved versions of the original chip have been characterized and employed in some of the work presented in later chapters. The operational amplifier blocks have remained identical to that of the original prototype and the schematic layout of the I/V conversion block also remained the same. The only significant changes were in the size of the output resistors, the implementation of the output resistors in polysilicon rather than p⁺ diffusion, and changes in the geometric width-to-length ratios of transistors M12 and M13.

The first redesigned version of the original prototype circuit included only minor modifications to the output circuit. The (polysilicon) output resistors were increased to 3.2 k Ω (the dimensions of the current mirror transistors were unchanged). The performance of this version of the integrated potentiostat circuit was therefore similar to that of the original prototype, except that the sensitivity has been slightly increased, and differences in the current sensitivities between the two potentiostat channels was virtually eliminated.

The performance of this version coupled to an actual sensing electrode was compared to that of a commercial three-electrode Pine RDE-4 potentiostat. A Pt electrode (0.823 mm²), coated with a thin membrane of Nafion polymer in order to decrease mass transport related noise, was used as the working electrode. A bias voltage of +0.7 V was applied between the WE and a Ag/AgCl wire which served as RE and cathode. The WE and RE were alternately switched between the IC and Pine potentiostats in order to obtain an electrode current measurement using each instrument in the same electrochemical cell, without moving the electrodes. Figure 2.11 shows a comparison of the output of the two systems as the concentration of Fe(CN)₆⁴⁻ is varied (*cf.* Figure 2.6). In this measurement, the cell was also stirred with an air-driven magnetic stirrer. The lower limit of current measurable with this version of the integrated potentiostat is less than 2 nA and the maximum current measurable (with a ± 5 V power supply) is 2 μ A, although this can easily be extended to more than 3 μ A if the power supply voltages are increased somewhat. The sensitivity of the output of the integrated potentiostat for currents of ~ 10 nA to 200 nA is 75 mV/ μ A, and the linearity of the cross correlation of the two instruments is $\pm 0.5\%$ over

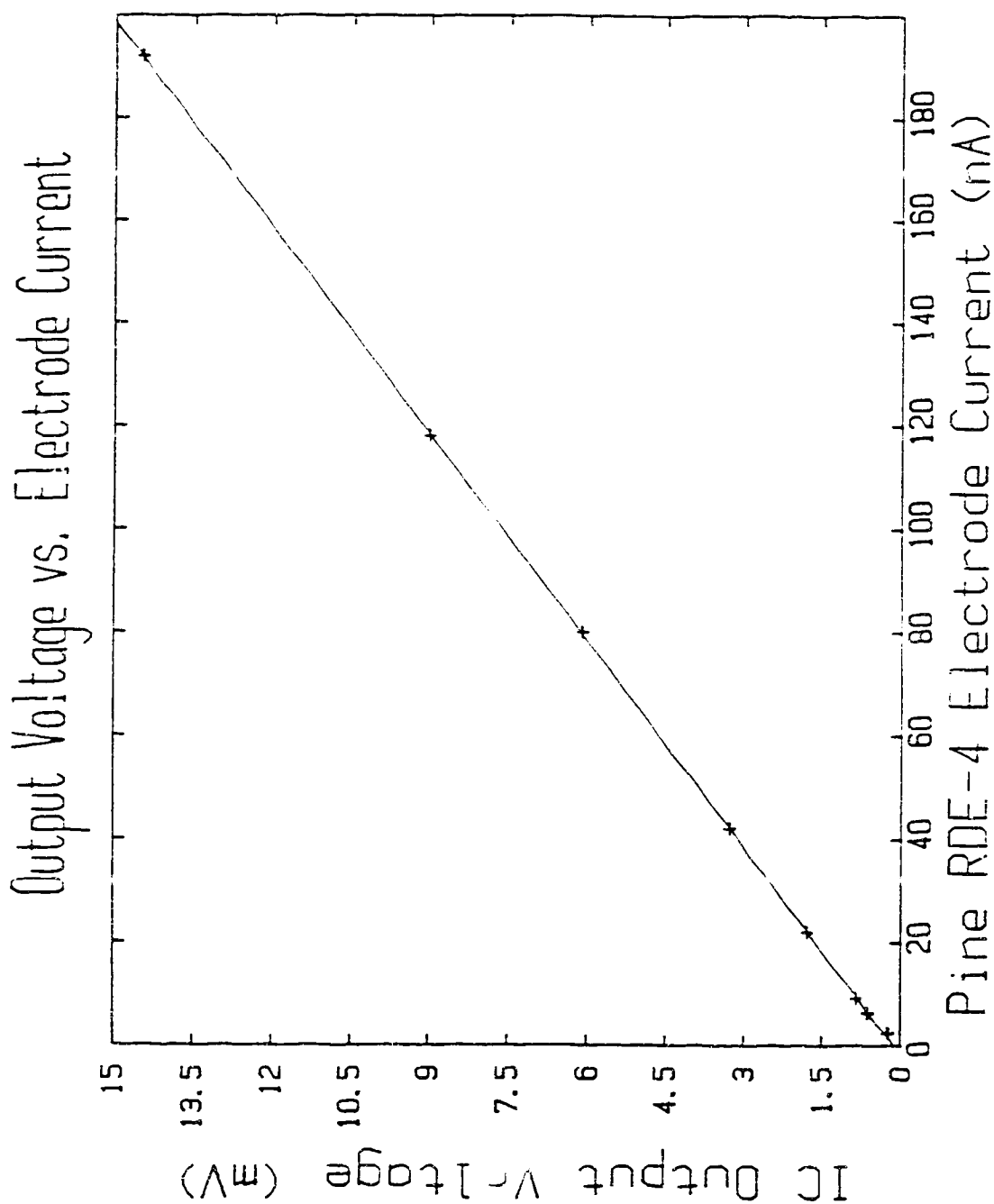


Figure 2.11 Cross correlation between the two-electrode integrated potentiostat circuit and a commercial three-electrode analytical potentiostat (Pine Instrument Company model RDE-4). Data correspond to $\text{Fe}(\text{CN})_6^{4-}$ oxidation currents at a Pt electrode coated with a thin ($< 0.5 \mu\text{m}$ thick) layer of Nafion polymer.

this range. Below approximately 10 nA the sensitivity is increased to 95 mV/ μ A, indicating some non-linearity of the circuit at very low currents. This version of the circuit is, in fact, the one that was employed in the Nafion membrane characterization studies presented in the following Chapter.

The output current mirror of the most recent version of the circuit has been redesigned to yield a considerably higher current sensitivity of 180 mV/ μ A, and a broader dynamic range of 10 nA to 10 μ A. In this version, the output resistors were increased to 5.7 k Ω , and the dimensions (*i.e.* ratios of W/L in μ m) of the current mirror transistors are M12 = 10/10 and M13 = 320/10. Again, the output resistors have been implemented in polysilicon, rather than p⁺ diffusion (in the original prototype), which has virtually eliminated any discrepancy in the slopes of the output voltages of the two independent channels. The difference in WE bias voltages between the two channels is less than 10 mV. The measured electronic performance characteristics of this redesigned version are shown in Figure 2.12 for the range of redox currents measurable with external power supply voltages of approximately ± 8 V (*cf.* Figures 2.4 and 2.5). The performance of this version of the circuit coupled with an implantable version of the glucose-sensitive electrode in whole blood (*in vitro*) is demonstrated in Chapter 5.

In one other recent version, a p⁺ resistor ($\sim 420 \Omega$) was placed in series with the compensation capacitor in order to realize an improvement in the phase margin. This version of the circuit was never actually used with a sensing electrode since process variations in the final CMOS 1B run resulted in poor matching between potentiostat channels. The circuit was stable and performed satisfactorily during tests with an electronic swept current source as before, although no oscillatory behavior was ever observed with other design versions either (*i.e.* those that did not utilize this compensation technique). No actual frequency response data were obtained for this or any other version of the circuit since only low frequencies are important to the present application.

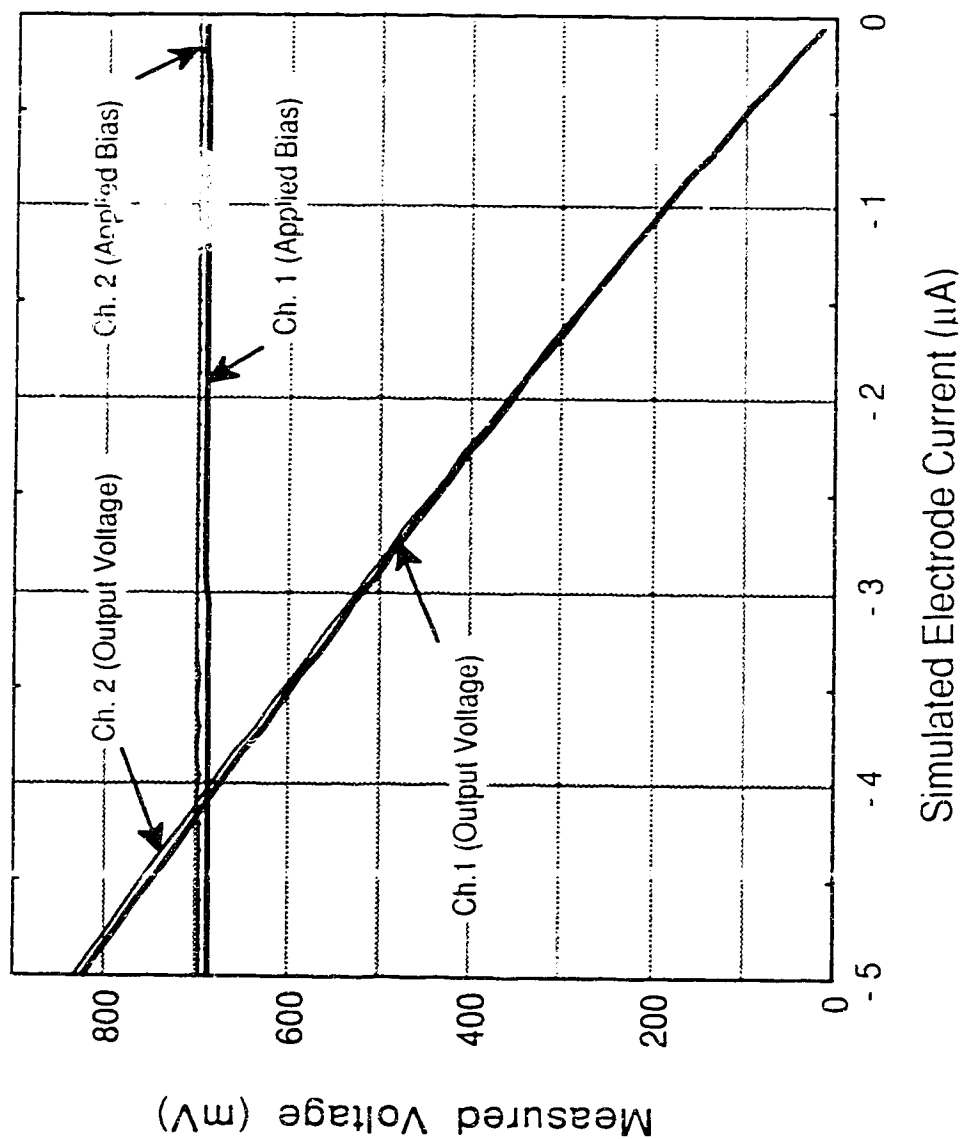


Figure 2.12 Electrical response characteristics of an improved version of the integrated bi-potentiostat circuit. The electrode current is simulated by a swept electronic current source connected to the reference and working electrode inputs.

2.5 CONCLUSIONS

We have presented a new CMOS integrated circuit that can be used to perform amperometric electrochemical assays with an accuracy comparable to those performed by a laboratory potentiostat. The circuit is specifically designed to measure small currents in order to facilitate its use with microelectrodes, which may or may not be integrated with the actual signal processing and control circuitry. Our experimental results demonstrate the utility of this circuit as a chemical sensor control system. Importantly, the circuit may be operated in a differential mode in order to null the effect of spurious interfering species not excluded either by the choice of the working electrode bias voltage, or the chemical selectivity of the membrane/electrode system employed. With minor modifications to the bias network, any electrochemically significant working electrode bias voltage can, in fact, be realized with this same basic design. And, the approach of taking the WE bias voltage reference levels from the internal OA bias network, lends itself to adaptation for programmable operation simply by controlling the power supply levels.

Several improvements to the original circuit have been incorporated into revised versions that further enhance the performance. For example, the output resistors have been implemented in polysilicon, rather than p^+ diffusion, which has virtually eliminated the differences in current sensitivity between the two channels. Modifications have also been made to the I/V conversion block in order to increase the sensitivity and expand the operating range. Unless otherwise noted, one of these improved versions was employed in all of the work presented in subsequent chapters involving the integrated potentiostat.

There exists a large variety of electrochemical assays that can be performed amperometrically, and a miniaturized integrated potentiostat provides tremendous flexibility in the design and application of chemical sensors based on this technique. For example, commercial benchtop glucose analyzers determine glucose amperometrically due to the inherent advantages this approach provides for glucose oxidase based electrode systems. The microelectronic circuit presented here offers the same

advantages for a miniaturized glucose sensor that can be used with microelectrodes which could potentially be implanted, for example, as part of an insulin delivery system for the treatment of Type I diabetes.

2.6 REFERENCES

- [1] H. Wohltjen, "Chemical Microsensors and Microinstrumentation", *Anal. Chem.*, Vol. 56, No. 1, pp. 87A-103A, 1984.
- [2] P.W.Cheung, D.G. Fleming, W.H. Ko and M.R. Neuman, Eds., *Theory, Design and Biomedical Applications of Solid State Chemical Sensors*, CRC Press, West Palm Beach, Fl., 1978.
- [3] J.S. Soeldner, Ed., "Symposium on Potentially Implantable Glucose Sensors", *Diabetes Care*, Vol. 5, No. 3, p. 147, 1982.
- [4] J.N. Zemel, "Ion Sensitive Field Effect Transistors and Related Devices", *Anal. Chem.*, Vol. 47, No. 2, pp. 255A-268A, 1975.
- [5] J. Janata and R.J. Huber, Eds., *Solid State Chemical Sensors*, Academic Press, London, 1985.
- [6] K. Cammann, *Working with Ion Selective Electrodes*, Springer-Verlag, Berlin, 1979.
- [7] S.D. Caras, J. Janata, D. Saupe and K. Schmitt, "pH-Based Enzyme Potentiometric Sensors", Part I, *Anal. Chem.*, Vol. 57, pp. 1917-1920, 1985. See also: Part II, *Ibid.*, pp. 1920-1923; and Part III, *Ibid.*, pp. 1924-1925.
- [8] J.A. Plambeck, *Electroanalytical Chemistry*, J. Wiley & Sons, New York, 1982.
- [9] W. Sansen and M. Lambrechts, "Glucose Sensor with Telemetry System", in *Implantable Sensors for Closed-Loop Prosthetic Systems*, W.H. Ko, Ed., Ch. 12, pp. 167-175, Futura, Mount Kisco, NY, 1985.

- [10] T. Yao, "A Chemically-Modified Enzyme Membrane Electrode as an Amperometric Glucose Sensor", *Anal. Chim. Acta*, Vol. 148, pp. 27-33, 1983.
- [11] G.G. Guilbault, *Analytical Uses of Immobilized Enzymes*, Marcel Dekker, New York, 1984.

CHAPTER 3

Characterization of Perfluorosulfonic Acid Polymer Coated Enzyme Electrodes for Glucose Analysis in Whole Blood†

The perfluorosulfonic acid polymer Nafion® leads to highly reproducible electrode preparation and performance when used as a dialysis membrane material on glucose oxidase/Pt electrodes in the determination of glucose in whole blood. Protection from enzyme electrode fouling in whole blood was demonstrated for a 1.7 μm thick Nafion membrane during 6 days of continuous *in vitro* measurement in fresh whole blood samples at 37°C. Nafion encapsulation yields enzyme electrodes with a linear response up to at least 28 mM glucose, and response times of 5-17 s which are superior to those for electrodes coated with cellulose dialysis membranes. A custom designed CMOS two-electrode potentiostat was used to control the electrode bias potential and measure electrode current. The current sensitivity of the circuit is approximately 75 mV/ μA , the response is linear over the range of 10 nA to 2 μA , and the current detection limit is <2 nA. The differential mode capability of the circuit permits nulling of the background current due to interfering species in whole blood, yielding an accuracy of $\pm 2\%$ relative to a Beckman glucose analyzer.

3.1 INTRODUCTION

Continuous monitoring of physiological glucose levels using an implantable glucose sensor based on glucose oxidase enzyme electrodes was proposed a number of years ago [1-3]. Since that time, research efforts have been directed toward improved design of the electrode and the necessary membrane materials required for proper operation of the sensor [3-10]. Miniaturization of both the sensor and the electronics for implantation has been addressed using pH sensitive ion sensitive field effect transistors (ISFET) coated with a glucose oxidase enzyme layer. This

† A version of this chapter has been published as:

D.J. Harrison, R.F.B. Turner and H.P. Baltes, "Characterization of Perfluorosulfonic Acid Polymer Coated Enzyme Electrodes and a Miniaturized Integrated Potentiostat for Glucose Analysis in Whole Blood", *Analytical Chemistry*, Vol. 60, No. 19, pp. 2002-2007, October 1988.

device is a potentiometric sensor with a response proportional to the logarithm of the glucose concentration [11,12]. Macroscopic potentiometric glucose sensors have been examined in detail and are found to suffer from sensitivity to buffer capacity, interfering species, and liquid junction potentials [13,14] to a much greater extent than glucose oxidase based amperometric sensors. A recent study of the enzyme coated ISFET demonstrates that the same difficulties also plague the miniaturized potentiometric device [12]. In fact, successful commercial bench-top glucose analyzers such as the Yellow Springs instrument are based on the amperometric approach.

With these considerations in mind, we developed the integrated CMOS based potentiostat [15] described in Chapter 2, which can be used for the amperometric determination of glucose and is sufficiently small, with low enough power demands, that it could easily be implanted as part of an artificial pancreas. Full integration of the transducing electrodes on the CMOS chip is not necessary to obtain high noise immunity since amperometry is inherently less sensitive to noise than high impedance potentiometry. This obviates many of the difficulties associated with packaging ISFET devices [16] since the entire silicon chip can easily be hermetically sealed.

The oxidation of glucose to produce gluconic acid and H_2O_2 in the presence of glucose oxidase is a well known means of obtaining a glucose selective electrode reaction. The choice of membrane system depends on whether O_2 or H_2O_2 is to be determined, and whether or not all the electrodes in the cell are located on the same side of the membrane. Lucisano, *et al.* have recently reviewed [17] the performance of O_2 electrodes of the Clark type with all electrodes on one side of the membrane, and the monopolar type where only the working electrode is membrane coated. All methods have advantages and disadvantages in terms of response time, stability and sensitivity to O_2 tension. We have elected to utilize H_2O_2 determination since, with this method, it is possible to easily reduce sensitivity to variations in O_2 tension in the analyte solution [5]. This is accomplished by using a semi-permeable membrane that reduces the ratio

of glucose to O_2 flux until the overall reaction rate is controlled by glucose mass transfer and not by O_2 .

One of the key difficulties in developing a H_2O_2 based implantable glucose sensor is in the design of a semi-permeable membrane structure [3,5-9] that ensures satisfactory electrochemical performance, yet prevents or at least reduces degradation of the sensor in the biological environment. A number of dialysis membranes have been suggested in the literature including cellulose and cellulose acetates [3,5,8,9], poly(urethane) [7], and poly(propylene) [8]. These membranes are semi-permeable to glucose, and decrease the rate of glucose mass transfer relative to O_2 , leading to reduced sensitivity to O_2 tension. However, they generally also serve another function. When a glucose oxidase membrane on a Pt electrode is directly exposed to blood, reversible fouling of the electrode occurs, presumably due to adsorption of species from solution, and the response to glucose is almost completely eliminated. The outer dialysis membrane must prevent this phenomenon, and may also reduce longer term effects such as clotting and fibrous encapsulation of the sensor. We have investigated cellulose and cellulose acetate membranes as dialysis layers, and we find it is difficult to reproducibly obtain satisfactory results with these materials. Similar concerns have been raised for poly(urethane) coatings [18].

In this paper, we present experimental results characterizing the DuPont perfluorinated ionomer Nafion® as a dialysis membrane material for use in whole blood. The chemical structure of the repeating unit of Nafion polymer is shown in Figure 3.1. Nafion has been used previously as a protective, selective coating on electrodes in intracellular fluids of nerve and brain tissue in order to reduce ascorbic acid response when determining various neurotransmitters [19-21]. We find that it also serves as an excellent dialysis membrane for use in whole blood when cast from solutions of the ionomer, allowing satisfactory voltammetry and high reproducibility of electrode preparation for membranes of approximately $0.8 \mu m$ thickness or greater. To our knowledge, this is the first report of the use of Nafion polymer as a dialysis membrane in the determination of glucose or other neutral species.

PERFLUOROSULPHONIC ACID (Nafion) IONOMER :

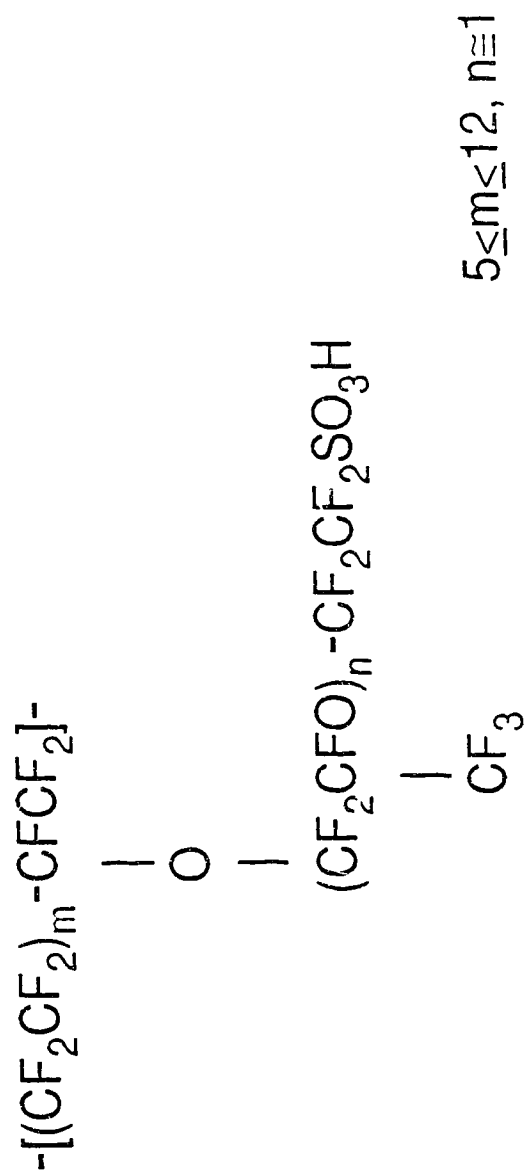


Figure 3.1 Chemical structure of repeating unit (mer) of perfluoro-sulfonic acid (Nafion) polymer. Nafion is a linear copolymer of tetrafluoroethylene and perfluorosulfonic acid first synthesized in the laboratories of E.I. du Pont de Nemours and Co. (also exists in a perfluorocarboxylic acid form).

3.2 MATERIALS AND METHODS

3.2.1 Reagents

High-purity glucose oxidase (EC 1.1.3.4) (Type X, from *Aspergillus niger*, 100,000-150,000 units/g), bovine serum albumin (Fraction V, 98-99% albumin) and glutaraldehyde (25% aqueous solution) were obtained from Sigma Chemical and used as received. All other chemicals were of reagent grade. Solutions were prepared using double-distilled, deionized water. Cellulose dialysis membrane (Spectra Por®) was obtained from Fisher Scientific and Nafion (5% solution, 1100 e.w) was obtained from Solution Technology. Canine whole blood from both healthy and diabetic animals was collected in heparinized Vacutainers® and stored at 4°C prior to use.

A stock buffer solution of pH 7.4 was prepared from phosphate salts ($\mu = 0.05$ M) with 5 mM sodium benzoate and 1 mM ethylenediamine tetraacetic acid (EDTA) as preservatives, and 0.1 M NaCl as supporting electrolyte. To this, glucose was added and allowed to mutarotate overnight at room temperature to yield a 0.1 M stock glucose solution that was subsequently stored at 4°C. Unbuffered solutions of 0.5% Nafion and 1% Nafion were prepared by dilution of the 5% solution with 1:1 isopropanol and water.

3.2.2 Electrode Preparation

Platinum wires (1.024 mm diameter) were sealed in glass tubing (5 mm o.d.), ground and polished to leave exposed a circular platinum electrode (0.823 mm²). Electrodes were polished using 1 μ m Al₂O₃ as the finish, etched for 1 minute in aqua regia, anodized at +1.9 V, and then cycled between -0.24 and +1.1 V vs. SCE in 0.5 M H₂SO₄ prior to coating. Electrodes were paired for differential measurements based on a comparison of areas by cyclic voltammetry.

Glucose-sensitive working electrodes were prepared by a method similar to that described by Yao [22]. That is, platinum electrodes were dipped in an acetate buffered solution (pH 5.5) containing 19.5 mg/mL glucose oxidase (GO), 73.2 mg/mL albumin (BSA) and 5 mg/mL glutar-

aldehyde, and then inverted to dry for at least two hours in air at room temperature. The resulting (dry) membrane composition is approximately 20% GO, 75% BSA and 5% glutaraldehyde. Glucose-insensitive working electrodes were prepared by dip-coating from a similar solution in which the GO component was replaced by an equivalent weight of additional BSA. Nafion dialysis membrane overcoats were applied by dip-coating the working electrodes in one of the Nafion stock solutions and inverting to dry for at least one hour. The procedure was repeated until a Nafion dialysis layer of desired thickness was obtained. It was found necessary to first coat with several dips in 0.5% Nafion solution, before making several dip-coats in 1% or 5% solutions. If the electrode was first dip-coated in the 5% solution as received, the enzyme activity was substantially reduced, whereas the procedure outlined above led to much more active electrodes. The reason for this is not clear since the solvent composition was the same for the more dilute Nafion solutions. It may be that the higher proton activity in the 5% solution is sufficient to partially denature the enzyme when there is no intervening Nafion coating to protect it.

Cellulose dialysis membranes were affixed to the electrodes by inserting both glucose active and inactive working electrodes into a length of dialysis tubing, folding the ends of the tubing together, gathering the excess membrane away from the electrode tips, and securing it with cellophane tape. Care was taken to avoid stretching the membrane and to ensure that it was in intimate contact with the working electrode tip over the entire active area of the electrodes.

3.2.3 Nafion Film Thickness

The thickness of the Nafion coatings on glass shrouded Pt electrodes (0.823 mm^2) were estimated electrochemically. $\text{Ru}(\text{NH}_3)_6^{3+}$ was ion exchanged into Nafion films coated on clean Pt electrodes from a solution of 5 mM $\text{Ru}(\text{NH}_3)_6^{3+}$ and 0.1 M KCl. The amount of Ru complex exchanged into the film was determined by integration of the cyclic voltammetric curve obtained in a solution of 50 μM $\text{Ru}(\text{NH}_3)_6^{3+}$ and 0.1 M KCl, where the complex was added to reduce loss from the film. The integral yielded the charge transferred during the cathodic scan, *viz.*

$$Q = zFA\Gamma_{\text{Ru}} \quad (3.1)$$

where z is the number of moles of electrons transferred per mole of $\text{Ru}(\text{NH}_3)_6^{3+}$ reduced ($z=1$); F is the Faraday constant (96,500 C/mol); A is the area of the electrode ($8.23 \times 10^3 \text{ cm}^2$); and Γ_{Ru} is the surface density of membrane bound Ru complex (mol/cm^2). Assuming $\Gamma_{\text{mem}}=3\Gamma_{\text{Ru}}$ (*i.e.* to account for the 3:1 ratio of RSO_3^- to $\text{Ru}(\text{NH}_3)_6^{3+}$ in the film) and substituting $\Gamma_{\text{mem}}=\rho\delta/(\text{e.w.})$, the membrane thickness δ is given by

$$\delta = 3 Q (\text{e.w.}) / zFA\rho \quad (3.2)$$

where e.w. is the equivalent molecular weight (1100 g/mol) and ρ is the mass density of the membrane ($1.58 \text{ g}/\text{cm}^3$). Cyclic voltammetric current obtained in the $50 \mu\text{M}$ $\text{Ru}(\text{NH}_3)_6^{3+}$ solution was independent of stirring of the solution, indicating only polymer confined $\text{Ru}(\text{NH}_3)_6^{3+}$ contributed significantly to the current measured. The sample data shown in Table 3.1 indicate that the results were approximately independent of scan rates of up to 20 mV/s. The table also shows that the actual amount of polymer coated per dip can vary, which is due to the fact that the dip-coating parameters can not be precisely controlled. However, a test of the ability of the membrane to exclude 5 mM $\text{Fe}(\text{CN})_6^{4-}$ can be used to evaluate a given coating.

To calibrate the electrochemical method several large area Pt flags were dip-coated in Nafion solution, the quantity of $\text{Ru}(\text{NH}_3)_6^{3+}$ exchanged into the films was determined electrochemically, and after exchanging out the Ru complex in NaCl solution the film thickness was measured using an Alpha Step surface profilometer (Tencor Industries) [23,24]. A portion of the film was removed with a scalpel to generate a step. The results indicate there is 1.2 ± 0.2 times as much Ru complex in the film as would be expected for a 3:1 polymer sulfonate to $\text{Ru}(\text{NH}_3)_6^{3+}$ ratio. The factor of 1.2 is found using a density of $1.58 \text{ g}/\text{cm}^3$ for the Nafion film [23], and assuming the nominal value of 1100 grams/ SO_3^- equivalent is correct in the calculation of $\text{Ru}(\text{NH}_3)_6^{3+}$ content from the measured thickness. The thicknesses of Nafion polymer coatings on GO/BSA membrane electrodes are estimated from the data obtained for Nafion coated, glass shrouded Pt

TABLE 3.1 Sample Nafion film thickness data as determined electrochemically by cyclic voltammetry of (membrane bound) $\text{Ru}(\text{NH}_3)_6^{3+}$ saturated membranes. Q is the measured total charge transferred during the cathodic scan, and δ is the membrane thickness calculated from $\delta=3Q(\text{e.w.})/zFA\rho$.

No. Nafion Dip Coats x [Nafion]	Scan=5 mV/s		Scan=10 mV/s		Scan=20 mV/s		$\text{Fe}(\text{CN})_6^{4-}$ Block ^a
	Q (μC)	δ (nm)	Q (μC)	δ (nm)	Q (μC)	δ (nm)	
1 x 0.5% ^b	2.522	66.3	2.229	58.6	2.323	61.1	~33%
4 x 0.5% ^c	NA	NA	16.69	439	18.75	493	~90%
4 x 0.5% + 2 x 1.0% ^b	12.20	321	12.61	331	10.04	264	~99%
4 x 0.5%+ 4 x 1.0%+ 1 x 5.0% ^b	39.60	1041	36.7	965	36.83	969	~99.9%

- (a) Determined by comparison of peak oxidation current, with and without Nafion membrane, in 5 mM $\text{K}_4\text{Fe}(\text{CN})_6$ solution.
- (b) These measurements were performed on the same electrode and the same membrane (*i.e.* at different stages in the coating procedure). The electrode surface was treated with N-trimethoxysilylpropyl-N,N,N-trimethyl ammonium chloride (TTACl) prior to coating.
- (c) This measurement was performed on the same electrode as (b), but a different membrane. In this case, the electrode surface was not treated with (TTACl) prior to coating.

electrodes prepared by the same dip-coating sequences, assuming there is no change in coating characteristics when the enzyme layer is present. The values are corrected for the excess $\text{Ru}(\text{NH}_3)_6^{3+}$ present in the Nafion films.

3.2.4 Electrochemical Measurements

Experimental assays were performed with a dual-channel CMOS integrated potentiostat, in a two-electrode configuration, with a Ag/AgCl reference. The applied potential between the common reference and each working electrode is derived from an on-chip voltage reference that is set by adjusting the external power supply voltages. The integrated circuit was fabricated [15] by Northern Telecom (CMOS 1B process; 5 μm feature size) in accordance with an agreement with the Canadian Microelectronics Corporation. The integrated potentiostat was generally operated in differential measurement mode using a pair of identical Pt working electrodes, one glucose sensitive, one glucose insensitive, each prepared as described above. The difference between the two output channels gives the net glucose current, independent of the background current at +0.7 V vs. Ag/AgCl.

A Pine RDE-4 potentiostat was used in three-electrode configuration for cyclic voltammetry and diagnostic amperometry. A three-neck glass round-bottom flask served as the electrochemical cell. Stirring was provided with an air driven magnetic stirrer, and cell temperature was monitored with a K-type thermocouple. Data were recorded using either a Hewlett-Packard x-y-t recorder (HP7015B) or strip chart recorder (HP7128A) and crucial voltages were monitored with a high-impedance multimeter (HP3478A). Control assays of blood samples and stock glucose solutions were obtained with a Beckman Glucose Analyzer 2, operated by a trained technician.

Working electrodes were potentiostated at +0.7 V vs. Ag/AgCl and calibrated in magnetically stirred stock buffer solutions (pH 7.4) under air by addition of aliquots of glucose stock (0.1 M). Whole blood and plasma glucose assays were performed by standard additions in the same manner.

In the lifetime study, a pair of working electrodes was operated continuously over a 24 h period in whole blood. A series of glucose standard additions was performed initially, and again after 24 h, to calibrate the electrodes. The blood was then exchanged for a fresh aliquot and the cycle repeated. A Corala Ultra Thermostat NB-34707 thermostated water bath maintained the cell at 37°C, and O₂ presaturated with H₂O (37°C) was passed over the sample. Response time of the electrodes in buffer (pH 7.4) was determined from the rise time of the signal following injection of an aliquot of glucose or H₂O₂ standard into a rapidly stirred cell.

3.3 RESULTS AND DISCUSSION

3.3.1 Nafion Dialysis Membranes

To evaluate enzyme electrodes in blood, it was necessary to use a dialysis membrane to obtain satisfactory electrode response. Several materials were used, but Nafion proved most satisfactory (*vide infra*). The electrodes were prepared by dip-coating a glucose oxidase (GO), bovine serum albumin (BSA) membrane coated electrode in a solution of Nafion, as described in the Materials and Methods section. The thickness of the Nafion overcoating on the enzyme electrodes was estimated by an electrochemical method, also described in the Materials and Methods section, involving ion exchange of Ru(NH₃)₆³⁺ into Nafion films on Pt electrodes. We estimate the accuracy in reported thickness values to be about ±20%, and the precision to be ±10%. Calibration of the electrochemical thickness determination using a profilometer indicates that 1.2 ± 0.2 times as much Ru(NH₃)₆³⁺ enters the Nafion film as would be expected based on charge neutrality considerations. The slight excess is consistent with results reported by White, *et al.* [24] indicating that Nafion films that are fully saturated with Os(bipyridyl)₃²⁺ or [N,N,N-trimethylaminomethyl]ferrocene exhibit an excess of the complex cation over the Nafion SO₃⁻ group content. Additionally, Szentirmay and Martin [23] have shown that Nafion has an extremely high affinity for Ru(NH₃)₆³⁺ that is not explained by electrostatic effects alone, and this could lead to extraction of excess complex into the film.

Figure 3.2 shows the response of GO membrane electrodes in stock buffer solution (pH 7.4), to aliquots of 0.1 M glucose stock solution, as measured with the integrated potentiostat. As expected, the response varies significantly as the thickness of the Nafion dialysis membrane coating increases. With no Nafion membrane, the response is non-linear, approximately obeying Michaelis-Menton kinetics, and the value of the apparent Michaelis constant is a function of O_2 concentration in solution as has been reported by others [5,6]. Surprisingly, a thin coat of Nafion (~50 nm) actually results in an increased response as shown in Figure 3.2. This effect has been observed repeatedly for many electrodes and may be due to the enhanced solubility of O_2 in Nafion membranes [25,26]. While the thin film may increase the local O_2 concentration, the thickness or uniformity of the film may be insufficient to significantly impede the rate of supply of glucose to the enzyme. Unfortunately such thin films do not adequately protect the electrodes in blood, and so the mechanism responsible for this effect was not pursued. Increasing the Nafion thickness to ~0.25 μm results in the curve marked Medium in Figure 3.2. A thick coating, ~0.83 μm , results in substantial limitation of glucose transport, decreasing the electrode sensitivity, but giving a linear response to glucose concentrations over the measured range of 0 to 28 mM. This is within the typical range expected in a diabetic patient with insufficient control over glucose levels (a relatively constant 5 mM level is maintained in healthy individuals).

The quality of the response to glucose of an enzyme electrode in whole blood is known to be strongly dependent on the nature of the dialysis membrane used [3,5-7]. In the case of Nafion coated electrodes, the thickness of the deposited membrane is important. With thinner coatings, less than ~0.5 μm , an electrode in whole blood shows an initial increase in response to an injection of additional glucose, which then decays to the original signal level over several minutes. After several injections, increasing the blood glucose concentration to ~10 mM or more, there is no change in response at all. This response pattern is sometimes observed for enzyme electrodes with no dialysis membrane, although more frequently we observed no response at all to added glucose at such electrodes. Nafion

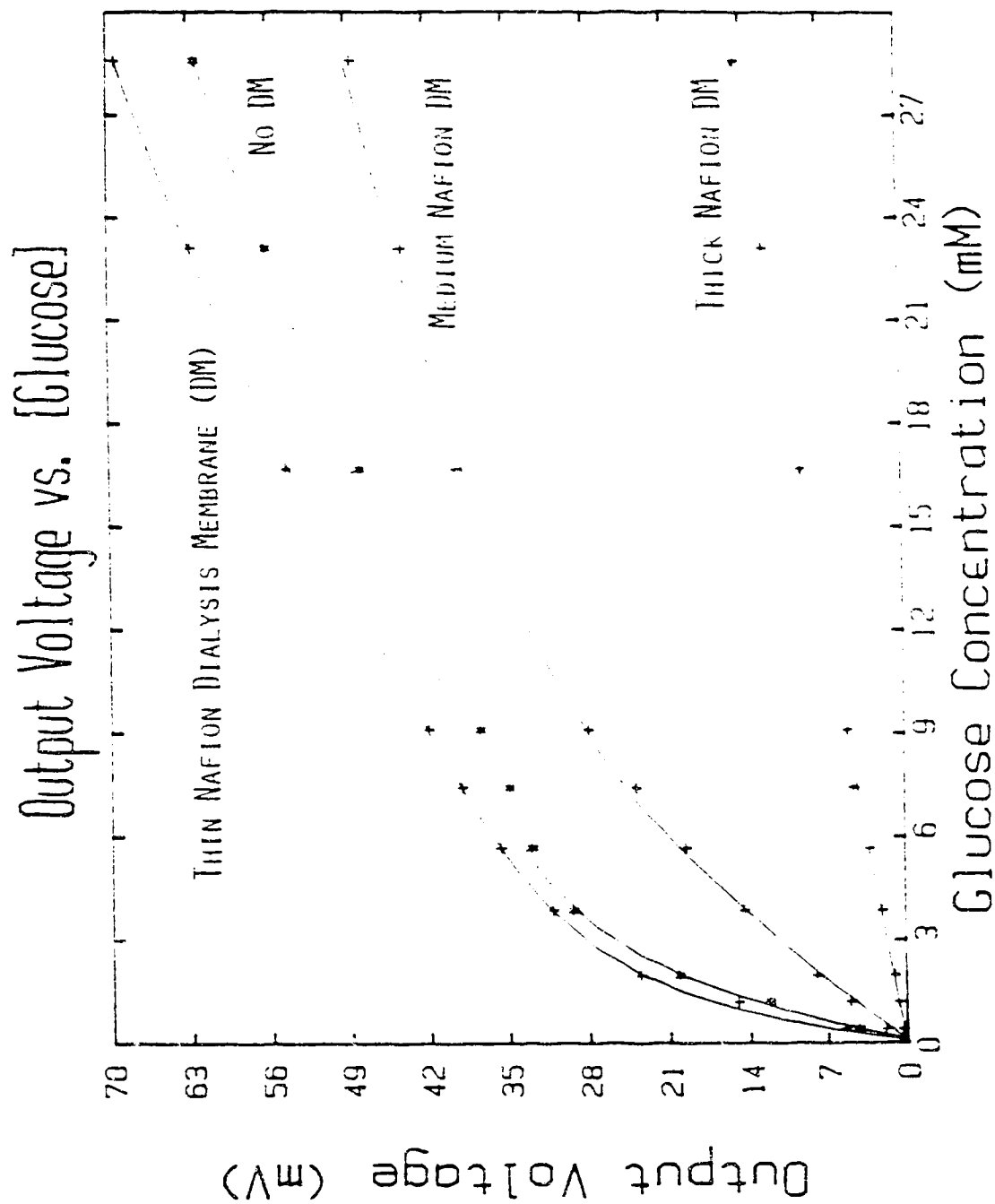


Figure 3.2 Typical sensor calibration curves in phosphate buffer showing the effect of Nafion membrane thickness on the response characteristic. Experimentally estimated thicknesses are: Thin, 50 nm; Medium, 250 nm; Thick, 830 nm.

overcoatings of 0.8 μm thickness or greater result in steady state response to additional glucose injections in blood, with stable response over at least 30 minutes.

Figure 3.3 shows the amperometric response of an enzyme electrode with a 1.7 μm thick Nafion overcoating in whole blood, during addition of glucose standard. The initial sharp rise evident with each glucose injection is due to inefficient mixing of the standard in whole blood on initial addition to the cell. The Grans plot in Figure 3.3 shows that the electrode response is linear over the range of standard glucose additions examined. The stability of response following each glucose addition, and the linearity of response, indicate satisfactory performance of the Nafion coated enzyme electrode in whole blood *in vitro*. In contrast, Figure 3.4 and Figure 3.5 show similar standard additions experiments in whole blood and blood plasma respectively, using conventional cellulose dialysis membranes (MWCO 12,000) in place of a Nafion membrane. Note the slower response time and the decaying response indicating electrode failure after approximately 20 minutes exposure (similar behavior was observed both in whole blood and in plasma). In this case, electrode failure is manifested in much the same manner as an electrode with a thin (*i.e.* less than $\sim 0.5 \mu\text{m}$) Nafion membrane.

Cyclic voltammograms in Figure 3.6 show the characteristic response of a Nafion coated (1.7 μm) enzyme electrode in phosphate buffer solution (pH 7.4) and in whole blood, before and after injections of additional glucose. It can be seen that the H_2O_2 oxidation curves show substantially the same behavior in both solutions, indicating that the Nafion is a successful dialysis membrane, maintaining a relatively protein and interferent free environment near the electrode surface. In contrast, cyclic voltammetry at an unprotected enzyme electrode in whole blood shows substantially depressed oxidation current that exhibits very little if any response to additional injected glucose. The reduction current observed at Nafion coated electrodes in Figure 3.6 is due to O_2 , and possibly H_2O_2 , reduction at the Pt substrate. The differences in the reduction currents between blood and buffer matrices likely reflects the decreased availability of O_2 in blood relative to buffer solution.

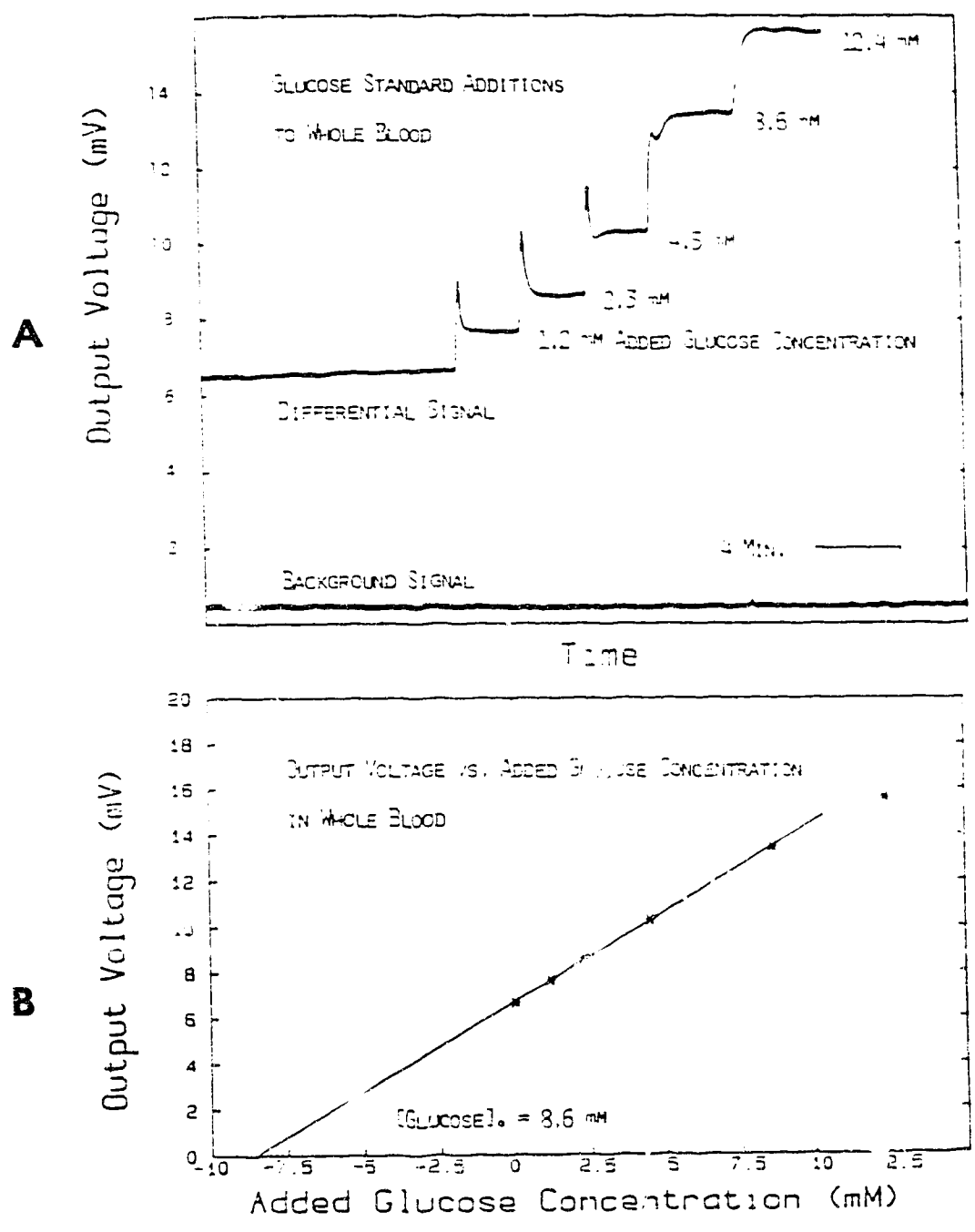


Figure 3.3 Typical glucose assay in whole blood by standard additions with a 1.7 μm thick Nafion dialysis membrane. (A) Sensor response versus time, showing a significant level of background signal which is eliminated by the differential measurement. (B) Grans plot of standard additions data.

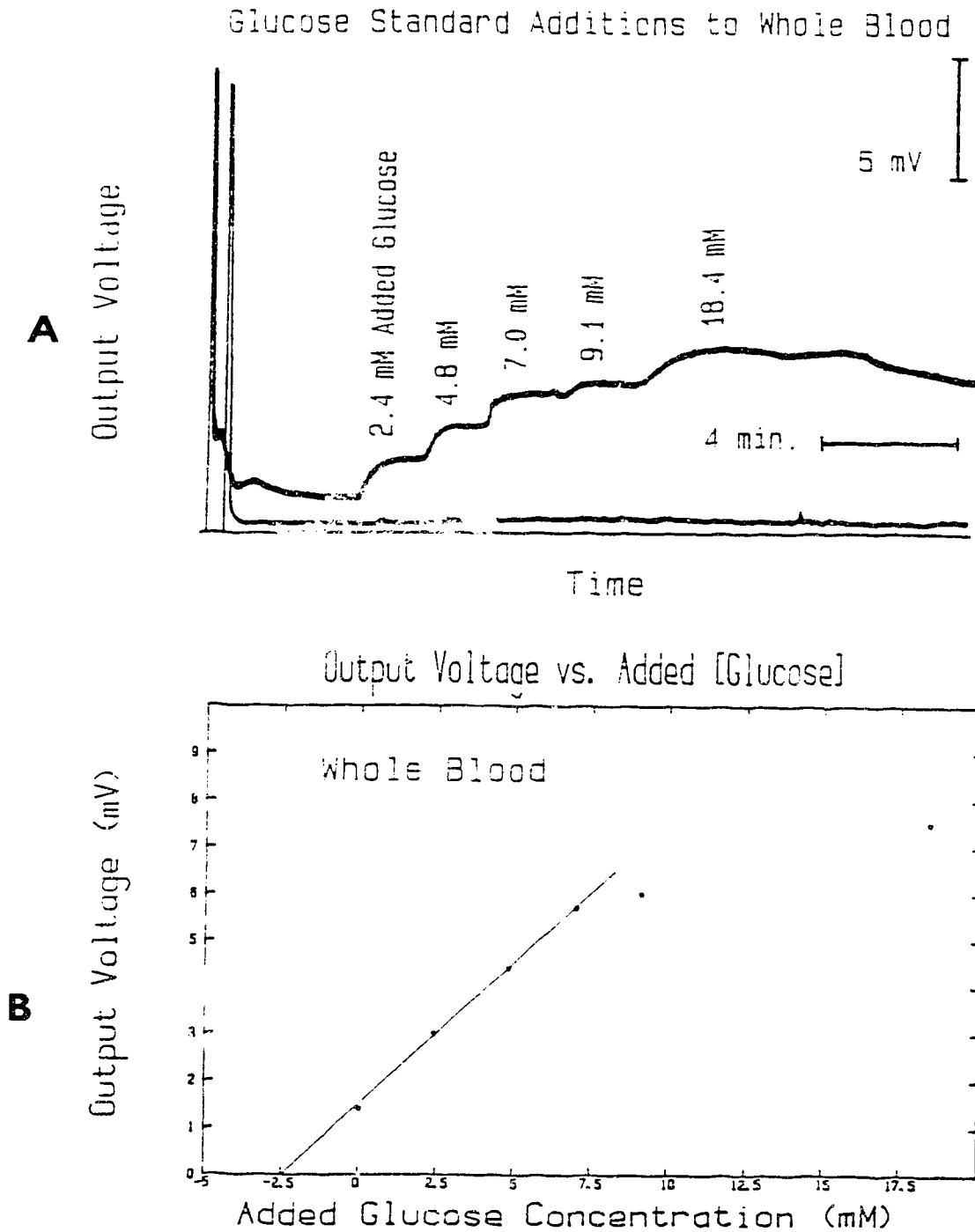


Figure 3.4 Typical glucose assay in whole blood by standard additions with a 12,000 MWCO cellulose dialysis membrane. (A) Sensor response versus time. (B) Grans plot of standard additions data.

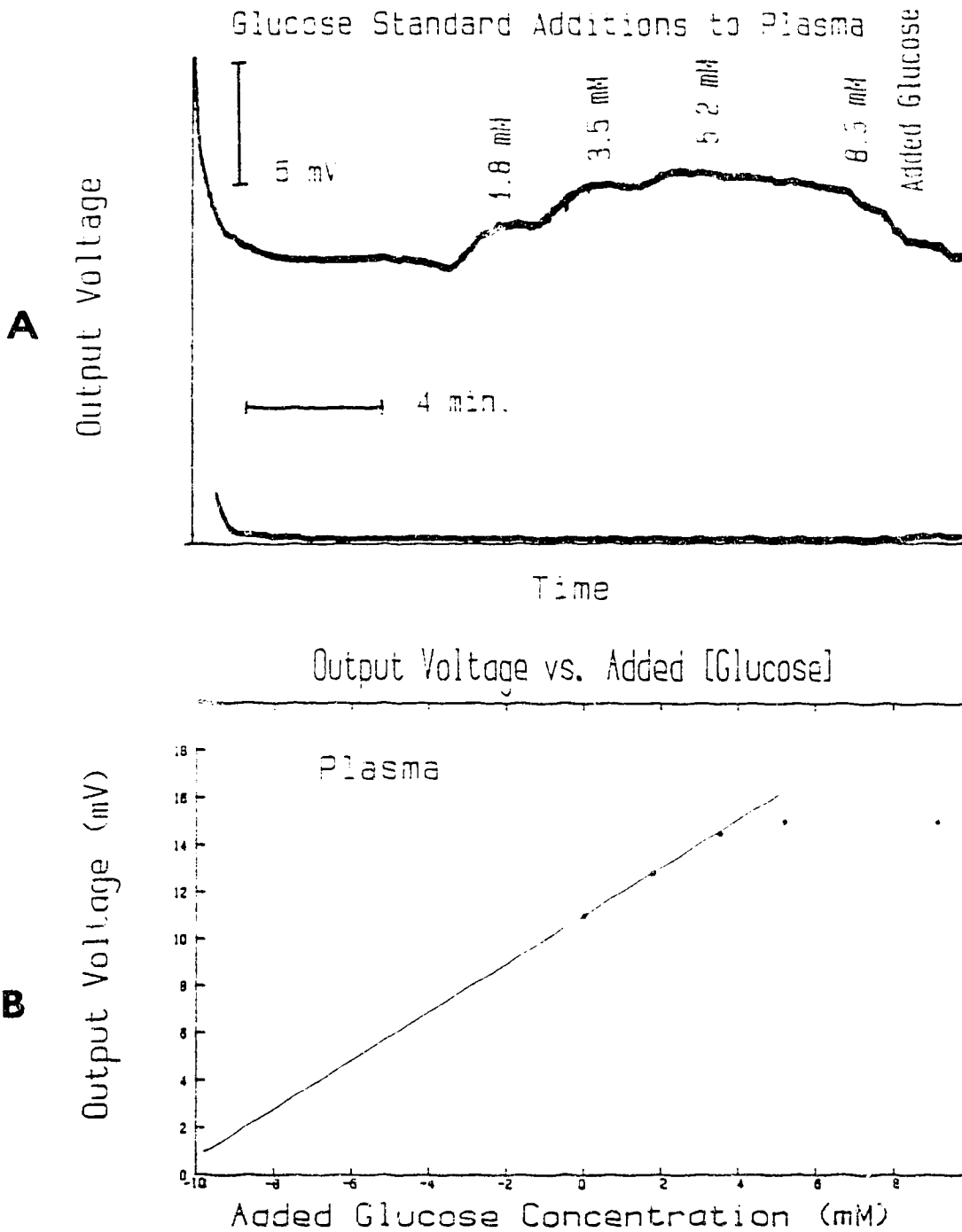


Figure 3.5 Typical glucose assay in blood plasma by standard additions with a 12,000 MWCO cellulose dialysis membrane. (A) Sensor response versus time. (B) Grans plot of standard additions data.

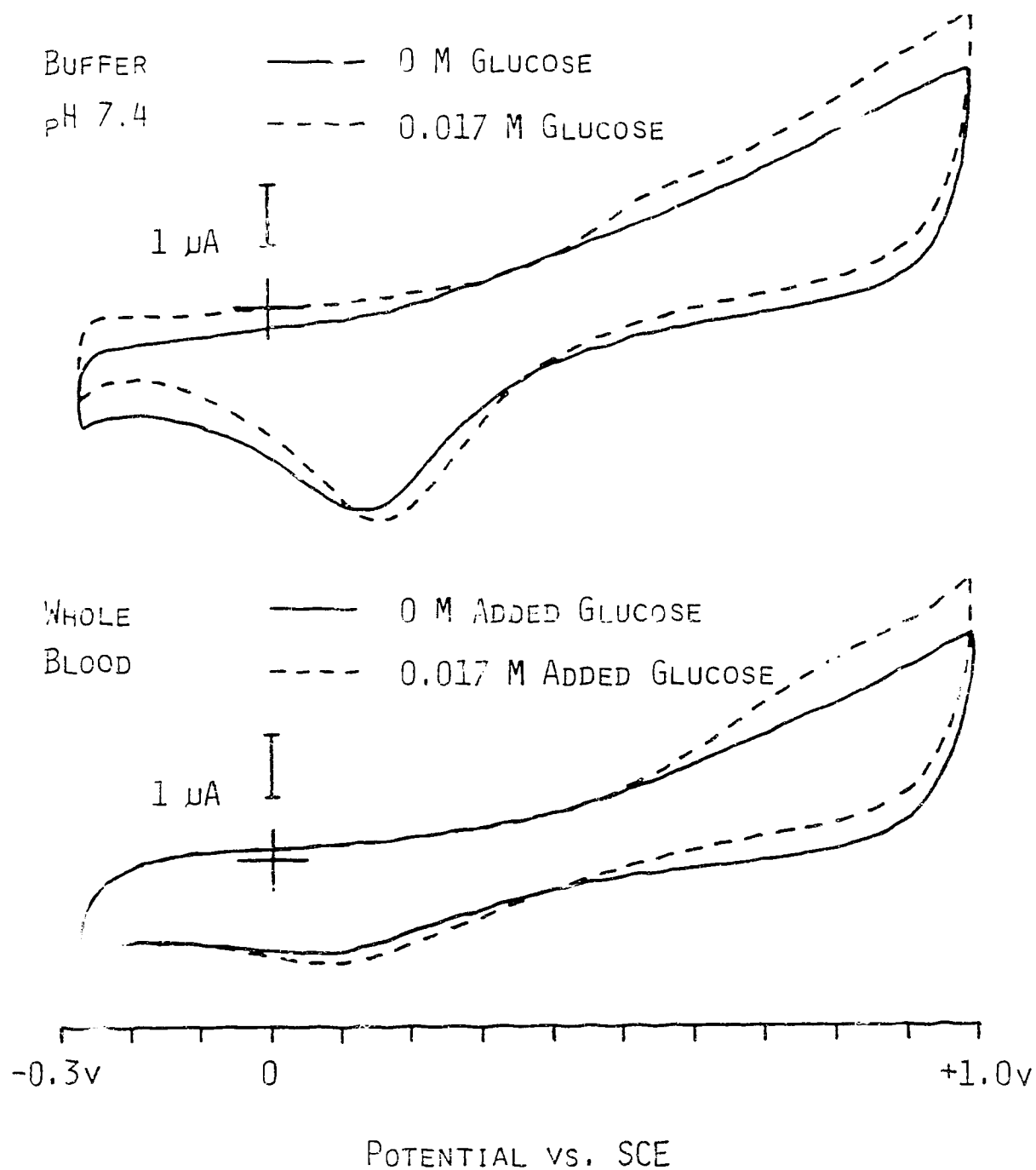


Figure 3.6 Cyclic voltammograms at 100 mV/s in buffer and whole blood showing the effect of added glucose. The whole blood sample used contained 4.8 mM of endogenous glucose (Beckman assay).

It is useful to know how thick a Nafion film is necessary to obtain satisfactory response in whole blood. We find that there is a correlation between the cyclic voltammetric response of Nafion coated electrodes to 5 mM $\text{Fe}(\text{CN})_6^{4-}$ in buffer solution, and their performance in whole blood. As would be expected due to the permselectivity of Nafion films [27], the current for $\text{Fe}(\text{CN})_6^{4-}$ decreases as film thickness increases, falling to ~1% of the response of a naked electrode for coatings of 0.25 μm , and showing a response of less than 0.1% for coatings of 0.8 μm or greater. Electrodes that perform satisfactorily in blood also prevent $\text{Fe}(\text{CN})_6^{4-}$ from reacting at the electrode, 0.1% response or less, while those Nafion coatings that are not satisfactory in blood show a larger response to 5 mM $\text{Fe}(\text{CN})_6^{4-}$ in buffer solution. Sufficiently thick films also result in limitation of the rate of glucose supply relative to O_2 , producing linear calibration curves up to at least 30 mM glucose. We find that Nafion coatings of 0.8 μm thickness or greater give satisfactory results in whole blood from one electrode to the next, unless the film is physically damaged through mishandling of the electrode. That is, the protective function of the Nafion layer is very reproducibly attained, even though film thickness and uniformity can vary from one preparation to the next. This is one of the key features of using Nafion as a dialysis membrane.

The above results make it apparent that in order to adequately protect either the enzyme function, the electrochemical H_2O_2 reaction at the Pt substrate, or both when an enzyme electrode is used in whole blood, a sufficiently thick Nafion film which significantly reduces permeation of small molecules and ions through the dialysis layer is required. We note that many cellulose encapsulated GO electrodes use a two-layer dialysis system with cellulose as the outer coating and a GO layer, and the ionomer cellulose acetate coated on the Pt electrode [3]. To gain some insight into the coating function, an electrode with the interfacial structure Pt/Nafion/GO, BSA copolymer was prepared and tested in whole blood. The electrode showed minimal response to added glucose, a result identical to that found for enzyme electrodes with no dialysis layer. Yet, when tested in buffer the activity of the Nafion undercoated enzyme electrode was similar to that of a standard enzyme electrode. Apparently, species present in whole blood

significantly decrease activity of the enzyme membrane itself. This may happen through adsorption of protein matter or cells on the surface, by direct inhibition of enzyme activity, or by reaction of H_2O_2 with catalase released as a result of peroxide induced haemolysis. The Nafion layer clearly prevents a decrease in enzyme function, and is expected to also protect the Pt electrode activity.

We have also examined a large number of Pt/enzyme film electrodes in whole blood with outer layers of various cellulose dialysis membranes obtained from several sources, ranging in nominal molecular weight cut-off from 12,000 to 2,000 Daltons. In most cases these dialysis layers failed to provide satisfactory performance in whole blood. Only 5% to 10% of the cellulose protected enzyme electrodes responded as shown in Figure 3.3 for the Nafion coated electrode. The remainder exhibited a behavior as shown in Figure 3.4 or Figure 3.5, which is similar to that described above for enzyme electrodes with no dialysis membrane, or very thin Nafion coatings. We were unable to determine what factors governed the variable performance of the cellulose dialysis membranes, as there was no correlation with the nominal molecular weight cut-off values.

The response time of glucose enzyme electrodes can be significantly affected by dialysis membranes, which may also affect the overall sensor performance. The effect of cellulose and Nafion membranes on response time to a concentration step from 0 to 5 mM glucose was evaluated in buffer solution (pH 7.4). The cellulose dialysis membranes, particularly for low molecular weight cut-off, have a very substantial effect on electrode response. Table 3.2 shows that response time, measured as the time taken for the signal to rise from 10 to 90% of the maximum following addition of glucose, is greatly increased over that of an uncoated GO electrode. The same is true when 0.2 mM H_2O_2 is added to the test solution, although H_2O_2 penetrates the cellulose film more rapidly than glucose. In contrast, the Nafion coating causes relatively little change in the rise time following either glucose or H_2O_2 injection. In fact, in the measurement as performed here, the observed rise time represents an upper limit, since the time of mixing in the cell following sample addition (2-5 s) is of the same order. While the response time of the sensor is not critical to most applications if it

TABLE 3.2 Comparison of response times of Nafion polymer versus cellulose dialysis membranes. Aliquots of buffered glucose or H₂O₂ were injected into a rapidly stirred cell initially containing only 0.1 M NaCl in phosphate buffer (pH 7.4). Data were obtained using the integrated potentiostat circuit connected to an x-y-t recorder with a calibrated time base.

Type of Dialysis Membrane ^a	Rise Time ^b (Seconds)	
	5 mM Glucose	0.2 mM H ₂ O ₂
No Membrane	7.3	5.3
Cellulose 12,000 ^c	61.0	18.0
Cellulose 3,500 ^c	75.0	19.0
Cellulose 2,000 ^c	>1,000.0	245.0
Nafion (0.25 μm)	4.5	7.5
Nafion (0.83 μm)	17.5	5.2

- (a) In all cases a GO/BSA membrane on a Pt indicating electrode was employed in order to achieve glucose sensitivity.
- (b) Rise time is defined here as the time required for a change from 10% to 90% of the final signal following a concentration step from 0 mM.
- (c) Manufacturer's specification (Spectrapor® Dialysis membranes from Fisher Scientific); value represents nominal molecular weight cut-off.

is less than a few minutes, it has been suggested [28] that a rapid response is desirable in the configuration of algorithms for insulin delivery. Also, if a non-steady state voltammetric approach were used in glucose analysis rather than steady state amperometry, such as in the catalytic Pt sensor studied by Giner [29] and others [30], the presence of a protective film which allows rapid transient response such as Nafion could perhaps enhance selectivity and performance.

3.3.2 Quantitative Sensor Performance and Lifetime

The effectiveness of the integrated potentiostat, Nafion coated enzyme electrode combination was evaluated in whole blood using the method of standard additions. Figure 3.3 shows a typical data set obtained with this combination, and the Grans plot for the standard addition of 50 μ L aliquots of stock 0.1 M glucose solution. The blood glucose concentration determined by this method was compared to values measured with a Beckman Glucose Analyzer. The Beckman instrument requires the whole blood sample be centrifuged to separate the plasma from the cells, resulting in a volume change for the solution. A correction factor of 1/1.12 is then applied to the plasma glucose value to account for the volume change. This is a standard value in common use [31], but may not always accurately reflect the actual volume change [32,33], and so introduces some inaccuracy in the cross-calibration. Despite this, we find agreement between the two methods is good if care is taken to limit, or account for, the time delay between analyses. It is known that stored blood shows a slow linear decline in glucose concentration over time [31]. The error between the two methods as determined by several measurements on different blood samples is $\pm 2\%$. The high linearity of the standard addition curves shown in Figure 3.3 is routinely obtained, indicating the precision of analysis with our glucose sensor is high.

Using a paired set of glucose active and glucose inactive working electrodes, differential measurement allows discrimination between glucose current and that arising from solution species oxidizable at +0.7 V vs. Ag/AgCl at the Pt substrate. We have previously shown that differential operation of the two channels of the integrated potentiostat

corrects for background currents when H_2O_2 is added to 5 mM glucose in buffer solution [15]. To further explore this feature the effect of added ascorbic acid and urea on the response at an uncoated Pt/enzyme electrode in glucose buffered solution was tested, since both of these species are present in whole blood. Differential measurement readily eliminated interference from both ascorbic acid and urea at concentrations up to 3 and 20 mM, respectively. It should be noted that when cellulose is used as the dialysis layer, interferences from electroactive species such as ascorbate will also be reduced due to the Donnan exclusion of these species [19-21,27]. In whole blood, background current is observed by the non-glucose active working electrode when either cellulose or Nafion serve as the dialysis layer. In Figure 3.3, for example, the background level is $\pm 8\%$ of the differential output signal, and typically varies from 5 to 20% from one blood sample to the next with both Nafion and cellulose membranes.

Physical implantation of a glucose sensor in the body requires that both the integrated potentiostat and the electrode membrane be durable in this harsh environment. However, lifetime of the enzyme electrode assembly in biological fluids such as blood, and the effect of the host immune system response on the electrodes, remains a critical difficulty. We report here some preliminary results on the response characteristics of a Nafion coated electrode over time, during continuous operation in whole blood *in vitro*.

A pair of electrodes for differential measurement of glucose with a $1.7\ \mu\text{m}$ Nafion overcoating, were operated continuously in a sample of whole blood for 24 h at room temperature. On initial introduction of the electrodes to the sample, a series of standard glucose additions showed a calibration slope of 14.5 nA/mM. After 24 h the electrodes were immediately transferred to a fresh whole blood sample at 37°C and showed a response of 11.4 nA/mM to a series of standard additions. After 5 days of continuous operation at 37°C in whole blood samples, replenished every 24 h, the calibration slope had changed to 13.6 nA/mM. The variability in slope may represent a change in electrode response over time as others have reported [34,35], however, the variability in mass transport rates due

to differing blood viscosity, electrode positioning, and stirring rates make the source of variation uncertain in this study.

On the sixth day of testing at 37°C, the electrode pair failed and examination showed the Nafion layer had separated from the glass shroud around the electrode, partially removing the enzyme film from the Pt surface. Poor adhesion of solution cast Nafion films on glass and Pt is a recognized problem. Szentirmay, *et al.* have developed [36] an adhesion promotion scheme that involves silanization of the substrate with N-trimethoxysilylpropyl-N,N,N-trimethylammonium chloride prior to casting of the film. We have used this and similar methods to pretreat electrodes prior to preparation of both the enzyme and Nafion membranes on the electrode. The resulting membrane assembly is much more strongly adherent and the films are also much less mechanically fragile. Details of these modification procedures will be presented in Chapter 5 along with a discussion of *in vivo* tests of an implantable version of the modified electrodes.

2.4 CONCLUSIONS

The performance characteristics of the integrated, two-electrode potentiostat allow several design criteria for sensor implantation to be met. The current detection limit of ± 2 nA for the electronics is sufficiently low that the small electrode dimensions required for implantation can be accommodated. The relatively low power draw (~ 0.5 mW) of the CMOS circuitry offers an advantage over assembly of the electronics from discrete components. Furthermore, the sensitive electronics are readily protected from the harsh *in vivo* environment by separating the sensing element from the chip in packaging of the sensor. Clearly, the same or similar type of potentiostatic control circuit could also act as the basis for other miniaturized or integrated chemical sensors.

The use of Nafion cast from solutions of the ionomer as a dialysis material appears to be an attractive approach to the determination of small neutral or cationic electroactive molecules in biological media. The reproducibility of dialyzing action from one Nafion coated electrode to another in whole blood, and the ease of film preparation, are important

features of this material. Perhaps also of significance is the fact that Nafion has many of the attributes that have been suggested as desirable for obtaining a significant level of biocompatibility [37]. These include having both hydrophilic and hydrophobic properties, being chemically inert, and being subject to relatively little adsorption of species from solution. While the preliminary lifetime study in whole blood *in vitro* is encouraging, it is necessary to evaluate the biocompatibility of Nafion polymer before pursuing further testing of this sensor *in vivo*. Finally, while we have focussed on the determination of glucose via H_2O_2 in whole blood, Nafion dialysis coatings on electrodes may also be a useful means of enhancing the measurement of other electrochemically assayable species in this medium.

3.5 REFERENCES

- [1] S.J. Updike and G.P. Hicks, "The Enzyme Electrode", *Nature*, Vol. 214, pp. 986-988, 1967.
- [2] A.M. Albisser, B.S. Leibel, T.G. Ewart, Z. Davidovac, C.K. Botz and W. Zingg, "An Artificial Endocrine Pancreas", *Diabetes*, Vol. 23, pp. 389-396, 1974.
- [3] L.C. Clark, Jr. and C.A. Duggan, "Implanted Electroenzymatic Glucose Sensors", *Diabetes Care*, Vol. 5, No. 3, pp. 174-180, 1982.
- [4] G.G. Guilbault and G.J. Lubrano, "Enzyme Electrode for Glucose", *Anal. Chim. Acta*, Vol. 60, pp. 254-255, 1972.
- [5] D.R. Thévenot, "Problems in Adapting a Glucose-Oxidase Electrochemical Sensor Into an Implantable Glucose-Sensing Device", *Diabetes Care*, Vol. 5, No. 3, pp. 184-189, 1982.
- [6] S.J. Updike, M. Shults and B. Ekman, "Implanting the Glucose Enzyme Electrode: Problems, Progress and Alternative Solutions", *Diabetes Care*, Vol. 5, No. 3, pp. 207-212, 1982.
- [7] M. Shichiri, R. Kawamori, Y. Goriya, Y. Yamasaki, M. Nomura, N. Hakui and H. Abe, "Glycaemic Control in Pancreatectomized

Dogs with a Wearable Artificial Endocrine Pancreas", *Diabetologia*, Vol. 24, pp. 179-184, 1983.

- [8] S. Ikeda, K. Ito, T. Kondo, K. Ichikawa, T. Yukawa and H. Ichihashi, "Prolongation of Life-Time of Enzyme Electrode Type Glucose Sensor for Artificial Pancreas", *Anal. Chem. Symp. Ser., Proc. Chem. Sensors*, Fukuoka, Japan, Sept. 19-22, Vol. 17, pp. 620-625, Elsevier, Tokyo, 1983.
- [9] D.A. Gough, J.Y. Lucisano and P.H.S. Tse, "Two-Dimensional Enzyme Electrode Sensor for Glucose", *Anal. Chem.*, Vol. 57, pp. 2351-2357, 1985.
- [10] A.E.G. Cass, G. Davis, G.D. Francis, H.A.O. Hill, W.J. Aston, I.J. Higgins, E.V. Potkin, L.D.L. Scott and A.P.F. Turner, "Ferrocene-Mediated Enzyme Electrode for Amperometric Determination of Glucose", *Anal. Chem.*, Vol. 56, pp. 667-671, 1984.
- [11] Y. Hanazato and S. Shono. "Bioelectrode Using Two Hydrogen Ion Sensitive Field Effect Transistors and a Platinum Wire Pseudo Reference Electrode", *Anal. Chem. Symp. Ser., Proc. Chem. Sensors*, Fukuoka, Japan, Sept. 19-22, Vol. 17, pp. 513-520, Elsevier, Tokyo, 1983.
- [12] S.D. Caras, D. Petelenz and J. Janata, "pH-Based Enzyme Potentiometric Sensors. Part 2. Glucose-Sensitive Field Effect Transistor", *Anal. Chem.*, Vol. 57, pp. 1920-1923, 1985.
- [13] L.B. Wingard, Jr., C.C. Liu, S.K. Wolfson, Jr., S.J. Yao and A.L. Drash, "Potentiometric Measurement of Glucose Concentration with an Immobilized Glucose Oxidase/Catalase Electrode", *Diabetes Care*, Vol. 5, pp. 199-202, 1982.
- [14] D.A. Gough and L. Leyboldt, *Applied Biochemistry and Bioengineering*, pp. 175-207, Academic Press, New York, 1981.

- [15] R.F.B. Turner, D.J. Harrison and H.P. Baltes, "A CMOS Potentiostat for Amperometric Chemical Sensors", *IEEE J. Solid-State Circuits*, Vol. SC-22, pp. 473-478, 1987.
- [16] J. Janata, "Chemically Sensitive Field Effect Transistors", Chapter 2 in *Solid State Chemical Sensors*, J. Janata, R.J. Huber, Eds., pp. 66-118, Academic Press, London, 1985.
- [17] J.Y. Lucisano, J.C. Armour and D.A. Gough, "In Vitro Stability of an Oxygen Sensor", *Anal. Chem.*, Vol. 59, pp. 736-739, 1987.
- [18] M. Koudelka, S. Gernet and N.F. de Rooij, "Voltammetry—A Powerful Tool for Evaluation and Process Control of Thin Film Electrodes", *Transducers '87*, 4th Intl. Conference on Solid State Sensors and Actuators, June 2-5, Tokyo, Japan, Digest of Technical Papers, pp. 41-44, 1987.
- [19] G.A. Gerhardt, A.F. Oke, F. Nagy, B. Moghaddam and R.N. Adams, "Nafion-Coated Electrodes with High Sensitivity for CNS Electrochemistry", *Brain Research*, Vol. 290, pp. 390-395, 1984.
- [20] G. Nagy, G.A. Gerhardt, A.F. Oke, M.E. Rice, R.N. Adams, R.B. Moore III, M.N. Szentirmay and C.R. Martin, "Ion Exchange and Transport of Neurotransmitters in Nafion Films on Conventional and Microelectrode Surfaces", *J. Electroanal. Chem.*, Vol. 188, pp.85-94, 1985.
- [21] E.W. Kristensen, W.G. Kuhr and R.M. Wightman, "Temporal Characterization of Perfluorinated Ion Exchange Coated Microvoltammetric Electrodes for *In Vivo* Use", *Anal. Chem.*, Vol. 59, pp. 1752-1757, 1987.
- [22] T. Yao, "A Chemically Modified Enzyme Membrane Electrode as an Amperometric Glucose Sensor", *Anal. Chim. Acta*, Vol. 148, pp. 27-33, 1983.

- [23] N.M. Szentirmay and C.R. Martin, "Ion-Exchange Selectivity of Nafion Films on Electrode Surfaces", *Anal. Chem.*, Vol. 56, pp. 1898-1902, 1984.
- [24] H.S. White, J. Leddy and A.J. Bard, "Polymer Films on Electrodes 8: Investigation of Charge Transport Mechanisms in Nafion Polymer-Modified Electrodes", *J. Am. Chem. Soc.*, Vol. 104, pp. 4811-4817, 1982.
- [25] Z. Ogumi, Z. Takehara and S. Yoshizawa, "Gas Permeation in SPE Method: I. Oxygen Permeation Through Nafion and NEOSEPTA", *J. Electrochem. Soc.*, Vol. 131, pp. 769-773, 1984.
- [26] S. Gottesfeld, I.D. Raistrick and S. Srinivasan, "Oxygen Reduction Kinetics on a Platinum RDE Coated with a Recast Nafion Film", *J. Electrochem. Soc.*, Vol. 134, pp. 1455-1462, 1987.
- [27] J. Redepenning and F.C. Anson, "Permselectivities of Polyelectrolyte Electrode Coatings as Inferred from Measurements with Incorporated Redox Probes or Concentration Cells", *J. Phys. Chem.*, Vol. 91, pp. 4549-4553, 1987.
- [28] J.T. Sorensen, C.J. Colton, R.S. Hillman and J.S. Soeldner, "Use of a Physiologic Pharmacokinetic Model of Glucose Homeostasis for Assessment of Performance Requirements for Improved Insulin Therapies", *Diabetes Care*, Vol. 5, pp. 148-157, 1982.
- [29] H. Lerner, J. Giner, J.S. Soeldner and C.K. Colton, "An Implantable Electrochemical Glucose Sensor", *Annals. N.Y. Acad. Sci.*, Vol. 428, pp. 263-278, 1984.
- [30] G.L. Richter, G. Luft and U. Beghardt, "Development and Present Status of an Electrocatalytic Glucose Sensor", *Diabetes Care*, Vol. 5, pp. 224-228, 1982.
- [31] W.T. Caraway, In *Fundamentals of Clinical Chemistry*, N.W. Teitz, Ed., pp. 154-155, W.B. Saunders, Philadelphia, 1970.

- [32] P. Ingram, S. Ingram, S. Turtle, S. Sturrock and D. Applegarth, "Comparison of Glucose Determinations Obtained from Whole Blood and Plasma", *Clin. Biochem.*, Vol. 4, pp. 297-301, 1971.
- [33] G.W. McDonald, G.F. Fisher and C.E. Burnham, "Difference in Glucose Determinations Obtained from Plasma or Whole Blood", *Public Health Reports*, Vol. 79, pp. 515-520, 1964.
- [34] G.G. Guilbault and G.J. Lubrano, "An Enzyme Electrode for the Amperometric Determination of Glucose", *Anal. Chim. Acta*, Vol. 64, pp. 439-455, 1973.
- [35] D.R. Thévenot, R. Sternberg and P.R. Coulet, "A Glucose Electrode Using High-Stability Glucose-Oxidase Collagen Membranes", *Diabetes Care*, Vol. 5, No. 3, pp. 203-206, 1982.
- [36] M.N. Szentirmay, L.F. Campbell and C.R. Martin, "Silane Coupling Agents for Attaching Nafion to Glass and Silica", *Anal. Chem.*, Vol. 58, pp. 661-662, 1986.
- [37] S.D. Bruck, *Blood Compatible Synthetic Polymers*, C. Thomas Charles, Springfield, Chapter 3, 1974.

CHAPTER 4

Preliminary *In Vivo* Biocompatibility Studies on Perfluoro-sulfonic Acid Polymer Membranes for Biosensor Applications†

The first biocompatibility studies on the DuPont perfluorosulfonic acid (Nafion) polymer are presented. Presterilized samples of commercially cast and solution cast Nafion membranes were implanted subcutaneously, intraperitoneally and intravenously in male Sprague-Dawley rats. Scanning electron microscopy and histological examination of explanted samples and surrounding tissues reveal little, if any, evidence of a severe acute or chronic foreign body inflammatory response. The fibrous capsules surrounding the implants remain nominally thin (<100 μ m) after more than 3 months *in situ*, and the surrounding tissues remain well vascularized. Nafion polymer is found to exhibit sufficient biocompatibility to make it a viable candidate for some implantable biosensor applications. It may, however, be necessary to compensate for the effects of the progression of fibrous encapsulation on sensor performance, particularly during the acute response stage.

4.1 INTRODUCTION

The potential for the realization of new clinical diagnostic and therapeutic devices has steered an enormous amount of research effort toward the development of biosensors for medical applications. Recent advances in analytical chemistry and related sensor technology have indeed allowed some previously complicated laboratory assay procedures to be accomplished with a single, miniaturized, solid state probe, at least *in vitro* [1,2]. However, implantable biosensors for long-term *in vivo* monitoring, have remained an elusive goal, primarily because conventional membrane materials that are biocompatible, are not necessarily "sensor compatible", and *vice versa* [3].

† A version of this chapter has been submitted for publication as:

R.F.B. Turner, D.J. Harrison and R.V. Rajotte. "Preliminary Biocompatibility Studies on Perfluorosulfonic Acid Polymer Membranes for Biosensor Applications", Submitted to *Biomaterials*, 1990.

Merging biocompatibility considerations with sensor membrane requirements results in an extremely challenging set of criteria. From a functional point of view, a sensor encapsulating (dialysis) membrane must ensure the stability of desirable mass transport conditions for analyte and electrolyte species and, ideally, the exclusion of interfering species. In fact, any significant changes in the permeability characteristics of the membrane, or the surrounding tissues, will affect the calibration of the sensor. Thus, in addition to the direct and obvious concerns regarding the well being of the host, biocompatibility is also involved in the requirements of the sensor itself. It is also important to realize that a proposed sensor encapsulation material must yield reproducible and structurally stable membranes without the need for high temperature processing, at least for the broad class of biosensors which employ temperature-sensitive proteins (e.g. enzymes) or micro-organisms in order to achieve the required specificity.

Our own efforts in this field have focused on the development of whole blood glucose sensors based on the enzyme glucose oxidase. Several polymer dialysis membrane materials have previously been proposed for use in whole blood including cellulose and cellulose acetates [4,5], polyurethane [6], polypropylene [7] and silicone rubber [8]. Unfortunately though, none of these materials have sufficiently satisfied the combined sensor and biocompatibility criteria so as to be considered suitable for long-term *in vivo* monitoring. We have, however, recently reported superior reproducibility and performance in whole blood *in vitro* with the use of perfluorosulfonic acid (Nafion®) polymer membranes [9]. Nafion membranes have previously been used to suppress ascorbate interference during acute *in vivo* determination of various neurotransmitters [10,11]. Biosensor dialysis membranes thus represent a novel and promising application of this material, although very little is presently known about its biological compatibility. To our knowledge, the only previous investigations of the biological response to Nafion polymer have been limited to acute toxicity (oral ingestion) and skin irritation tests [12].

Nafion is a linear copolymer derived from tetrafluoroethylene and either perfluorosulfonic acid or perfluorocarboxylic acid monomers.

Structurally, Nafion is a close relative of Teflon® except that the saturated fluorocarbon backbone is randomly substituted with perfluorinated side chains that terminate in either sulfonic acid or carboxylic acid groups. Detailed studies of the morphology, as well as the chemical, thermal and mechanical properties of Nafion membranes have been reported elsewhere [13]. Nafion is commercially available both as a thermally cured solid sheet, and in a dissolved form that can be solvent cast in the laboratory to produce thin films. Morphological differences exist between these two forms that lead to differences in permeability and solvent swelling characteristics.

Our objective here was to examine the biocompatibility of Nafion polymer, in order to determine whether or not it would be feasible to pursue the development of implantable biosensors based on Nafion encapsulating membranes. The scope of our investigation is conceptually limited to aspects of the tissue and blood response of most immediate concern to such applications. These results are preliminary in the sense that we have not attempted to undertake a comprehensive evaluation, and we acknowledge that further testing would be required before any clinical use of this material could be contemplated. In this study, we have considered both morphological forms of the polymer—commercially cast films cured at high temperature, and the uncured form cast from the soluble form of the polymer. We sought an overview of both the short-term (1-4 days) and long-term (several months) biological response. The approach involved implanting samples of the two forms of the polymer at several *in vivo* sites regarded as potentially important to biosensor applications, and examining the response using histochemical and microscopic methods.

4.2 MATERIALS AND METHODS

4.2.1 Biosensor Considerations

Certain aspects of the methodology employed here, specifically the choice of sterilization technique and the choice of implant sites and duration *in situ*, reflect the proposed application as a membrane material for biosensor encapsulation. Enzyme based biosensors are, of course, non-autoclavable due to the temperature sensitivity of the protein components.

Furthermore, exposure of solution cast Nafion membranes to high temperatures is known to cause morphological changes in the polymer [14] which, in turn, have undetermined effects on the performance of the dialysis membrane. Ethylene oxide sterilization was investigated as an alternative (to alcohol), however it was found that the ethylene oxide reacted with solvent residues in solution cast Nafion films and the products were retained in the film. The implant sites employed in this study correspond with sites previously proposed for *in vivo* glucose sensor implantation [15-17], and the c. 100 day durations *in situ* are considered nominally useful durations for implantable sensor applications. Short duration implants of 1 to 43 days were included in order to provide some indication of the acute response, and to determine whether in fact a relatively stable tissue environment around the implant could be expected in the short-term.

4.2.2 Implant Preparation

Commercially precast sheets of DuPont Nafion 117 membrane (thickness 0.20 mm) was obtained from The Electrosynthesis Co., Inc. (East Amherst, N.Y.). Subcutaneous and abdominal cavity implants were cut from the precast sheets in the shape of circular discs with diameters of 6 mm, 10 mm and 16.5 mm. Intravenous implants were also cut from the precast sheets in narrow strips with a rectangular cross section (approximately) 0.6 mm by 0.2 mm, and a length of approximately 5 cm. Implants were thoroughly cleaned by repeated cycles of rinsing in distilled, deionized water and sonicating in a 1:1 solution of isopropanol and distilled, deionized water. Implants were then transferred to a sterilizing solution of concentrated (100%) ethanol or isopropanol.

Dissolved Nafion polymer (1100 E.W., 5% solution in lower aliphatic alcohols and water) was obtained from Solution Technology, Inc. (Mendenhall, Penn.). Thermally cured Nafion films are structurally very stable and are the obvious substrate on which to cast uncured membranes in order to avoid artifacts in the biological response due to the introduction of another material. Thus, in order to simulate an uncured membrane such as would be used for sensor encapsulation, some of the sterilized commercially cast Nafion samples described above were dip-coated twice using the 5% Nafion solution. These films were allowed to air dry at room

temperature, and the coated implants were then transferred back to a (separate) sterilizing solution. All samples remained immersed in alcohol for at least 48 hrs. prior to implantation.

For comparison purposes, similar implants were fabricated from Silastic® Medical-Grade implant materials obtained from Dow Corning Corp. (Midland, Mich.). Circular disc shapes (diameter 6 mm, thickness 1.02 mm) were cut from Silastic 501-7 Subdermal Implant sheeting for subcutaneous and abdominal cavity implants. Intravenous implants were formed from Silastic tubing (O.D. 0.64 mm) filled with Silastic Type A adhesive. These control implants were cleaned exactly as the Nafion implants, and similarly sterilized in alcohol for at least 48 hrs. prior to implantation.

4.2.3 Implant Procedures and Treatment of Recovered Specimens

Male Sprague-Dawley rats (200-400 g at time of implantation) were anaesthetized with sodium pentobarbital (40 mg/kg IP) and surgically implanted, under aseptic conditions, with a prescribed combination of each of the implant types described above. Subcutaneous implants were placed unanchored in a pocket formed by blunt dissection under the skin of the medial aspect of both inner thighs and the anterior aspect of the upper abdomen. Abdominal cavity implants were anchored with sutures (4-0 silk) to the omentum and to the rectus abdominis muscle of the abdominal wall. Intravenous implants were introduced into the inferior vena cava through venipuncture sites made using a 22 gauge hypodermic needle. Approximately 1-2 cm of the implant length was retained outside the vessel, which was sutured (4-0 silk) to the psoas muscle. All animals received penicillin as Derapen-C® (0.2 ml IM) immediately following implant surgery.

Animals were sacrificed after 1, 2, 4, 43, 95, 103, 105 or 206 days and the implants were recovered along with surrounding tissues, rinsed briefly in normal saline and placed in an appropriate fixing solution. Specimens intended for general histological examination were fixed in 10% formaldehyde (in acetate buffer, pH 7.0), dehydrated in a graded series of ethanol (70%-95%) and mounted in poly(methyl methacrylate) blocks.

Transverse sections were stained with methylene blue-basic fuchsin and viewed under a light microscope. Some selected specimens were mounted in paraffin blocks and transverse sections were stained by the Ledrum Acid Picro-Mallory method (Culling) [18] in order to differentiate between collagen and fibrin. Specimens intended for scanning electron microscopy (SEM) were fixed in 2.5% glutaraldehyde (in Millonig's buffer, pH 7.2), post-fixed in 1% osmium tetroxide, dehydrated in a graded series of ethanol (50%-100%) and critical point dried. Dehydrated specimens were then mounted on stubs and sputter-coated with gold/palladium prior to viewing. In all, 121 specimens were examined from 25 different rats. Of these, 60 samples were recovered from subcutaneous sites, 37 were recovered from abdominal cavity sites and 24 from intravenous sites. The distribution among specific implant sites is shown in Table 4.1 along with the durations *in situ*.

4.3 RESULTS AND DISCUSSION

4.3.1 Short-Term Implants

Subcutaneous and Intraperitoneal Sites

Subcutaneous and abdominal cavity implants removed at the 1-4 day stage were coated with a clear viscous fluid, but appeared to be free of any tissue adhesions at the time of removal. No inflammation was visible in nearby tissues, including the subcutaneous implant pockets. The overviews depicted in Figures 4.1(a) and 4.2(a) (1 day and 4 days, respectively) show patches of dehydrated transudated fluid over some regions of the implant surface, and remnants of what appears to be early stages of fibrosis. Fibroblasts are indeed visible in close-up views, and the size and surface morphologies of some of the other species visible in Figure 4.2(b), for example, indicate some monocyte/macrophage activity. The average populations of these cells, however, do not suggest a severe inflammatory response. Histological examination of similar implants also revealed a few inflammatory cells, but again a severe response was not indicated.

TABLE 4.1 Distribution of recovered specimens among specific implant sites. Each entry specifies the number of specimens times the number of days *in situ*. The subcutaneous sites include the medial aspect of both inner thighs and the anterior aspect of the upper abdomen. The abdominal cavity sites include the omentum (attached by a 4-0 silk suture) and the anterior abdominal wall (sutured to the rectus abdominis muscle).

INTRAVENOUS SITES			SUBCUTANEOUS SITES			ABDOMINAL CAVITY SITES		
Plain ^a	Coated ^b	Silastic ^c	Plain	Coated	Silastic	Plain	Coated	Silastic
4x1d.			6x1d.			4x1d.		
4x2d.			6x2d.			4x2d.		
4x4d.			6x4d.			4x4d.		
1x43d.	1x43d.	1x43d.	3x43d.	3x43d.	3x43d.	2x43d.	2x43d.	2x43d.
2x95d.			7x95d.	4x95d.		2x95d.	1x95d.	
1x103d.	1x103d.	1x103d.	3x103d.	3x103d.	3x103d.	2x103d.	2x103d.	2x103d.
2x105d.	1x105d.	1x105d.	5x105d.	3x105d.	3x105d.	3x105d.	3x105d.	2x105d.
			2x206d.			1x206d.		

(a) Uncoated, unmodified commercially precast Nafion polymer; implants were cut to form either narrow strips (IV only) or circular discs with diameters of 6 mm, 10 mm or 16.5 mm.

(b) As above, but coated with solution-cast Nafion polymer (Solution Technologies 5%).

(c) Medical grade Silastic® silicone rubber tubing (IV only) (0.64 mm o.d.) or circular discs (3 mm dia.).

Intravenous Sites

The sections of inferior vena cava which hosted the intravenous implants were excised without removal of the implant from the vessel and hence no immediate visual observation of the implant surface could be made. However, except for attachments around the actual venipuncture site, the implants appeared to move freely inside the lumen of the vessel. The specimens shown in Figures 4.3 and 4.4 (1 day and 4 days, respectively) were cut from a part of the implant exposed by contraction of the distal end of the vessel from the point of excision. The encapsulation visible in the overviews of Figures 4.3(a) and 4.4(a) is clearly more developed than that surrounding the extravascular implants, and several trapped or adhering cell species were found over some areas of the capsule. The populations of these cells do not suggest gross inflammation at this stage, although substantial thrombosis is manifest over the entire surface after 1 day of implantation as shown in Figure 4.3(a). Figure 4.3(b) shows a close-up view of a region near the centre of the field of Figure 4.3(a). A fibrin deposit can be seen with a significant number of platelets and white blood cells visible on the surface. After 4 days of implantation, the fibrous tissue growth has become more dense as shown in Figure 4.4(b). Histology samples were stained using the Ledrum Acid Picro-Mallory method [18] in order to differentiate between collagen and fibrin. This stain showed that after 4 days a re-organization of the fibrous tissue is well advanced, with both fibrin and collagen present. Complete re-organization to collagen occurs after long-term implantation (*vide infra*). Remnants of newly formed thrombi over the outer surface of the encapsulated regions shown in Figure 4.4(a) may have resulted from the surgical procedures, since blood from the lower extremities was impaired for several minutes prior to removal, and some evidence of thrombus formation was visible in the pooled blood that was cleared in the saline rinse following removal.

Figures 4.1 through 4.4 indicate that a Nafion encapsulated sensor would invoke a short-term biological response that, although not severe, is likely to cause a drift in the calibration characteristic. The present study was not designed to resolve the time evolution of this short-term response. Rather, a series of long-term implants were studied to determine what, if

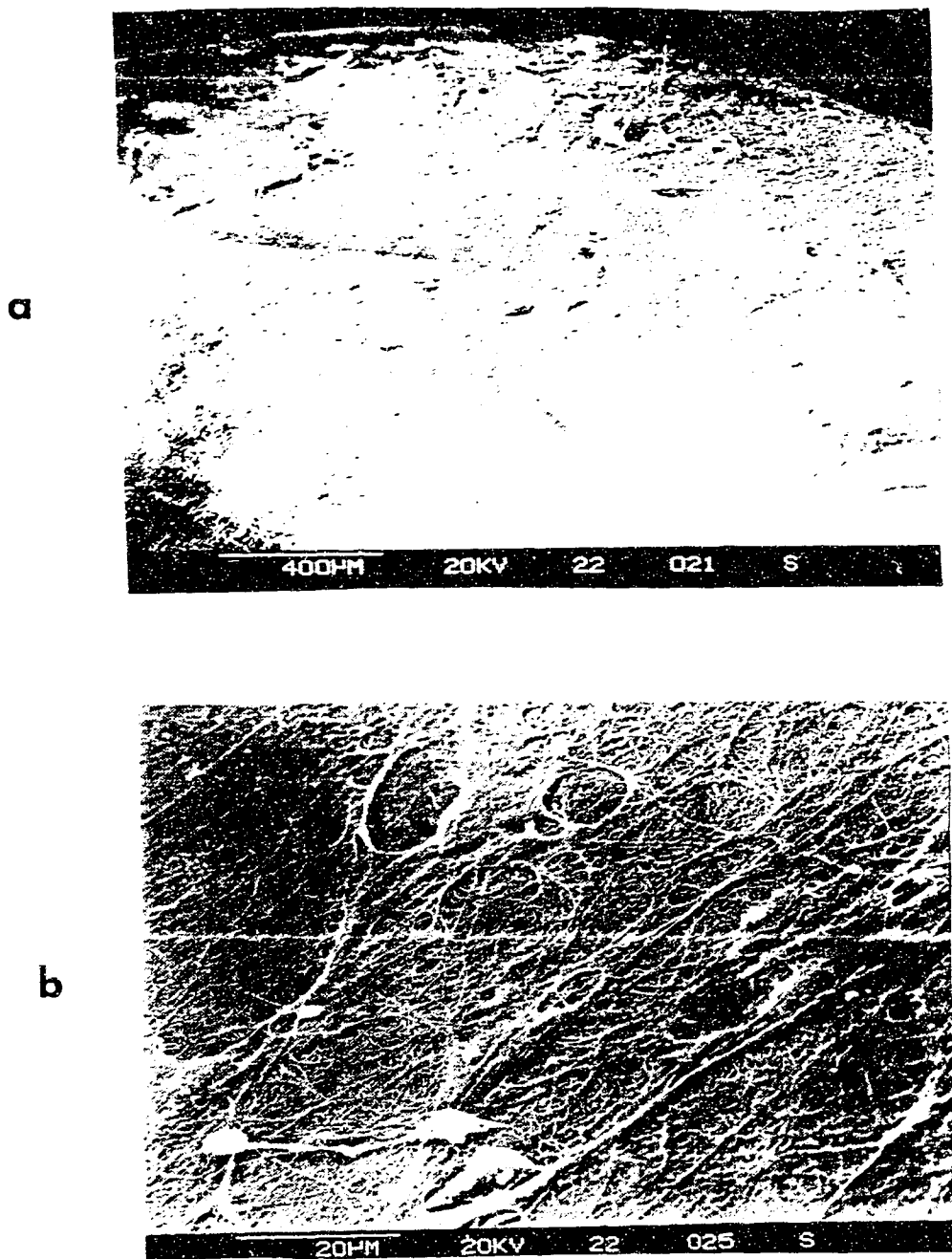


Figure 4.1 Scanning electron micrographs showing surface features of subcutaneous (L. thigh) disc shaped Nafion implant after 1 day *in situ*: (a) typical overview near edge (original magnification 52x); (b) close-up view near center of field in (a) (original magnification 1060x).

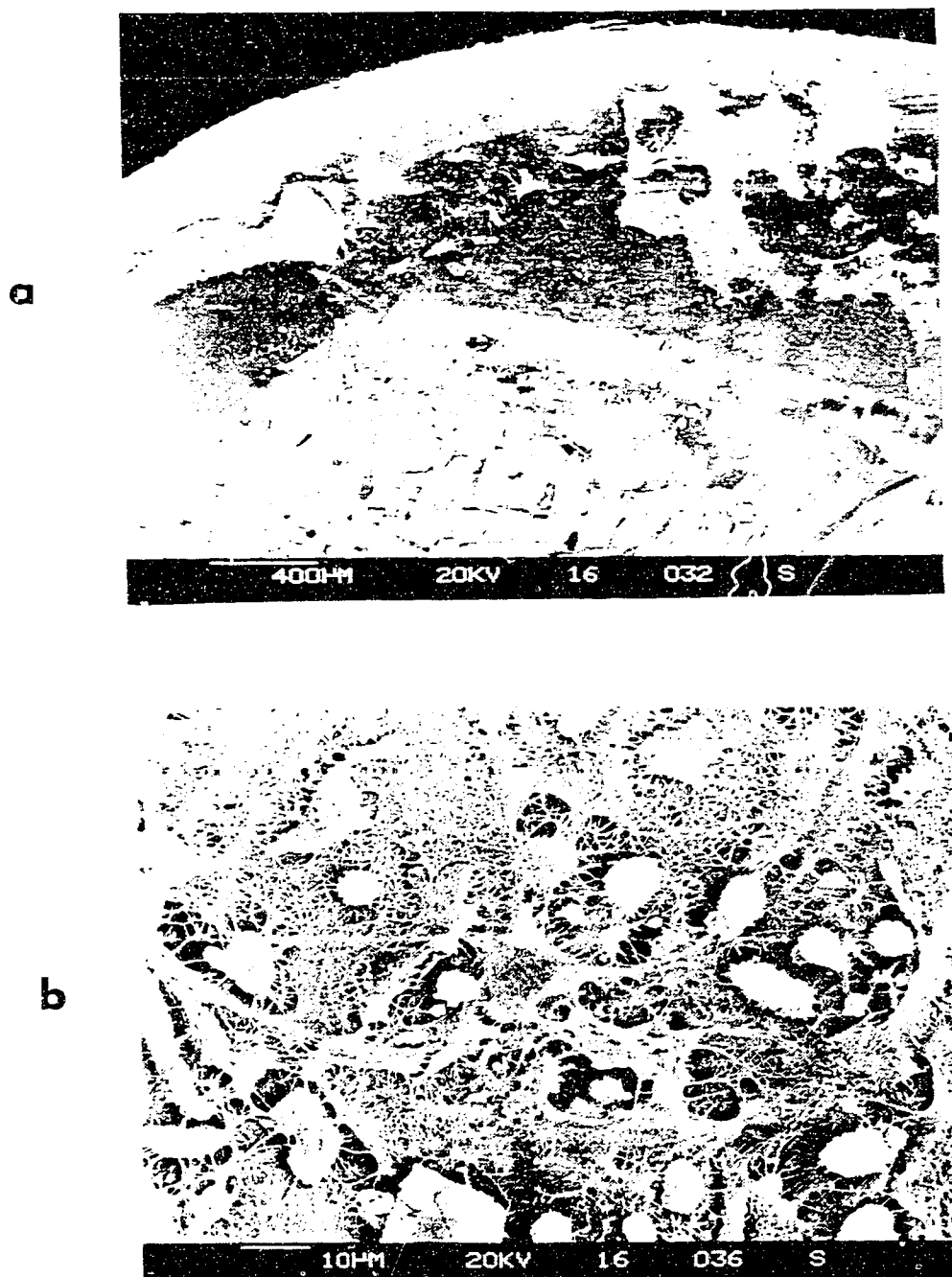


Figure 4.2 Scanning electron micrographs showing surface features of subcutaneous (L. thigh) disc shaped Nafion implant after 4 days *in situ*: (a) typical overview near edge (original magnification 32x); (b) close-up view of fibrous region slightly right of center of field in (a) (original magnification 600x).

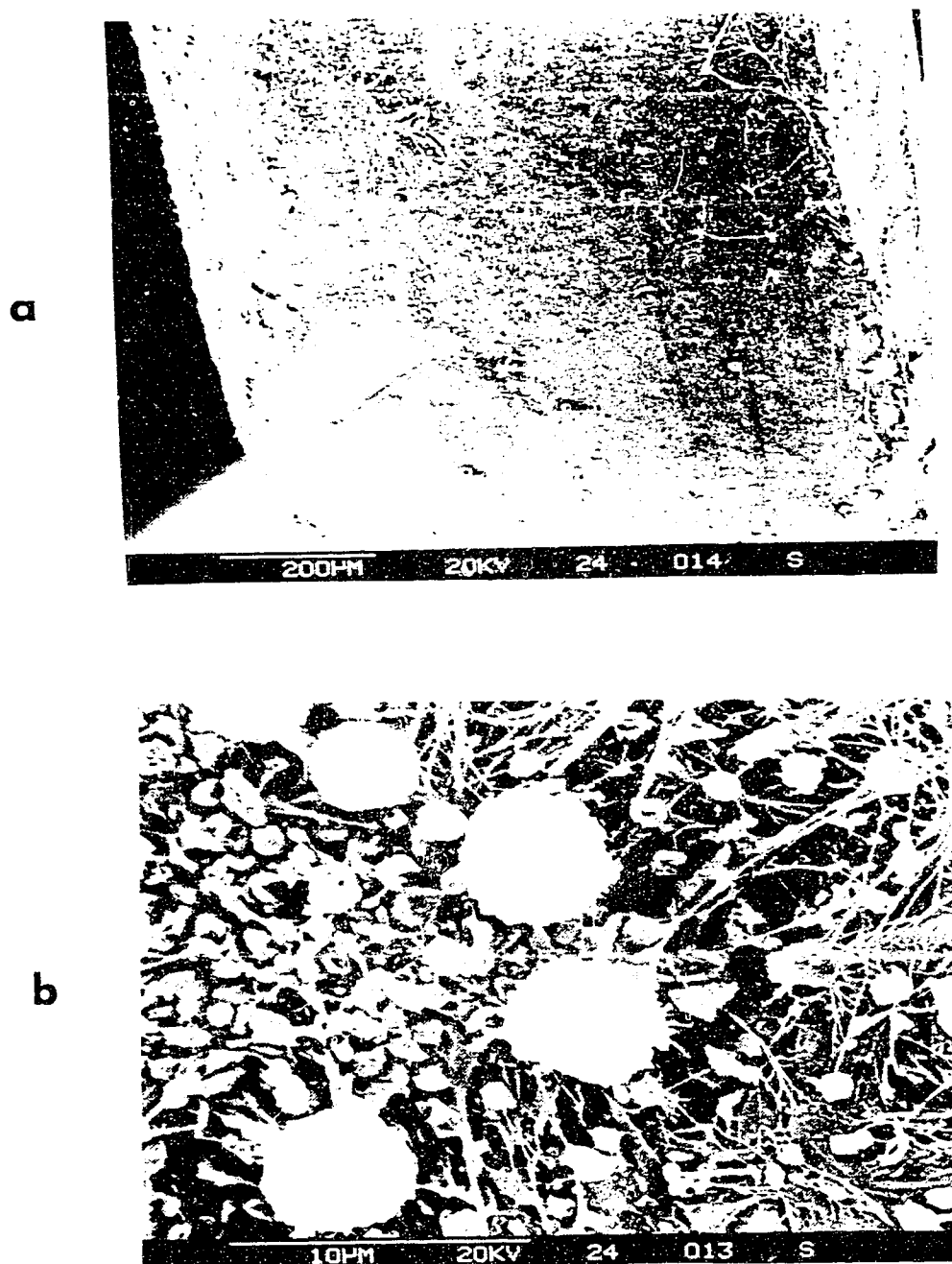


Figure 4.3 Scanning electron micrographs showing surface features of intravenous (inferior vena cava) cannula shaped Nafion implant after 1 day *in situ*: (a) overview showing both anterior and lateral aspects (original magnification 100x); (b) close-up near center of field in (a) (original magnification 3900x).

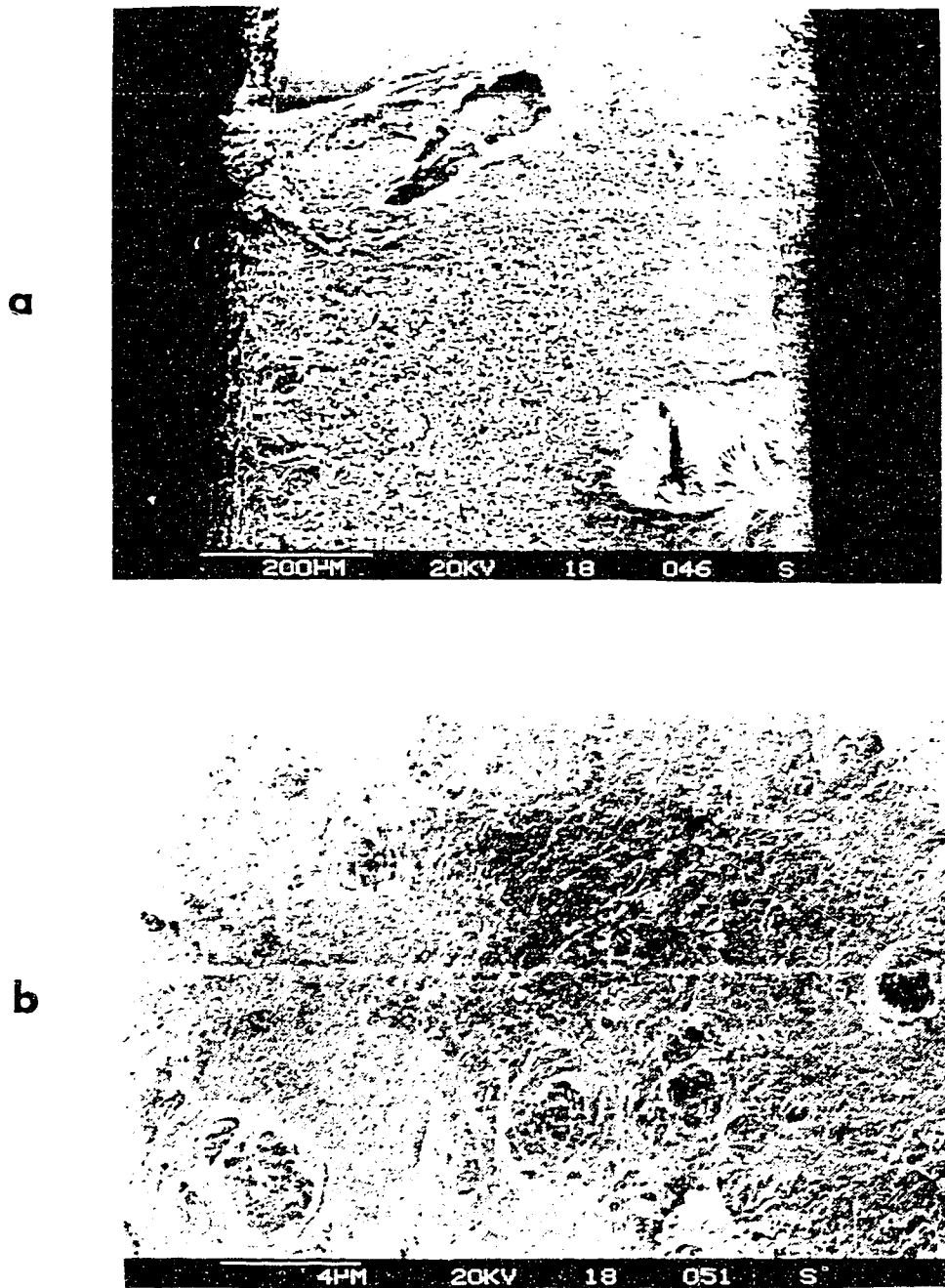


Figure 4.4 Scanning electron micrographs showing surface features of intravenous (inferior vena cava) cannula shaped Nafion implant after 4 days *in situ*: (a) overview of anterior aspect (original magnification 115x); (b) close-up view of fibrous capsule upper right from center of field in (a) (original magnification 4300x).

any, steady state situation develops. In any case, some means of recalibrating an implanted sensor *in situ* would seem to be required, and should be provided for, in the design of the sensor electronics.

4.3.2 Long-Term Implants

Subcutaneous Sites

Long-term subcutaneous implants were removed by dissecting the loose connective tissue surrounding the encapsulated implant. No obvious inflammation or infection was evident in these tissues at the time of explantation in any of the cases studied. In most cases, the fibrous capsule itself was recovered intact in order to preserve the relationship between capsular features and the surface of the implant. The few implants that were removed from the fibrous tissue capsule at the time of explantation were free of adhesions, and subsequent examination by SEM revealed surface features that were similar to those depicted in Figure 4.2(a).

Two different morphological forms of Nafion polymer were employed in the long-term studies. Commercially cast film cured at high temperatures (referred to here as Type I), and the uncured form prepared by casting a thin film of 5% Nafion solution on a commercial film substrate (referred to here as Type II). The specimens shown in Figures 4.5 and 4.6 are typical of Type I and Type II subcutaneous Nafion implants respectively, after 100 ± 5 days *in vivo*. In all cases, these implants were characterized by a well defined and relatively thin (~ 10 - $100 \mu\text{m}$) fibrous capsule, surrounded by healthy, well vascularized loose connective tissue.

In Figure 4.5, some residual components of the transudated capsular fluid are visible at the surface of this Type I implant, and along some regions of the interior surface of the capsule. In some cases, a few multinucleated giant cells, histiocytes and macrophages could be identified in the residuum, although these were sparse and no other evidence of a chronic inflammatory response was observed. No attempt was made to determine the composition of the transudated fluid lining the capsule *in vivo*, and it therefore remains to be verified that the analyte and electrolyte concentrations in this fluid are indeed in dynamic equilibrium with



Figure 4.5 Partial transverse section of subcutaneous (L. thigh) disc shaped plain (*i.e.* Type I) Nafion implant and surrounding tissues after 105 days *in situ*. The original dimensions of this implant were: 6 mm dia., 0.2 mm thick. (original magnification 50x).

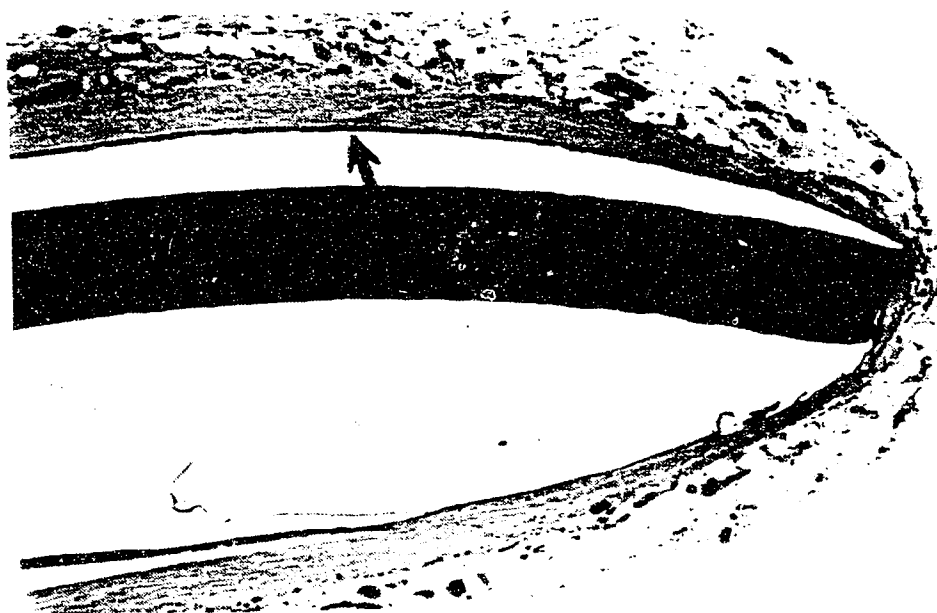


Figure 4.6 Partial transverse section of subcutaneous (L. thigh) disc shaped coated (*i.e.* Type II) Nafion implant and surrounding tissues after 105 days *in situ*. The arrow identifies the thin solution cast Nafion film, which has separated from the underlying solid Nafion substrate. The original dimensions of this implant were: 6 mm dia., 0.2 mm thick. (original magnification 100x).

the corresponding plasma concentrations. This condition depends on the particular analyte species of interest, but it is believed that glucose and electrolytes should be able to permeate a thin fibrous capsule that is surrounded by well vascularized tissue [19].

Similar observations to those discussed above for Type I implants also apply to Type II Nafion, as depicted in Figure 4.6. Unfortunately, Nafion does not exhibit good adhesion to most non-porous substrates following water uptake, unless the surface can be modified with adhesion-promotion reagents [20]. Consequently, the thin ($<10\ \mu\text{m}$) solution cast Nafion coating of the Type II implant can become dislodged from the surface of the solid Nafion substrate. For example in Figure 4.6, the solution cast film actually lines the interior surface of the capsule as indicated by the arrow. Whether dislocated or not, the solution cast Nafion coating did not appear to elicit a significantly greater biological response than the bare (*i.e.* uncoated) solid Nafion implants.

In order to evaluate the stability of the fibrous capsules, samples of Type I and Type II subcutaneous Nafion implants were examined after 43 days *in vivo*. Type I samples were also examined 206 days after implantation. The fibrous tissue encapsulation associated with these implants was similar in thickness ($10\text{-}100\ \mu\text{m}$) to that observed for the 100 day implants, with surrounding tissues appearing similar to that seen in Figure 4.5 and 4.6. The histology specimens from all three periods of long-term implantation were essentially indistinguishable, indicating that the fibrous encapsulation had stabilized by 43 days.

The section shown in Figure 4.7 is typical of the specimens involving subcutaneous Silastic implants after 100 ± 5 days. In all cases, the Silastic material itself became dislodged from the intracapsular space during microtome sectioning and, in many cases, some tissue loss or damage was also incurred. However, enough of the fibrous capsule remains intact to give a qualitative comparison between the response to Nafion and the response to a known biocompatible material evaluated using the same protocol. In general, the capsules surrounding the Silastic implants are thinner over the planar aspects of the implants, but considerably thicker



Figure 4.7 Partial transverse section of subcutaneous (L. thigh) disc shaped Silastic implant and surrounding tissues after 105 days *in situ*. Note that the long axis of the cross section shown is rotated 90° with respect to that of Figures 4.5 and 4.6 in order to accommodate the full thickness of the implant in the field of view. The original dimensions of this implant were: 6 mm dia., 1.02 mm thick. (original magnification 50x).

around the edges. Unfortunately, the geometries of the Nafion implants were significantly different from the Silastic implants, and the magnitude of the reaction around the perimeter of the Silastic implants may be partly a result of mechanical irritation due to the greater thickness of the implant itself. Geometric effects were not addressed in this study. However, the geometry of the Nafion implants employed here represents a worse situation with respect to mechanical irritation and other geometrical factors than a small, smooth, rounded sensor implant such as would be used in practice.

Intraperitoneal Sites

All of the abdominal cavity implants were anchored by a single 4-0 silk suture placed near the perimeter of the implants. In all cases the most significant reaction was clearly concentrated near the suture site. Regions far from the suture site were often free of fibrous tissue, although an extremely thin fibrous capsule was observed in some cases. The sections of Figures 4.8 through 4.10 (105 days) were all taken from implants that were sutured to the omentum and thus remained fairly mobile within the abdominal cavity. Other samples were sutured to the interior surface of the anterior abdominal wall, and a similar response was observed near the suture site. For these latter samples there was a somewhat greater tendency towards complete encapsulation of the implant, with considerable variability in the capsule thickness. The omentum, pancreas, spleen and other abdominal organs appeared normal and healthy at the time of explantation based on visual inspection. Subsequent histological examination of the tissues surrounding the actual implant did not reveal a severe chronic inflammatory response.

Figure 4.8 includes a portion of the scar tissue that developed around the region near the suture site. In this case, the fibrous capsule did not actually enclose the implant. The tissue visible in Figure 4.8 extends approximately a millimeter beyond the field of view, and the remaining roughly two-thirds of the section has the same appearance as the entire opposing planar aspect, which remains unencapsulated even at 105 days.



Figure 4.8 Partial transverse section of disc shaped plain (*i.e.* Type I) Nafion implant and surrounding tissues after 105 days *in situ* in the abdominal cavity (attached to the omentum). The original dimensions of this implant were: 6 mm dia., 0.2 mm thick. (original magnification 50x).

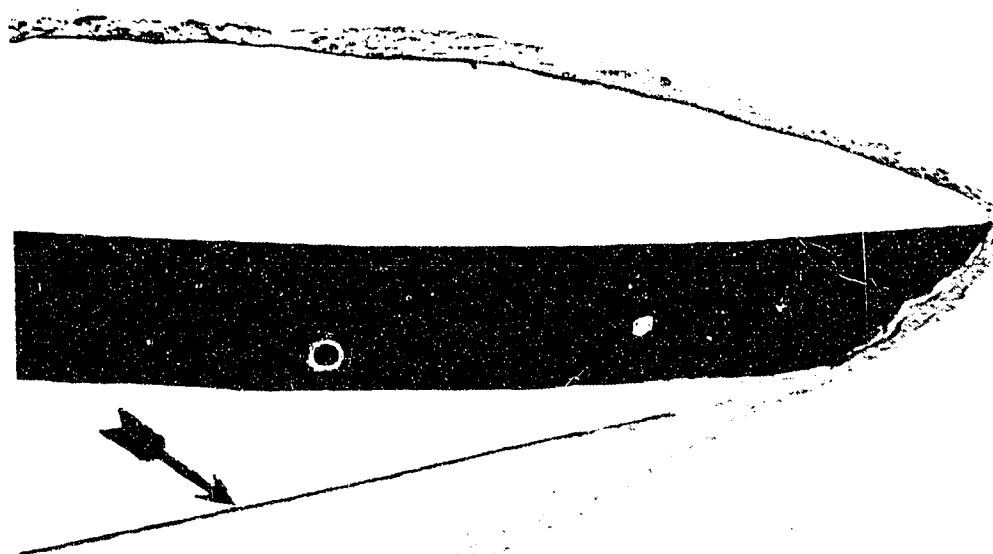


Figure 4.9 Partial transverse sections of disc shaped coated (*i.e.* Type II) Nafion implant and surrounding tissues after 105 days *in situ* in the abdominal cavity (attached to the omentum). The arrow identifies the thin solution cast Nafion film, which has partially separated from the underlying solid Nafion substrate. The original dimensions of this implant were: 6 mm dia., 0.2 mm thick. (original magnification 100x).

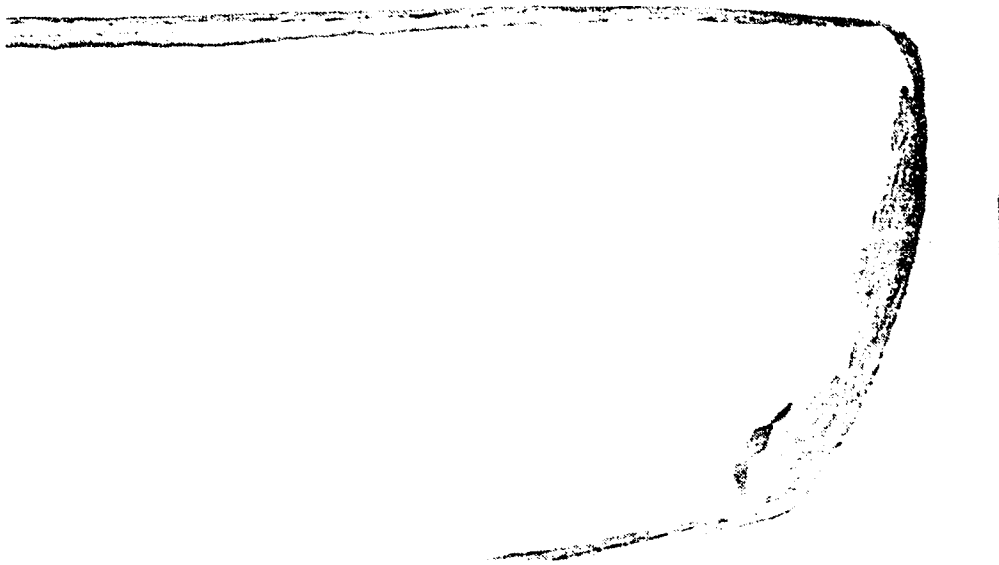


Figure 4.10 Partial transverse sections of disc shaped, Silastic implant and surrounding tissues after 105 days *in situ* in the abdominal cavity (attached to the omentum). The original dimensions of this implant were: 6 mm dia., 1.02 mm thick. (original magnification 50x).

A significant number of inflammatory cells are, however, visible at or near the exposed surfaces.

Figure 4.9 shows a section taken from a Type II Nafion implant recovered after 105 days. Again, the film of solution cast Nafion has become detached from the solid Nafion "substrate" and lines the fibrous capsule over one planar aspect, and appears to be free of both the capsule and the solid Nafion implant over the opposing aspect. In this case the capsule encloses the entire implant, but seems to be comprised mainly of well vascularized granulation tissue with very little organized collagenous connective tissue. Only one of the Nafion implants exhibited a more developed capsule than that shown in Figure 4.9. The general characteristics of Figures 4.8 and 4.9 were observed for both Type I and Type II Nafion samples implanted for periods of 43, 100±5 and 206 days, indicating the relative stability of the tissue encapsulation.

Specimens obtained from Silastic implants were particularly susceptible to microtome damage during sectioning and hence the actual implant material was not retained in these sections. The tissue associated with these specimens was retained and Figure 4.10, for example, shows the fibrous capsule that originally enclosed a 105 day Silastic implant. As with the subcutaneous Silastic implants, the capsule is very thin about the planar aspects and thicker around the perimeter. In Figure 4.10, there is very little vascularized tissue around the capsule, although more was observed for other samples. Virtually all of the long-term Silastic implants showed similar collagenous capsule formation.

Intravenous Sites

The long-term intravenous implants were removed by a similar procedure as described above for the short-term implants. No visual examination of the actual implant could be made at the time of explantation, but the liver and other tissues of the abdominal viscera showed no obvious inflammation or abnormal coloration. There was, however, significant scarring in the vicinity of the original incision of the peritoneum and the site where the implant was sutured to the psoas muscle.

The intravenous implants occupied a substantial volume (e.g. 15-20%) within the original lumen of the vessel, although this partial obstruction did not result in the loss of any experimental animals. Consequently the size and geometry of these implants are likely to be significant determining factors with respect to the overall biological response, somewhat complicating the interpretation of the results [21,22]. The sections shown in Figures 4.11 and 4.12 are typical of Type I and Type II Nafion implants respectively, after 100 ± 5 days in the inferior vena cava. In all of the cases studied, the fibrous capsules were substantially thicker than those associated with extravascular implants. Differential (Culling) staining of the histology specimens identified the fibrous encapsulation as collagen, indicating re-organization of the original fibrin deposits, as depicted in Figures 4.3 and 4.4, is complete. For all samples some evidence was observed of endothelialization of the capsule tissues resulting, ultimately, in total exclusion of the implant from the active lumen of the vessel. The fibrous encapsulation of implants recovered after 43 days was similar to that of the longer term implants, although there was no evidence of endothelialization at this stage.

Notice that in Figure 4.12 the solution cast Nafion film remains relatively intact over most of the surface of the Type II implant. A few small pieces of the solution cast film have been dislodged and subsequently isolated by, or rather imbedded in, the main implant capsule, yet this did not greatly perturb the structure of the capsule itself. In some cases, displaced solution cast Nafion pieces were actually found outside the main implant capsule and did not really exhibit a well defined fibrous encapsulation at all, and nearby tissues remained well vascularized. Too few instances of this behavior were observed to permit further discussion here, although it is suggestive that it would perhaps be worth pursuing further testing involving small fragments or microspheres of solution cast Nafion.

Figure 4.13 shows a typical section of the fibrous capsule that originally surrounded a Silastic implant after 105 days in the vena cava. Typically, the capsules surrounding intravenous Silastic implants were substantially thinner than those surrounding the Nafion implants. There

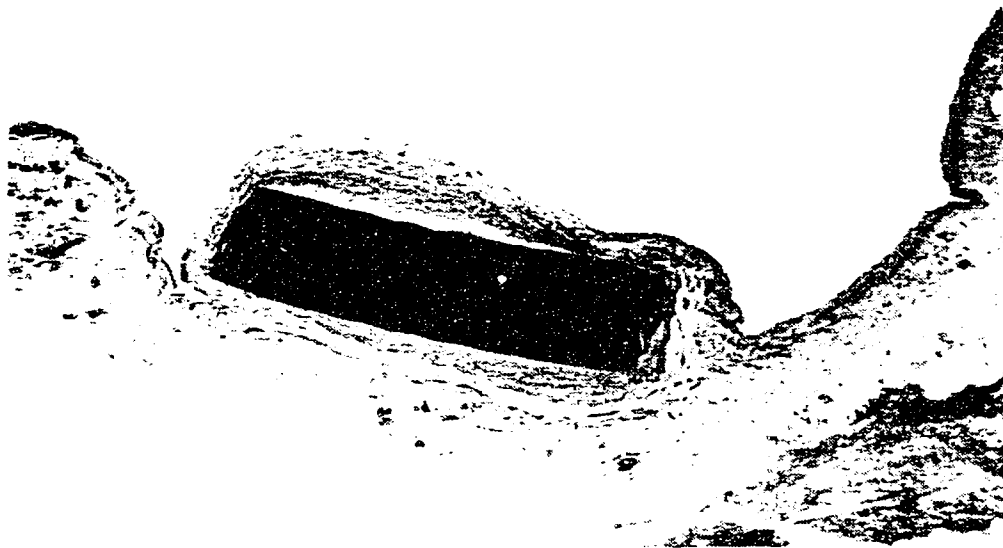


Figure 4.11 Transverse sections of intravenous (inferior vena cava) cannula shaped plain (*i.e.* Type I) Nafion implant after 105 days *in situ* showing surrounding vessel wall (original magnification 50x).

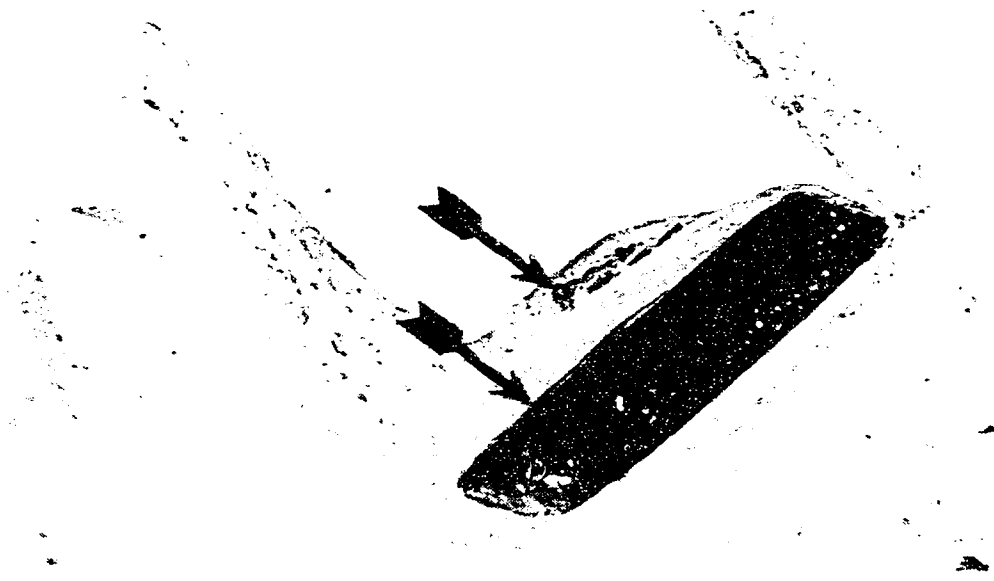


Figure 4.12 Transverse sections of intravenous (inferior vena cava) cannula shaped coated (*i.e.* Type II) Nafion implant after 105 days *in situ* showing surrounding vessel wall. The arrow

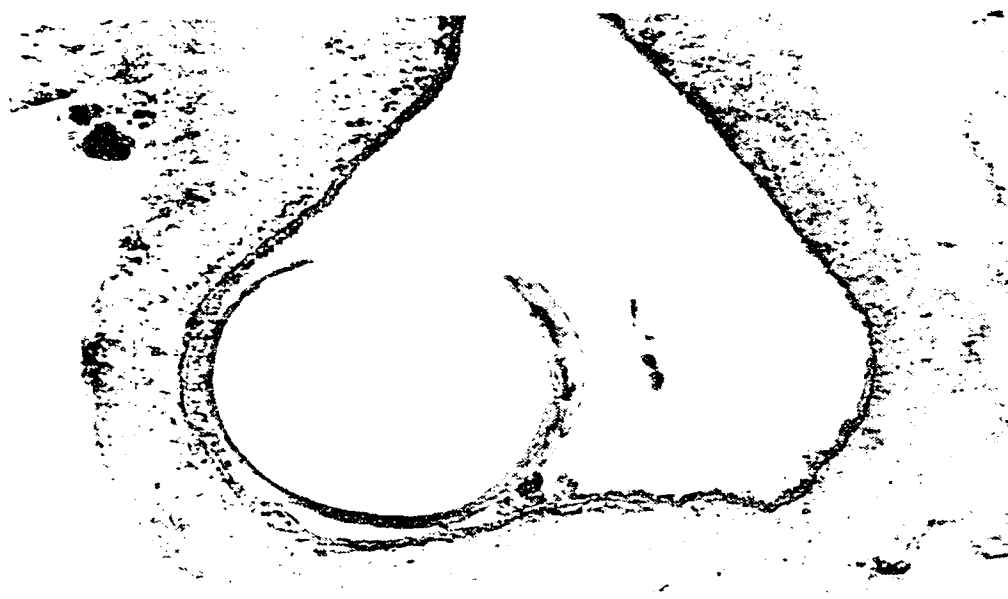


Figure 4.13 Transverse sections of intravenous (inferior vena cava) cannula shaped Silastic implant after 105 days *in situ* showing surrounding vessel wall (original magnification 50x).

generally appeared to be less progress toward endothelialization of the fibrous capsule, although some evidence was observed.

4.4 CONCLUSIONS

A first look at the short and long-term biocompatibility of Nafion polymer has been presented. A severe acute inflammatory response was not evident from SEM and histological examination of 1 and 4 day implants. However, the onset of fibrosis associated with subcutaneous implants was evident even at these early stages, and significant thrombosis occurred around the surface of intravenous implants. No significant chronic inflammation was observed at 43, 95, 105 or 206 days, and no obvious systemic abnormalities were noted. There was no significant difference between the response to thermally cured (*i.e.* Type I) Nafion implants and uncured, solution cast (*i.e.* Type II) Nafion implants. In our hands, Nafion polymer did not appear to invoke a substantially more severe biological response than silicone rubber (Silastic).

Considerable variability was observed in the thickness of the fibrous capsules of longer-term subcutaneous implants, both from sample to sample, and from region to region of the same sample. Capsules do, however, remain nominally thin ($<100\ \mu\text{m}$) and the surrounding tissues well vascularized. Comparison of capsular thickness of 43, 95, 105 and 206 day subcutaneous implants suggests a nearly steady state situation has been attained at the 43 day stage, whereas fibrosis associated with intravenous implants continued to progress up to at least the 100 day stage. With regard to implantable sensors, frequent recalibration would likely be required during the progressive phase of capsular formation, regardless of the operational stability of the sensor itself. Abdominal cavity implants (secured to the omentum) actually appeared to invoke the least severe biological response, and the peritoneal cavity may in fact be a suitable site for some types of implantable sensors [17].

The intravenous implants were likewise not characterized by severe chronic inflammation, but the fibrous tissue capsules were notably thicker, exceeding $200\ \mu\text{m}$ in some cases. Notwithstanding the surgical consider-

ations, intravenous sites are clearly the most inciteful of a biological response, and the thicker capsules (and later sequestering by endothelial tissues) would seem to negate any practical advantages over subcutaneous or abdominal cavity sites as sensor locations. However, it is conceivable that implant size and geometrical factors may have affected the outcome of the intravenous implant study, and so we intend to pursue the *in vivo* testing of small, streamlined Nafion coated sensors both in whole blood and interstitially.

In general, Nafion polymer appears to possess a degree of biocompatibility comparable to silicone rubber. Given the outstanding chemical and electrochemical properties of Nafion polymer it would seem to offer considerable promise for some implantable biosensor applications, particularly interstitially placed sensors. More comprehensive studies are clearly required in order to establish to what extent geometrical factors are important, and whether constituents of interest in the transudated fluid surrounding the implant accurately reflect the corresponding plasma concentrations.

4.5 REFERENCES

- [1] Guilbault, G.G. and Luong, J.H., Biosensors—current status and future possibilities, *Chimia* 1988, **42**, 267-271.
- [2] Czaban, J.D., Electrochemical sensors in clinical chemistry: yesterday, today, tomorrow, *Anal. Chem.* 1985, **57**, 345A-352A.
- [3] Regnault, W.F. and Picciolo, G.L., Review of medical biosensors and associated materials problems, *J. Biomed. Mater. Res.* 1987, **21**, 163-180.
- [4] Clark, Jr., L.C., and Duggan, C.A., Implanted electroenzymatic glucose sensors, *Diabetes Care* 1982, **5**, 174-180.
- [5] Gough, D.A., Lucisano, J.Y. and Tse, P.H.S., Two-dimensional enzyme electrode sensor for glucose, *Anal. Chem.* 1985, **57**, 2351-2357.

- [6] Schichiri, M., Kawamori, R., Goriya, Y., Yamasaki, Y., Nomura, M., Hakui, N. and Abe, H., Glycaemic control of pancreatectomized dogs with a wearable artificial endocrine pancreas, *Diabetologia* 1983, **24**, 179-184.
- [7] Ikeda, S., Ito, K., Kondo, T., Ichikawa, T., Yukawa, T. and Ichihashi, H., Prolongation of life-time of enzyme electrode type glucose sensor for artificial pancreas, *Anal. Chem. Symp. Ser., Proc. Chem. Sensors (Japan)* 1983, **17**, 620-625.
- [8] Grenshaw, M.A. and Jones, J.E., Whole blood glucose enzyme electrode, *J. Electrochem. Soc.* 1989, **136**, 414-417.
- [9] Harrison, D.J., Turner, R.F.B. and Baltes, H.P., Characterization of perfluorosulfonic acid polymer coated enzyme electrodes and a miniaturized integrated potentiostat for glucose analysis in whole blood, *Anal. Chem.* 1988, **60**, 2002-2007.
- [10] Gerhardt, G.A., Oke, A.F., Nagy, F., Moghaddam, B. and Adams, R.N., Nafion-coated electrodes with high sensitivity for CNS electrochemistry, *Brain Res.* 1984, **290**, 390-395.
- [11] Kristensen, E.W., Kuhr, W.G. and Wightman, R.M., Temporal characterization of perfluorinated ion exchange coated microvoltammetric electrodes for *in vivo* use, *Anal. Chem.* 1986, **59**, 1752-1757.
- [12] E.I. du Pont de Nemours and Co., Nafion® perfluorinated membranes—safety in handling and use, Bulletin E-38524, Polymer Products Dept., Wilmington, Delaware, 1983.
- [13] Eisenberg, A. and Yeager, H.L., Eds., Perfluorinated ionomer membranes, ACS symposium series 180 (M.J. Comstock, series ed.), American Chemical Society, Washington, D.C., 1982.
- [14] Moore, III, R.B. and Martin, C.R., Procedure for preparing solution-cast perfluorosulfonate ionomer films and membranes, *Anal. Chem.* 1986, **58**, 2569-2570.

- [15] Rebrin, K., Fischer, U., v. Woedtke, T., Abel, P. and Brunstein, E., Automated feedback control of subcutaneous glucose concentration in diabetic dogs, *Diabetologia* 1989, **32**, 573-576.
- [16] Wolfson, S.K., Jr., Tokarsky, J.F., Yao, S.J. and Krupper, M.A., Glucose concentration at possible sensor tissue implant sites, *Diabetes Care* 1982, **5**, 162-165.
- [17] Kondo, T., Ito, K., Ohkura, K., Ito, K. and Ikeda, S., A miniature glucose sensor, implantable in the blood stream, *Diabetes Care* 1982, **5**, 218-221.
- [18] G.L. Humason, *Animal Tissue Techniques*, 4th Edition, pp. 242-244, W.H. Freeman, San Francisco, 1979.
- [19] Woodward, S.C., How fibroblasts and giant cells encapsulate implants: considerations in the design of glucose sensors, *Diabetes Care* 1982, **5**, 278-281.
- [20] Turner, R.F.B., Harrison, D.J., Rajotte, R.V. and Baltus, H.P., A biocompatible enzyme electrode for continuous *in vivo* monitoring in whole blood, *Sensors & Actuators* 1990, **22 (B)**, 561-564.
- [21] Wood, N.K., Kaminski, E.J. and Oglesby, R.J., The significance of implant shape in experimental testing of biological materials: disc vs. rod, *J. Biomed. Mater. Res.* 1970, **4**, 1-12.
- [22] Matlaga, B.F., Yashenchak, L.P. and Salthouse, T.N., Tissue response to implanted polymers: the significance of the sample shape, *J. Biomed. Mater. Res.* 1976, **10**, 391-397.

CHAPTER 5

Design and *In Vivo* Testing of a Prototype Implantable Glucose Sensor for Continuous Monitoring in Whole Blood[†]

Electrode fouling and biocompatibility problems remain the greatest obstacles to the development of a stable glucose sensor for continuous *in vivo* monitoring in whole blood. Nafion encapsulation successfully prevents electrode fouling, and substantially improves the stability and performance of whole blood and plasma glucose sensors *in vitro*. Nafion polymer also appears to invoke a minimal chronic biological response. A prototype enzyme electrode system is thus proposed, based on Nafion polymer encapsulation, which has a suitable size and geometry to be tested as an (acute) implantable sensor. Pilot test results are presented which, although inconclusive as an evaluation of the technology, yield valuable information regarding modifications for a next prototype; these are discussed.

5.1 INTRODUCTION

The feasibility of maintaining glucose homeostasis in patients with severe Type I diabetes by an artificial device was first demonstrated by Albisser, *et al.* [1] more than fifteen years ago. Since that time, a great deal of research has been directed toward the development of a sufficiently stable and accurate glucose sensor that could be used to realize an implantable version of the so called Artificial Beta Cell. Progress has been slow, primarily because of the severity of biocompatibility problems which depend, to some extent, on the implantation site and type of body fluid in which the sensor is operated. Intravenous monitoring of whole blood glucose is generally recognized as being ideal, but unlikely to prove successful due to the proficiency and extreme prejudice with which the body reacts to foreign objects in the blood stream. The most encouraging results thus far, at least in short-term studies, have been reported involving subcutaneous monitoring of glucose in the interstitial fluid [2-5]. However,

[†] Parts of this chapter have been published as:

R.F.B. Turner, D.J. Harrison, R.V. Rajotte and H.P. Baltes, "A Biocompatible Enzyme Electrode for Continuous *In Vivo* Glucose Monitoring in Whole Blood", *Sensors and Actuators*, Vol. 22 (B), No. 1, pp. 561-564, January 1990.

Rebrin, *et al.* [4] report that 10 out of 35 of their electrodes failed to respond when implanted subcutaneously, and raise concerns about further progress in this area, regardless of the implantation site, until the difficult problems relating to biocompatibility (and hence stability) can be resolved. Toward this end, we have proposed an enzyme electrode system [6], based on a novel dialysis membrane material, that performs well in whole blood *in vitro*, and appears to present a biocompatible interface to the body.

We have previously demonstrated the exceptional performance of perfluorosulfonic acid (Nafion®) polymer as a dialysis membrane material for enzyme-based glucose sensors in whole blood, *in vitro* [7]. Nafion encapsulation effectively excludes blood cells, plasma proteins and other blood constituents that denature the enzyme and/or cause fouling of the platinum electrode surface. We have also demonstrated that Nafion polymer exhibits a degree of biocompatibility comparable to that of silicone rubber and is considerably better, in this respect, than any conventional dialysis materials used for biosensor applications [8]. It remains to be shown, however, that the ensemble sensor/membrane system performs successfully *in vivo*. Since our experience with this system is mainly derived from glucose assays in whole blood and blood plasma, we have chosen to test the first prototype electrodes in circulating blood.

5.2 MATERIALS AND METHODS

5.2.1 Electrode Preparation

The indicating electrodes employed in the earlier development stages of the sensor/membrane system used here were designed for multiple reuse, ease of fabrication and handling, and exhibited well behaved electrochemical and mass transport properties. The active surface was a polished planar disc and was sealed in glass tubing which also enclosed the lead wire. The physical size and geometry of this type of electrode was, of course, unsuitable to be employed in a test of the system performance *in vivo*, and was therefore redesigned. The implantable version is required to be smaller, streamlined and should not expose the host to any non-biocompatible material. A cross sectional view of the structure of the implantable electrode is shown in Figure 5.1.

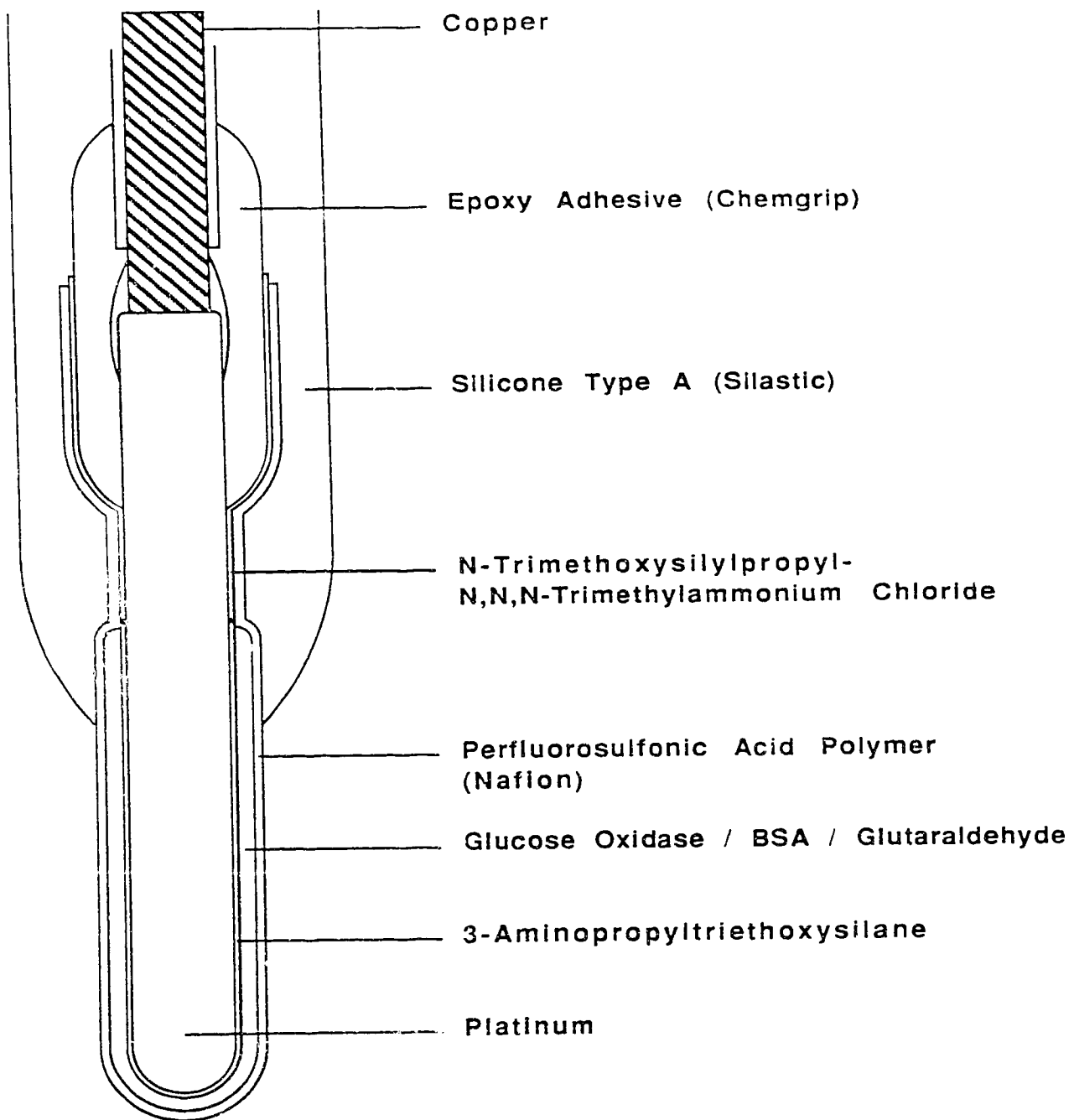


Figure 5.1 Cross sectional view of a prototype implantable electrode used for *in vivo* glucose monitoring in whole blood.

The platinum indicating electrode is joined to a stranded copper wire lead by a solder junction and sealed in Chemgrip® epoxy adhesive (Norton Performance Plastics, Wayne, NJ). The composition and procedure for applying the glucose oxidase (GOx)/bovine serum albumin (BSA) membrane and the overlying Nafion dialysis membrane are essentially the same as described previously for glass-shrouded planar electrodes [7], except that additional coats of Nafion solution are required in order to build up a sufficiently thick membrane. Also, the small cylindrical geometry of the implantable electrode gives rise to substantial membrane adhesion problems, which prevents the direct application of the planar electrode technology to the implantable electrodes. These problems have been overcome by the following procedure.

The clean platinum wire electrode (1.024 mm dia.) is anodized at +1.1 vs. SCE for approximately 5 minutes in order to form a monolayer of platinum oxide on the surface, which facilitates derivatization with silanizing reagents. A portion of the tip of the electrode (see Figure 5.1) is then treated by exposure to 1% 3-aminopropyltriethoxysilane (Petrarch) in anhydrous benzene for approximately 20 minutes, followed by a thorough rinse in dry benzene. The entire platinum electrode is then exposed to 5% N-(trimethoxysilylpropyl)-N,N,N-trimethylammonium chloride (Petrarch) in anhydrous methanol, following the procedure described by Szentirmay, *et al.* [9]. This treatment leaves a monolayer of primary amine groups exposed over a region of the tip of the electrode which facilitates covalent attachment of the GOx/BSA membrane as described by Yao [10]. The RNMe³⁺ moiety is present over the entire surface, which greatly enhances adhesion of the overlapping dialysis membrane by virtue of electrostatic interaction with the sulfonate groups in the Nafion [9]. Multiple coats of Nafion polymer (Solution Technology, Mendenhall, PA) are then applied by dip coating as previously described [7], except that one additional layer of 3% Nafion solution and one additional layer of 5% Nafion solution was applied. Also, the orientation of the electrode during the drying cycle for each successive Nafion application was alternated between inverted and non-inverted (*i.e.* between "tip down" and "tip up" orientations).

The lead wire and proximal end of the platinum indicating electrode are gloved in biocompatible Silastic® Medical-Grade tubing (1.47 mm i.d., 1.96 mm o.d.), and sealed with Silastic adhesive which is formed to give a smooth topology near the electrode tip. The only other material that would be exposed directly to the body is the Nafion dialysis membrane which encapsulates the active portion of the electrode tip. The Ag/AgCl reference and platinum counter electrodes are similarly gloved in Silastic and coated over the active portion with a thin layer of Nafion (less than 1 μm thick).

5.2.2 *In Vitro* Characterization

These trials involved three glucose electrodes, designated B1, B2 and B3, which were prepared according to the above procedures. Electrode B3 was used to obtain intermediate calibration data at various steps during the Nafion coating procedure, and was also used to verify that the redesigned electrodes performed satisfactorily in whole blood (*in vitro*). Calibration data, for each electrode, are shown in Figure 5.2 as measured in phosphate buffer (pH 7.4) with 0.1 M NaCl as supporting electrolyte using a Pine RDE-4 analytical potentiostat. The value of the apparent (*i.e.* observed) Michaelis constant K_m , which depends on the mass transport rate of glucose relative to oxygen through the dialysis membrane, gives an indication of the linearity of the electrode response. The observed response times were 5-50 s for concentration steps smaller than 5 mM (where the total glucose concentration is less than 10 mM total). These response times are somewhat slower than previous versions of the (planar) Nafion encapsulated electrode, but still faster than cellulose membrane encapsulated electrodes.

Before proceeding to the *in vivo* animal testing, one of the redesigned versions of the electrode (B3) was tested in canine whole blood *in vitro* using the method of standard additions as described in Chapter 3. In this case, the most recent version of the potentiostat chip described in Chapter 2 was used as the controller. It should be noted that a simultaneous (*i.e.* differential) measurement could not be made in this case, since a suitably matched dummy electrode was not available. A measurement of the background current in the whole blood sample was therefore obtained

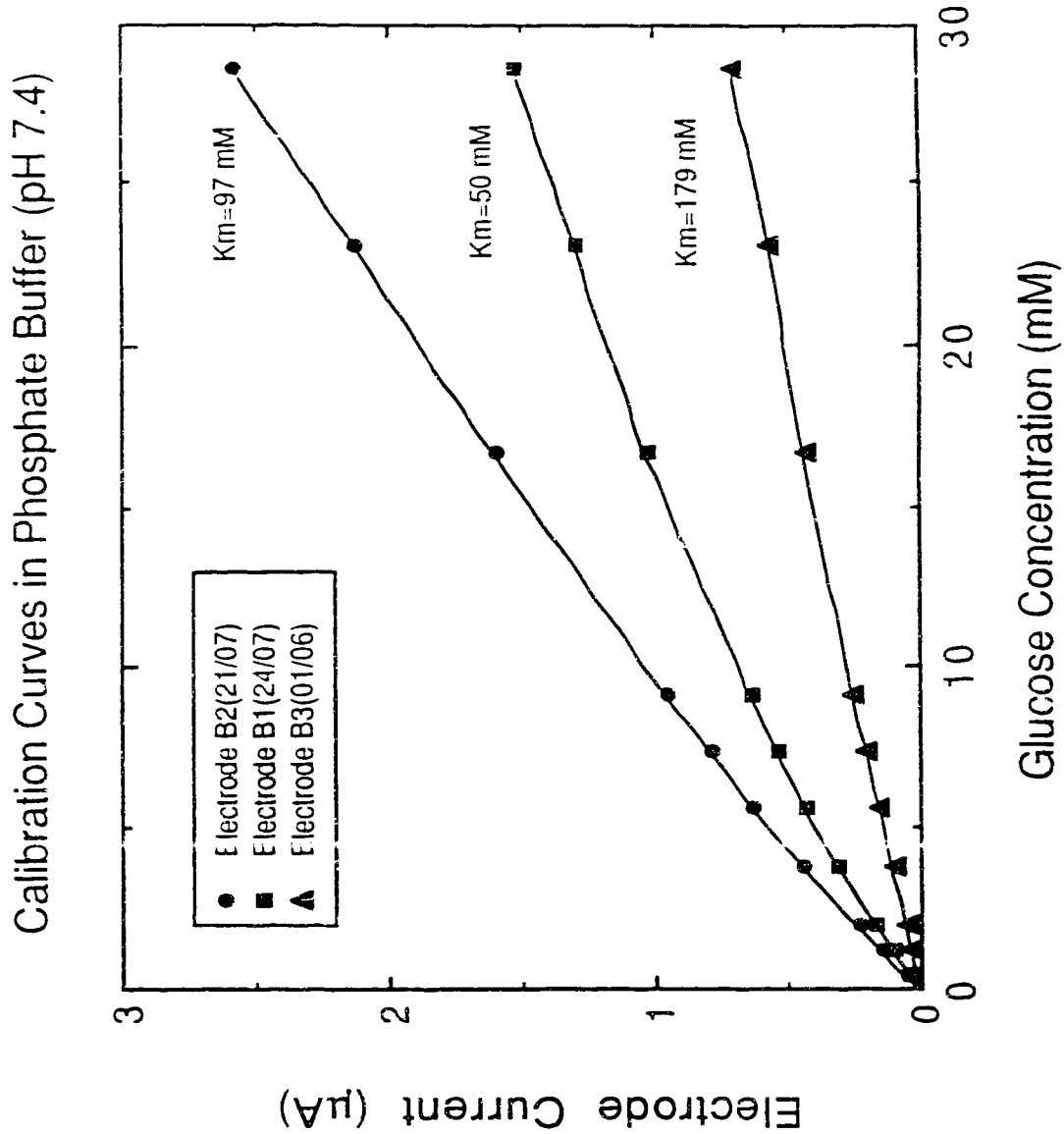


Figure 5.2 *In vitro* calibration curves for the prototype electrodes in phosphate buffer solution (pH 7.4). The apparent Michaelis constants (K_m) were determined from Lineweaver-Burke plots of the calibration data.

after the standard additions procedure was completed, using electrode B3 itself following thermal denaturation of the enzyme. Figure 5.3 shows a Grans plot of the standard additions data obtained from electrode B3 in whole blood (*in vitro*) which demonstrates linearity and precision comparable to that obtained in earlier studies with Nafion encapsulated planar electrodes. The initial glucose concentration in the sample was determined to be 3.12 mM, which agrees to within 6% of the value (2.95 mM) previously determined by a calibrated Beckman glucose analyzer. Note that the Beckman instrument measures plasma glucose values, which can be greater than the corresponding whole blood concentration by up to 20%. A correction factor of 15% was therefore applied to the Beckman reading in order to obtain an estimate of the whole blood glucose concentration in the sample. Hence, except for the slower response time, the performance of this electrode in whole blood *in vitro* was found to be comparable to the glass shrouded planar electrodes discussed in Chapter 3. Electrodes B1 and B2 were assumed to be similar, but were not actually tested in whole blood at this stage.

5.2.3 Implant Procedures and Instrumentation

Canine models have been extensively used for live animal studies in diabetes research. The canine system has thus been well characterized *vis à vis* the systemic response to glucose challenges and endogenous insulin, both in the normal and diabetic states. Canine subjects were therefore chosen for the *in vivo* experiments described here. Electrodes B1 and B2 were tested in two separate animals, designated K-118 and J-518. Animals underwent standard pre-operative care and all surgical procedures were conducted in an operating theater under sterile or aseptic conditions. Both dogs were anaesthetized with sodium pentobarbital (30 mg/kg IV), and supplemental pentobarbital was administered intravenously as required in order to maintain subjects at the surgical plane. Both dogs also received normal saline (drip) throughout all surgical and experimental procedures. The first subject (K-118) had undergone a total pancreatectomy immediately prior to the implant surgery and was hence acutely diabetic; the second subject (J-518) was normal and had not prev-

Grans Plot of Standard Additions Data (in Whole Blood, in vitro)

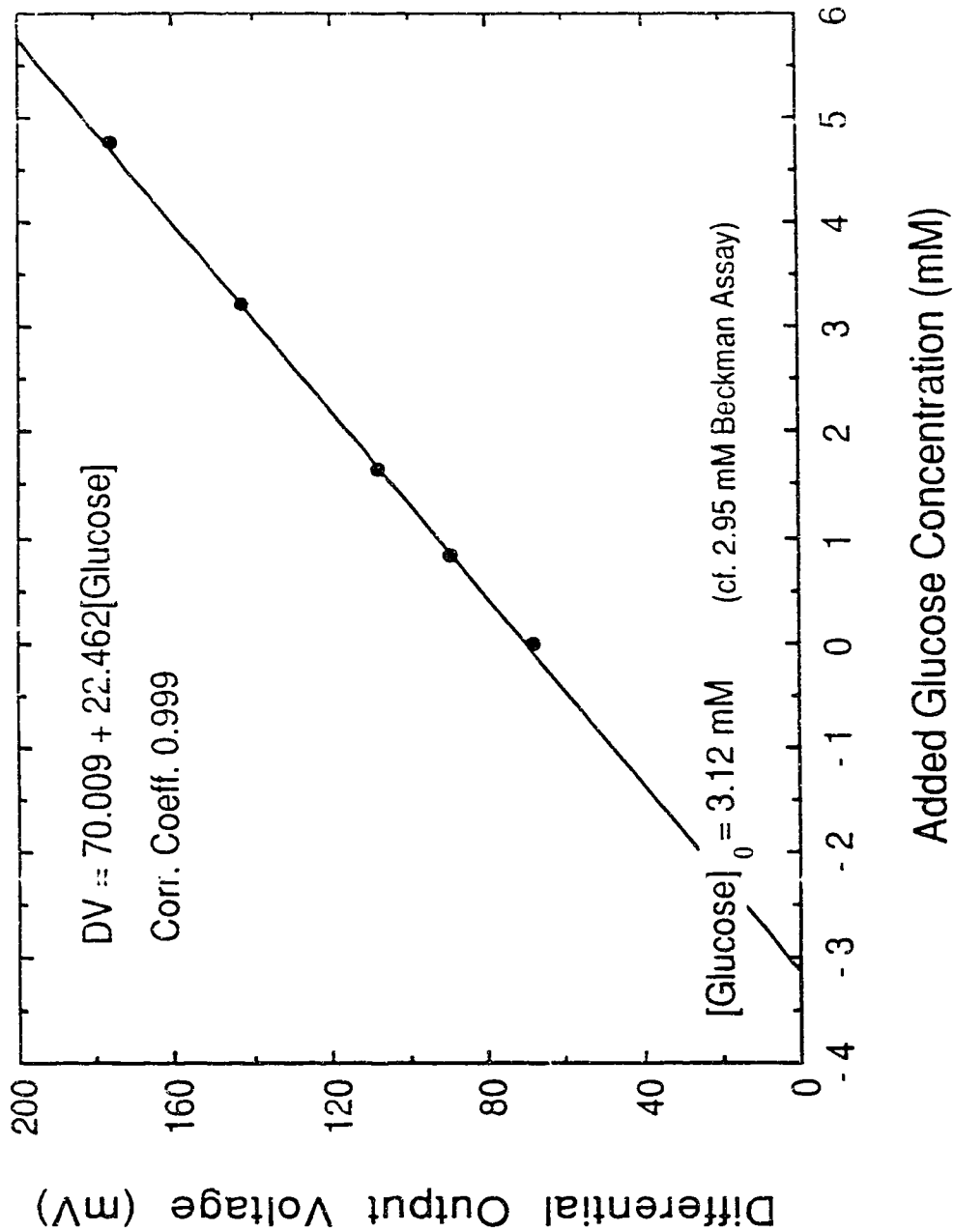


Figure 5.3 Grans plot of standard additions data obtained *in vitro* using electrode B3 in canine whole blood at room temperature. The initial glucose concentration (3.12 mM) was determined from the slope and intercept of the regression line.

iously undergone major surgery. Prototype electrodes were placed intravenously in both subjects according to the following procedure.

The inferior vena cava was selected as the implant site in order to accommodate the physical size of the electrodes without excessively perturbing the blood flow around the electrodes. The abdomen was opened through a midline laparotomy incision and abdominal viscera were retracted laterally and packed with saline soaked lap sponges. A section of the inferior vena cava, approximately midway between the confluence of the renal vein and the bifurcation into the illiac veins, was exposed by blunt dissection. The adventitia was cleared by sharp dissection and a partially occluding (Debakey) vascular clamp was applied in order to isolate and control the region surrounding the proposed venipuncture sites. A 14 gauge biopsy needle was used to puncture the wall of the vena cava and the electrodes were introduced. A separate puncture was made for each electrode (*i.e.* indicating and reference/counter electrodes) approximately 1 cm apart. The Debakey clamp was removed and the electrodes were further inserted another 5-6 cm. Stay sutures (3-0 silk) were used to anchor the electrode lead wires to the vessel wall near the venipuncture site. The exposed end of the lead wire was also sutured to the fascia of the anterior abdominal wall in order to prevent accidental tension on the implanted electrodes. In order to obtain venous blood samples, the right femoral vein was exposed by a cut-down procedure and a 16 gauge (Quik-Cath®) Teflon catheter was introduced, and secured by stay sutures to subcutaneous fascia.

The electrode lead wires were connected to a Pine model RDE-4 analytical potentiostat which was, in turn, connected to a Hewlett-Packard model HP 7128A strip chart recorder in order to obtain a continuous time record of the electrode current. The electrode bias potential was set to +0.7 V vs. Ag/AgCl and was monitored periodically with a Hewlett-Packard model HP 3478A high impedance multimeter. At specified intervals throughout the experiment, venous blood samples were collected in heparinized centrifuge tubes and immediately assayed using a Beckman Glucose Analyzer 2, operated by a trained technician. The general physiological condition of each dog was ascertained from blood gas,

haematology and electrolyte data determined before and after each experiment. These data are compiled in Table 5.1 along with reference (control) data for each variable.

5.2.4. Experimental Glucose Challenge Protocols

The objectives of these *in vivo* pilot tests were to monitor the response of the implanted electrode during induced changes in the dog's blood glucose level, and to compare this response with an independent determination of the glucose level at prescribed time intervals. The independent determination, as indicated in the previous section, was obtained by an *in vitro* assay of sampled venous blood using a calibrated Beckman glucose analyzer. In a normal animal, a temporary and predictable hyperglycaemic state can be induced by simply administering a bolus glucose challenge, either orally or intravenously. The subject's blood glucose then rises sharply to a level that depends on the original glucose dose. This load stimulates the pancreas to secrete additional insulin, which slowly returns the blood glucose to a normal level. This is, in fact, the basis for routine glucose tolerance testing (GTT) commonly used to obtain diagnostic data regarding a subject's own natural blood glucose control mechanisms. Variations on this type of protocol were used in the two experiments reported here. As mentioned above, the first subject (dog K-118) had been pancreatectomized prior to the experiment, and hence a slightly different protocol was employed in each case.

In the first experiment, dextrose 50% injectable solution (Abbott) was administered intravenously in a sequence of steps according to a calculated protocol based on an approximate distribution volume corresponding to 25% body mass. The actual dosages are indicated in the caption of Figure 5.4 for each step. In order to lower the dog's blood glucose level, Iletin II U-100 Regular insulin (Lilly) was administered intravenously in steps based on an assumed drop of approximately 200 mg% for each 100 mU/kg of insulin given. Again, the actual dosages used are indicated in the caption of Figure 5.4 along with the results. In the second experiment, a simple intravenous glucose tolerance test (IVGTT) protocol was used where a single IV injection of dextrose was administered as indicated along with the results.

TABLE 5.1 Blood gas, haematology and electrolyte data obtained from venous blood samples collected from Dogs K-118 and J-518 before and after each experiment. Normal (canine) values are also given for comparison.

Dog ID	pH	PCO ₂ (torr)	PO ₂ (torr)	HCO ₃ (mM)	Ttl.CO ₂ (mM)	Hct (%)	Hgb (g/dl)	Na ⁺ (mM)	K ⁺ (mM)
K-118 (Initial)	7.35	46.1	43.0	24.3	25.7	44	16.7	149.6	4.2
K-118 (Final)	7.25	50.2	41.2	21.3	23.2	43	16.2	138.9	3.6
J-518 (Initial)	7.18	69.9	42.7	25.2	27.4	36	13.4	NA	NA
J-518 (Final)	7.13	92.1	38.5	29.2	32.0	39	13.7	142.4	3.9
Normal ^a (Std. Dev.)	7.21 0.04	45.9 6.3	48.9 8.8	17.5 1.5	18.9 1.6	46 4	15.0 1.5	145.0 2.8	4.5 0.4

(a) Refer to normal values for venous blood.

5.3 RESULTS AND DISCUSSION

5.3.1 *In Vivo* Performance Tests

Figure 5.4 shows a comparison of the glucose profiles from subject K-118 measured (continuously) by electrode B1 and (at discrete intervals) by the Beckman analyzer. In this case, only the electrode currents corresponding to the times at which blood samples were taken have been plotted. The actual strip chart record from this experiment shows positive transient current steps that in fact coincide with glucose injections, at least until step 3. However, the signal exhibits a steady negative drift over the interval between injections, and the magnitude of the steps do not reflect the magnitude of the changes in plasma glucose level as measured by the Beckman instrument. In any case, the electrode fails to respond at all beyond step 4 (*i.e.* exhibits only the steady negative drift), and the current is clearly not well correlated with the Beckman data over any appreciable interval. The behavior of this electrode was similar to that observed in many previous experiments *in vitro*, where the encapsulating dialysis membrane was either damaged or not of sufficient thickness to adequately protect the electrode.

The experiment was terminated after approximately 4 h elapsed time, and the electrodes were carefully removed for visual inspection. Most of the electrode was clean, but a significant thrombus had formed over part of one side of the electrode near the tip. A small portion of the reference electrode also exhibited thrombus formation. The lengths of the intravenous portions of the electrodes were such that the two electrodes could well have been crossed in the lumen of the vessel, forming a kind of platelet "trap" to facilitate clot formation. Thrombosis alone should not have caused the observed failure of this electrode, but damage to the Nafion membrane could have resulted from friction if the electrodes were indeed crossed. Subsequent inspection under a (light) microscope was inconclusive in that no cracks or ruptures in the membrane could be identified, although some surface irregularities were apparent. The electrode was then washed with distilled water and tested in phosphate buffer solution where it was found to respond normally to glucose injections, although the

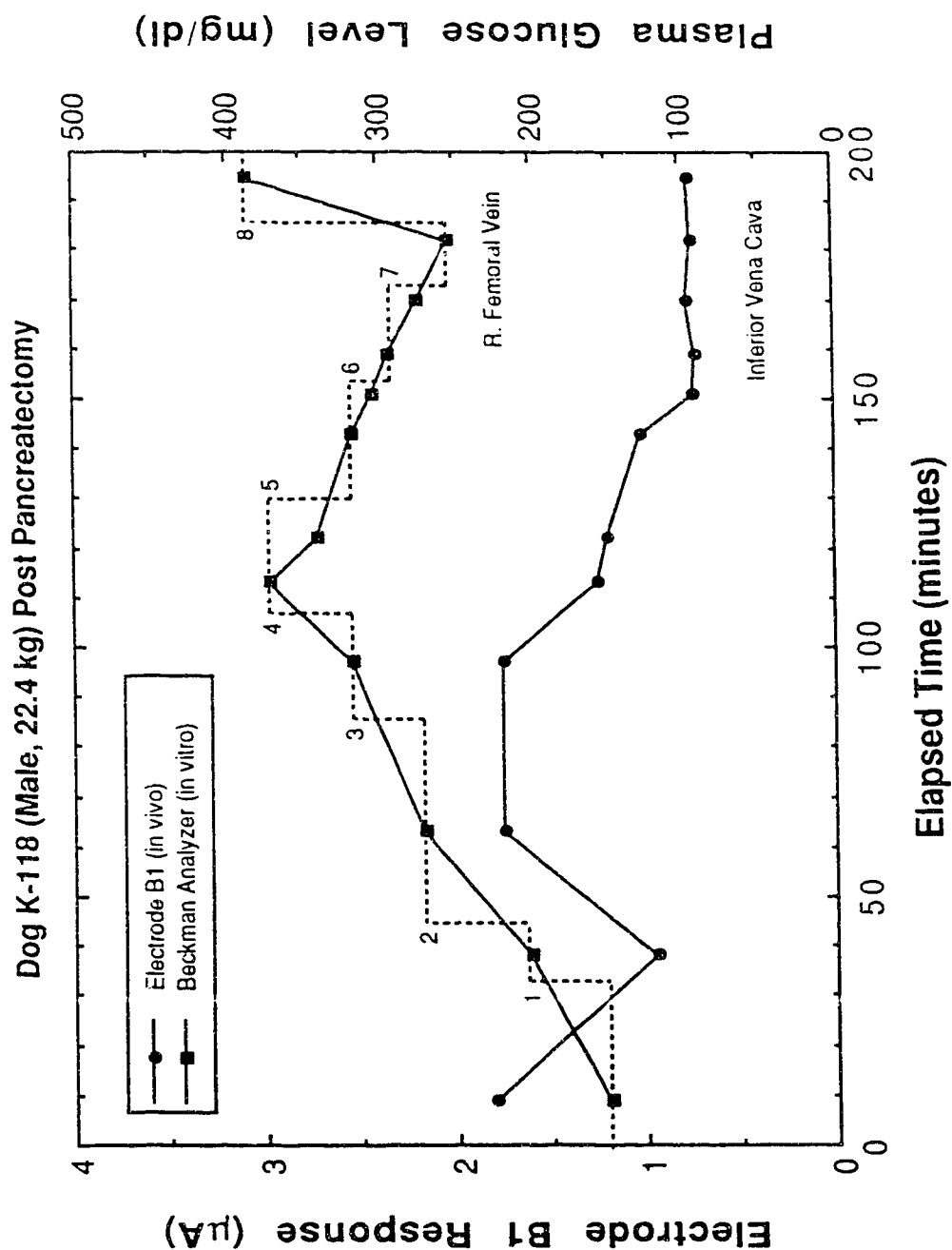


Figure 5.4 Electrode B1 response and Beckman plasma glucose profiles from Dog K-118 (male, 22.4 kg) post pancreatectomy. The numbered steps indicate intravenous bolus injections of dextrose/insulin as follows: 1=67 mg/kg dextrose, 2=3=4=223 mg/kg dextrose, 5=9 mU/kg insulin, 6=11 mU/kg insulin, 7=27 mU/kg insulin, 8=446 mg/kg dextrose.

current levels were somewhat higher than those measured (in buffer) prior to the *in vivo* experiment. This electrode was then washed again in distilled water and stored in a clean, dry test tube for later evaluation in whole blood samples.

In the second experiment, care was taken during the intravenous placement of the indicating electrode to ensure that the tip was downstream from the reference and counter electrodes in order to avoid possible damage. Figure 5.5 shows a comparison of the glucose profiles from subject J-518 measured by electrode B2 and, again discretely, by the Beckman analyzer. Initially at least, the electrode responded well and the signal was far more stable from the outset than in the previous experiment. However, the response time of the electrode was apparently not adequate to accurately resolve the hyperglycaemic peak in blood glucose concentration, and the response falls to a lower than expected level near the end of the experiment.

The actual signal from electrode B2 was found to be modulated by periodic (but non-sinusoidal) oscillations, which appeared to correlate with the animal's respiration. Assuming the perturbation due to the presence of the electrodes does not grossly disrupt the (approximately) laminar flow behavior, the oscillatory component may be explained as arising from positional variations of the sensor within the lumen of the vessel. That is, the velocity profile varies as a function of radial position over the cross-sectional plane, and exhibits a strong gradient near the wall of the vessel. The regular and heavy respiratory movements presumably caused slight variations in the position of the sensor in this cross-sectional plane, thus exposing the sensor to periodic variations in flow rate. The output signal from the sensor should reflect these variations, since the electrode current depends on flow rate (*i.e.* glucose mass transport rate). The electrode response shown in Figure 5.5 has been smoothed using a "moving average" type algorithm, where $W=13$ consecutive data points were averaged to yield a smoothed data point representing the central value within the temporal window. The averaging (window) function was "moved" along the time axis to generate the smoothed data set. The envelope of the original oscillatory response is shown in Figure 5.6 along with the smoothed response.

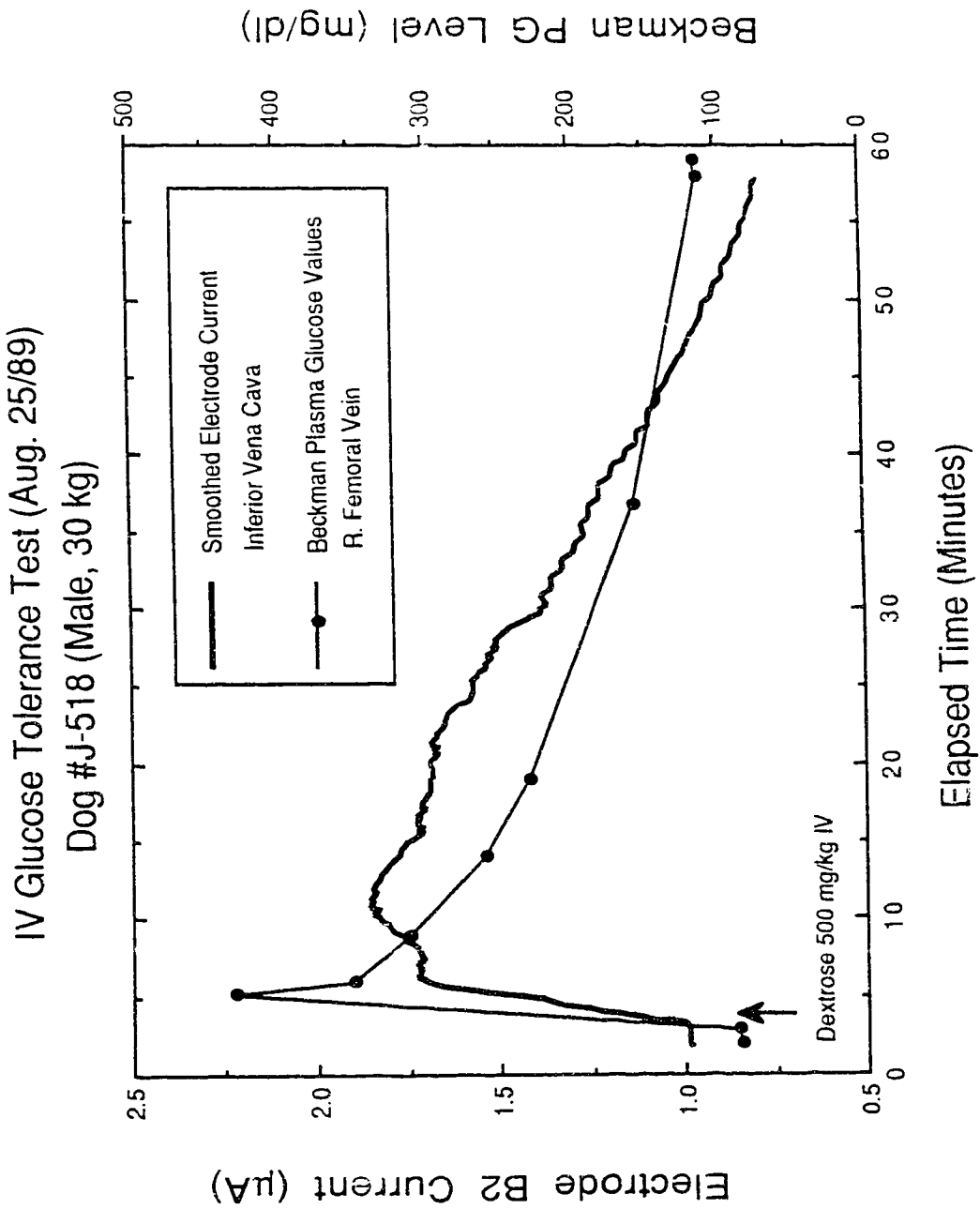


Figure 5.5 Smoothed electrode B2 response and Beckman plasma glucose profiles from Dog J-518 (male, 30 kg). An intravenous bolus injection of dextrose (500 mg/kg) was administered in order to elicit the initial rise in plasma glucose. The return to normoglycaemia was due to the dog's own endocrine response.

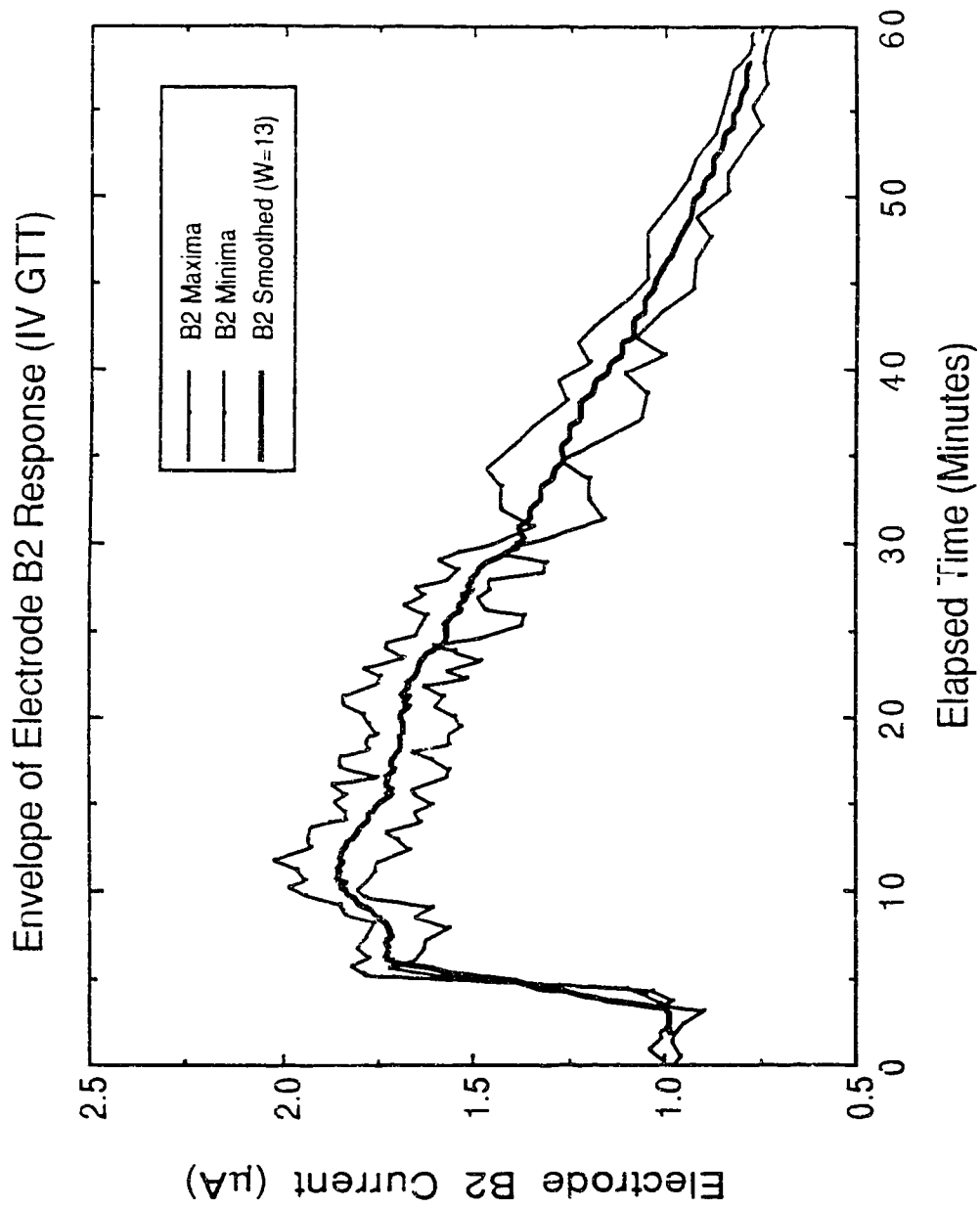


Figure 5.6 Envelope of actual oscillatory response of electrode B2 obtained during IVGTT on dog J-518. A window of 13 points ($W=13$) was applied in the "moving average" algorithm used to generate the smoothed version of the B2 response.

Figure 5.7 shows a cross correlation between the response data from electrode B2 and the Beckman readings obtained at the time intervals indicated on Figure 5.5. Assuming the Beckman data is accurate, Figure 5.7 indicates that the signal from electrode B2 is not well correlated with the actual plasma glucose level. However, the three highest glucose readings (immediately following a 350 mg/dl concentration "step") occurred within a time interval of only 4 minutes. Yet the response time of electrode B2 to a glucose concentration change of that magnitude is at least on the order of 1 to 2 minutes. If the three points corresponding to the highest glucose readings are omitted from the data, the correlation coefficient increases to 0.94. It is conceivable that the cross correlation might improve considerably if the concentration had not changed so abruptly near the start of the experiment, although response time considerations do not explain the poor accuracy later in the experiment.

Two subsequent follow-up IVGTT's were performed on dog J-518 during which electrode B2 failed to give a response that correlated with the Beckman data. The experiment was then terminated, after approximately 3.5 h total elapsed time, and the electrodes were carefully removed for visual inspection. Again, most of the electrode was clean, but some thrombus had formed around the central portion of the electrode tip. No further cleaning or visual inspection was performed at this stage; rather, the electrode was immediately fixed in 2.5% glutaraldehyde (in Millonig's buffer, pH 7.2) for later examination by scanning electron microscopy.

5.3.2 Post-Operative Evaluation of Electrodes

The glucose profile shown in Figure 5.8 was determined by the Beckman analysis of venous blood samples obtained during the final follow-up IVGTT on dog J-518. Each of the samples taken during the run were divided into two sub-samples—one for plasma glucose assay by the Beckman, and one for *in vitro* assay (in whole blood) using electrode B1, which had previously been implanted in dog K-118. This electrode, which had performed poorly *in vivo*, actually performed surprisingly well in whole blood *in vitro*. That is, it responded well during standard additions type assays (on eight separate samples), and the resulting Grans plots indicated

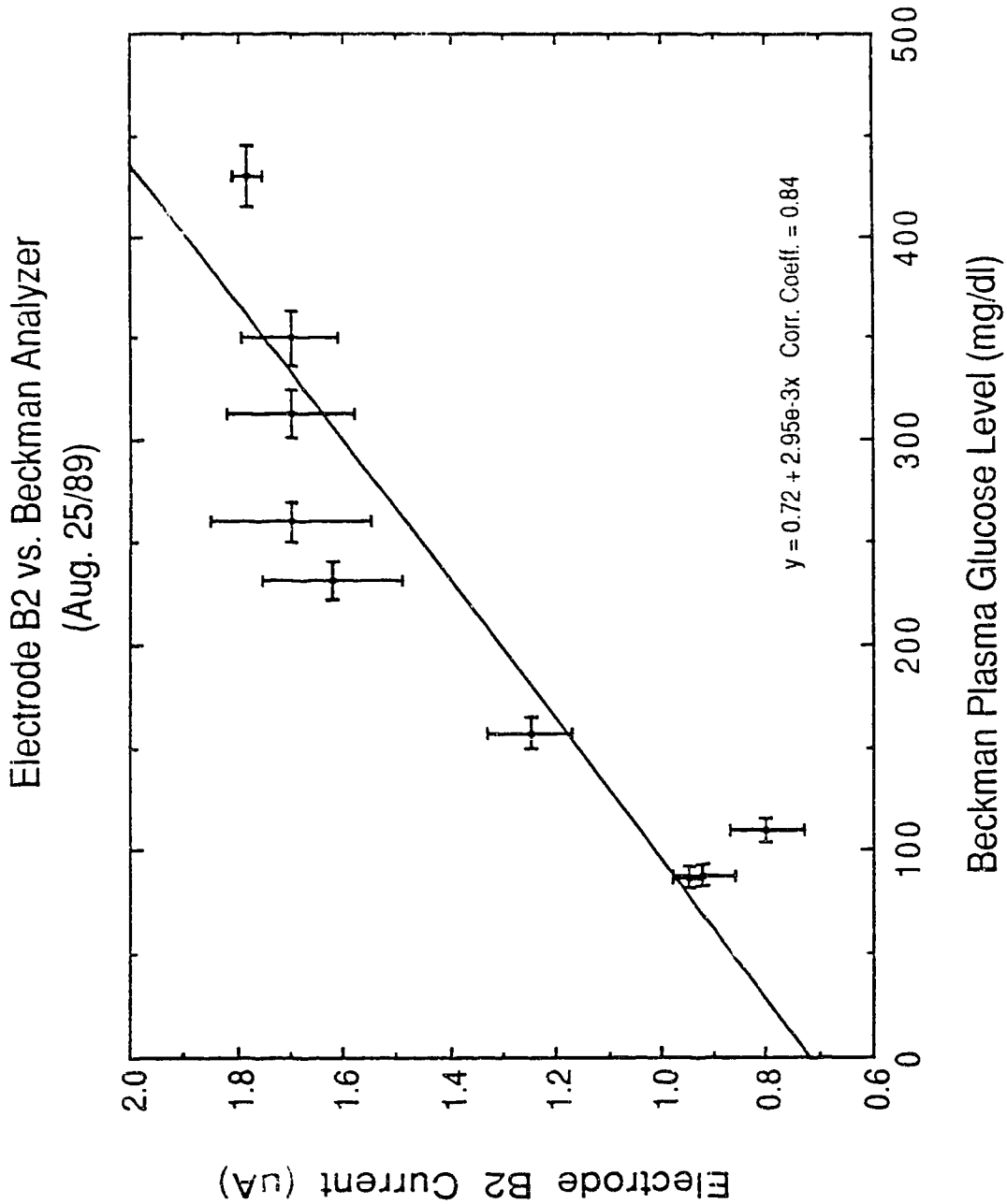


Figure 5.7 Cross correlation between the *in vivo* response of electrode B2 and (*in vitro*) plasma glucose readings obtained from sampled venous blood.

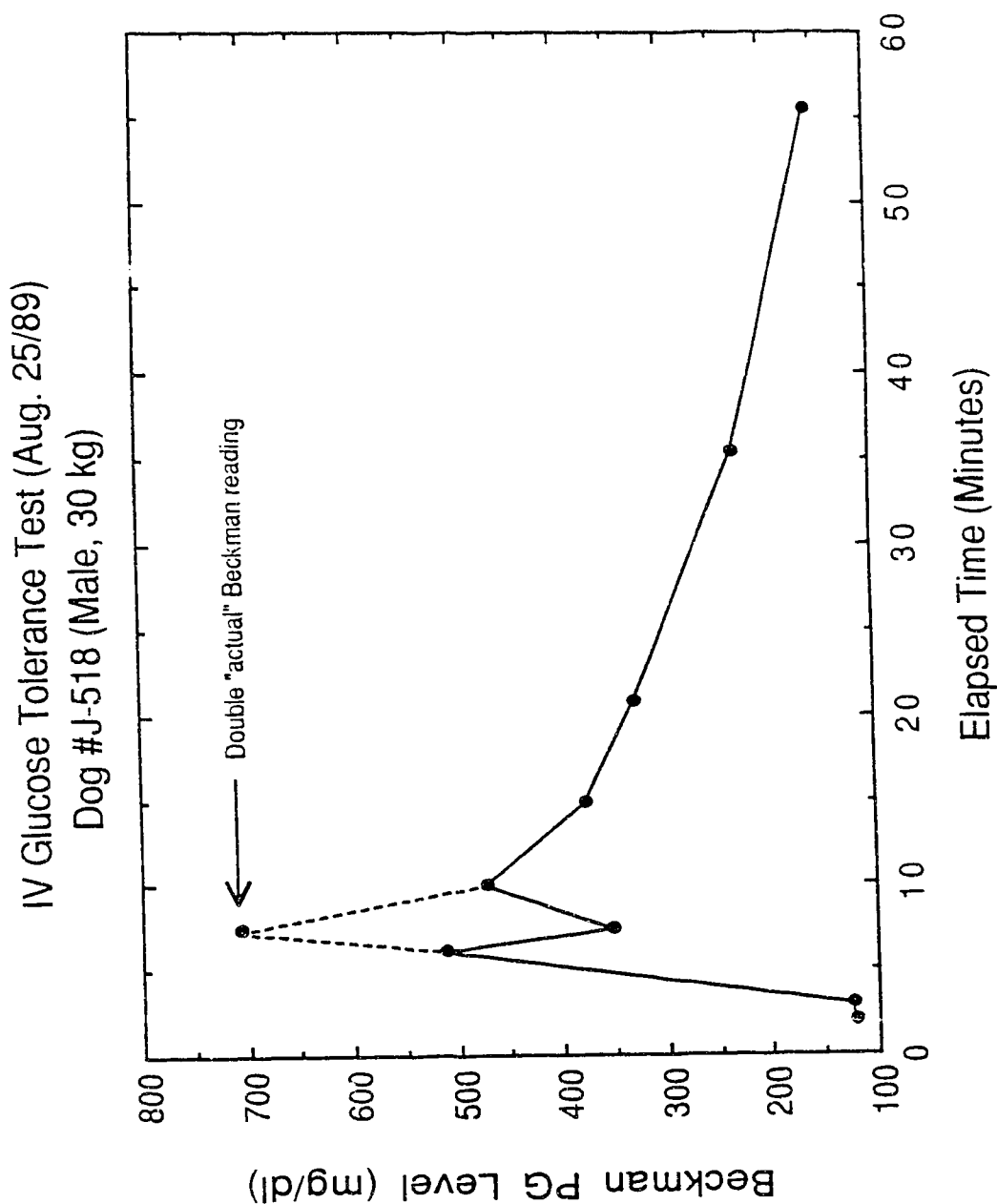


Figure 5.8 Response of Dog J-518 to intravenous glucose challenge (833 mg/kg) as determined by Beckman analyses of sampled venous blood. The magnitude of the fourth Beckman reading is questionable and the dashed portion of the profile represents the case where the actual reading has been doubled (see discussion).

good precision. These data were compared with the corresponding Beckman readings as depicted in the cross correlation plot shown in Figure 5.9. This correlation seems convincing, although no previous data are available for comparison as this was the first time that a graded series of blood samples of the same age and from the same animal were assayed by both the Beckman and a Nafion coated electrode.

It would be appropriate to include a note here about the interpretation of the curves shown in Figures 5.8 and 5.9. Unfortunately, the Beckman reading from the sample closest to the peak plasma glucose level is questionable in this case, as indicated in Figure 5.8. The problem arose because a considerably larger than normal dose of glucose had been administered at $t=0$ which resulted in a plasma glucose level that far exceeded the linear range of the Beckman instrument. The Beckman operator therefore had to dilute the sample (more than once?) and later admitted that the reported value could have been in error by a factor of two. Hence the dashed portion of the profile in Figure 5.8 and highest magnitude point in the data set of Figure 5.8, incorporate this scenario. If this point is excluded from the data set, the cross correlation coefficient becomes 0.91 and the slope $6.43 \times 10^{-4} \mu\text{A}/\text{mg}\%$. In either case, the correlation between electrode response and the plasma glucose level is far better for the *in vitro* assay than for the continuous *in vivo* measurement.

One further electrochemical test was performed on this electrode. Recall that, in Chapter 3, it was noted that a correlation appeared to exist between the Nafion thickness required to block $\text{Fe}(\text{CN})_6^{4-}$ and the thickness required for adequate protection of the electrode in whole blood *in vitro*. However, no ferrocyanide electrochemistry was observed in the cyclic voltammetric response of electrode B1 obtained in N_2 saturated solution of $\text{K}_4\text{Fe}(\text{CN})_6$ (1.0 mM) with KCl (0.1 M) as supporting electrolyte. Yet this electrode clearly did not perform in whole blood *in vivo*, which shows that the ferrocyanide test is not a helpful criterion for *in vivo* applications. A better criterion may be the magnitude of the apparent Michaelis constant K_m , since the value measured for electrode B1 was roughly half that measured for electrode B2. And, although electrode B2 eventually failed as well, it did perform better than B1 *in vivo*.

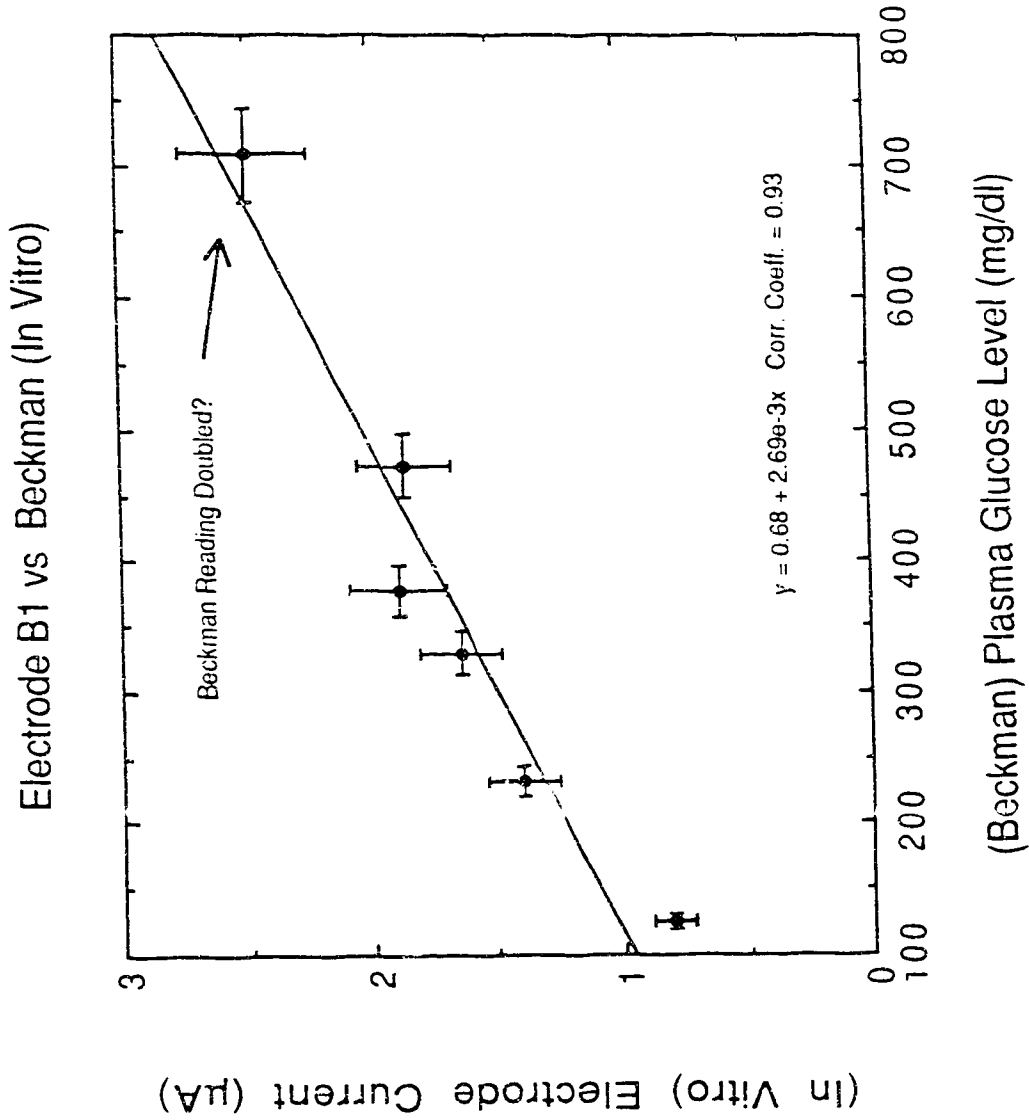


Figure 5.9 Cross correlation between the *in vitro* response of electrode B1 and (Beckman) plasma glucose readings obtained from sampled venous blood during subsequent IVGTT on Dog J-518. The validity of the peak Beckman reading is questionable (see discussion).

Electrode B2, which had previously been implanted in dog K-118, was examined by scanning electron microscopy in order to determine whether or not the Nafion encapsulation had been damaged during the course of the *in vivo* testing. Figure 5.10(a) shows a scanning electron micrograph of a portion of the electrode near the margin of the GOx/BSA membrane that was cast over the tip of the electrode. A crack in the Nafion polymer encapsulation is clearly visible approximately in the center of the field of view. It appears that the enzyme membrane has lifted slightly at this point (which could even have occurred during the *in vitro* characterization) and the resulting stress caused a small crack to form in the overlying Nafion membrane. The close-up view in Figure 5.10(b) shows adhering blood cells within the crack, indicating that interfering or poisoning species in the blood could have invaded the GOx/BSA membrane and underlying platinum surface from this point. Note, however, that the uncompromised areas of the electrode surface (*i.e.* that remain protected, externally at least, by a Nafion membrane) are devoid of adhering cells.

5.4 CONCLUSIONS

We have proposed a prototype version of an implantable glucose electrode, based on Nafion polymer encapsulation, which overcomes previous problems associated with membrane adhesion. The *in vitro* performance of the prototype electrodes was satisfactory both in buffer solution and in whole blood. However, the *in vivo* performance during these initial pilot tests was disappointing from the point of view of stability and lifetime of the sensor/membrane system. The transition from discrete *in vitro* glucose assays in the laboratory, to continuous *in vivo* monitoring was expected to be an iterative process involving a number of design/testing cycles. The results presented here represent the first step in this process, and a number of points can be made which should prove to be of value in designing the next version of the implantable electrode:

- (1) The fact that electrode B1 performed satisfactorily in whole blood *in vitro*, ~~after~~ failing abysmally in whole blood *in vivo*, indicates that some fundamental differences exist between the dialysis membrane requirements for whole blood glucose assays *in vitro* versus *in vivo*. There

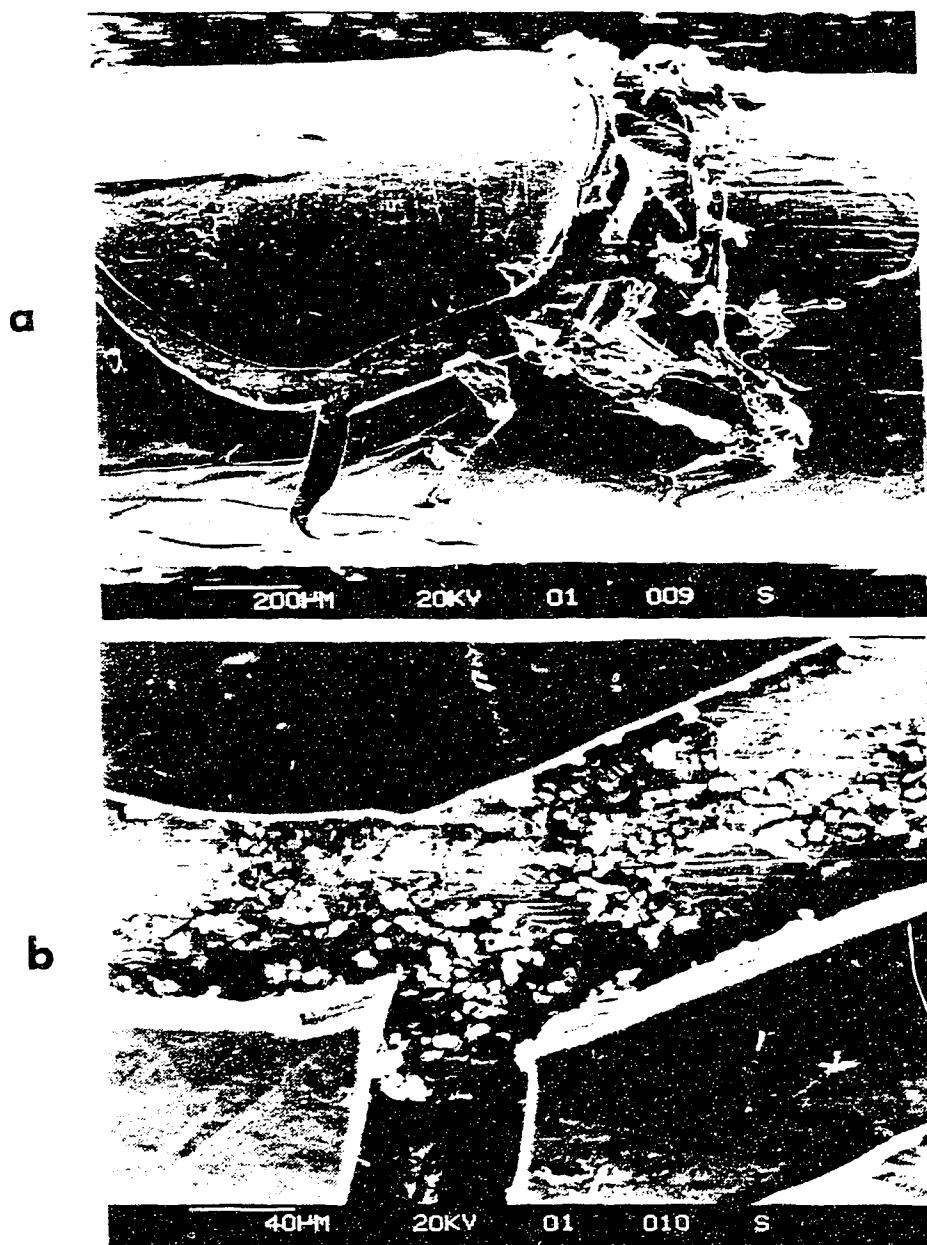


Figure 5.10 Scanning electron micrographs of electrode B2 following *in vivo* testing in Dog J-518. (a) crack discovered in Nafion dialysis membrane. (b) close-up view showing adhered blood cells in crack.

appear to be different types and/or concentrations of interfering species present in these two "media". Whether these effects are systemic or localized to regions surrounding the electrodes is unclear, but obviously the presence of the electrodes must somehow trigger these effects. This points again to biocompatibility problems which are apparently not completely obviated by the use of Nafion encapsulation, at least under the conditions employed in this study. Whether or not a thicker Nafion membrane would perform better remains to be shown, but should be investigated.

(2) The Nafion encapsulation process may require some modification in order to achieve better uniformity in the characteristics from one electrode to another. Recall that electrodes B1 and B2 had drastically different K_m values, yet underwent exactly the same coating regimen. It is likely that the shape and size of the platinum indicating electrode are important here, although early versions of the glass shrouded planar electrodes also varied somewhat in performance characteristics, so it is perhaps not unreasonable to expect that time is required in order to gain experience with this new geometry. In comparing electrodes, the relative values of K_m might serve as a helpful measure of the uniformity (and thickness) of the Nafion membrane. Furthermore, since electrode B1 passed the ferrocyanide test but still failed to perform *in vivo*, a different test species that is less easily excluded by the Nafion membrane should be investigated (e.g. ascorbate). It would also be helpful to establish whether or not a correlation exists between the value of K_m measured *in vitro* (in buffer) and the electrode performance *in vivo*.

(3) The crack found in electrode B2 was not evident from *in vitro* testing carried out in buffer solution or from close visual inspection of the dry membrane before the *in vivo* experiment. Hence, better methods of *in vitro* characterization must be implemented. Perhaps the ferrocyanide test would be more useful here (i.e. for "leak" detection). Closer attention must also be given to quality control during electrode fabrication. For example, the fact that the crack appeared around the margin of the GOx/BSA membrane suggests that the silanization treatment was faulty. Furthermore, the Silastic sheath should have extended further toward the

tip so as to cover the margin of the GO_x/BSA membrane (as shown in Figure 5.1).

(4) The size of electrodes B1 and B2 required their placement in the vena cava, which has the highest flow rate of any vein. Whether or not this adversely affected the tests described here is unclear, but thrombus formation over part of the electrode tip was observed after both experiments. In any case, smaller electrodes would be better from a biocompatibility point of view and would also permit testing in smaller veins, although membrane adhesion problems may arise again due to the increased curvature of a smaller electrode. A smaller electrode area would also be less sensitive to variations in the flow rate (recall the modulation in the response of electrode B2 attributed to flow rate variations). It would also be better to integrate the working (enzyme) electrode and the reference/counter electrode in a single probe, in order to decrease mechanical irritation to the host and reduce perturbations to the blood flow.

Intravenous implantation may not, ultimately, be the approach of choice for the clinical application of *in vivo* glucose sensors. However, intravenous sites are the most demanding for research testing and, notwithstanding the poor performance of both of these electrodes, these results were instructive (and encouraging). Further experimentation is obviously required, and the reported observations from this pilot study, and the points noted above, should provide direction for the next phase of this work.

5.5 REFERENCES

- [1] A.M. Albisser, B.S. Leibel, T.G. Ewart, Z. Davidovac, C.K. Botz and W. Zingg, "An artificial endocrine pancreas", *Diabetes*, Vol. 23, pp. 389-396, 1974.
- [2] L.C. Clark, Jr. and C.A. Duggan, "Implanted electroenzymatic glucose sensors", *Diabetes Care*, Vol. 5, pp. 174-180, 1982.
- [3] Y. Yamasaki, "The development of a needle-type glucose sensor for wearable artificial endocrine pancreas", *Med. J. Osaka University*, Vol. 35, pp. 25-34, 1984.

- [4] K. Rebrin, U. Fischer, T. v. Woedtke, P. Abe and E. Brunstein, "Automated feedback control of subcutaneous glucose concentration in diabetic dogs", *Diabetologia*, Vol. 32, pp. 573-576, 1989.
- [5] M. Shichiri, N. Askawa, Y. Yamasaki, R. Kawamori and H. Abe, "Telemetry glucose monitoring device with needle-type glucose sensor: A useful tool for blood glucose monitoring in diabetic individuals", *Diabetes Care*, Vol. 9, pp. 298-301, 1986.
- [6] R.F.B. Turner, D.J. Harrison, R.V. Rajotte and H.P. Baltes, "A Biocompatible Enzyme Electrode for Continuous *In Vivo* Glucose Monitoring in Whole Blood", *Sensors and Actuators*, Vol. 22 (B), No. 1, pp. 561-564, 1990.
- [7] D.J. Harrison, R.F.B. Turner and H.P. Baltes, "Characterization of perfluorosulfonic acid polymer-coated enzyme electrodes and a miniaturized potentiostat for glucose analysis in whole blood", *Anal. Chem.*, Vol. 60, pp. 2002-2007, 1988.
- [8] R.F.B. Turner, D.J. Harrison and R.V. Rajotte, "Preliminary *In Vivo* Biocompatibility Studies on Perfluorosulfonic Acid Polymer Membranes for Biosensor Applications", Submitted to *Biomaterials*, 1990.
- [9] M.N. Szentirmay, L.F. Campbell and C.R. Martin, "Silane coupling agents for attaching Nafion to glass and silica", *Anal. Chem.*, Vol. 58, pp. 661-662, 1986.
- [10] T. Yao, "A chemically modified enzyme membrane electrode as an amperometric glucose sensor", *Anal. Chimica Acta*, Vol. 148, pp. 27-33, 1983.
- [11] R.F.B. Turner, D.J. Harrison and H.P. Baltes, "A CMOS potentiostat for amperometric chemical sensors", *IEEE J. Solid-State Circuits*, Vol. SC-22, pp. 473-478, 1987.

- [12] P. Abel, A. Mueller and U. Fischer, "Experience with an implantable glucose sensor as a prerequisite of an artificial beta cell", *Biomed. Biochem. Acta*, Vol. 43, pp. 577-584, 1984.
- [13] U. Fischer, R. Ertle, P. Abel, K. Rebrin, E. Brunstein, v. Hahn, H. Dorsche and E.J. Freyse, "Assessment of subcutaneous glucose concentration: Validation of the wick technique as a reference for implanted electrochemical sensors in normal and diabetic dogs", *Diabetologia*, Vol. 30, pp. 940-945, 1987.
- [14] D.R. Mathews, E. Brown, T.W. Beck, E. Plotkin, L. Lock, E. Gosden and M. Wickham, "An amperometric needle-type glucose sensor tested in rats and man", *Diabetes Med.*, Vol. 5, pp. 248-252, 1988.

CHAPTER 6

Concluding Remarks

The purpose of this chapter is to present a brief summary of the goals attained in this work, specifically addressing the objectives set forth in Chapter 1, and to comment on the contribution of this research toward the ultimate goal of realizing an artificial beta cell. Also included here are several suggestions for further research in this field, including extensions of the present project. Finally, some of the other possible applications of this work are mentioned.

6.1 SUMMARY OF CONTRIBUTIONS

The first stated objective of this project was to develop improved instrumentation for implantable (amperometric) sensors. The integrated potentiostat circuit described in Chapter 2 provides the capability, with a single integrated circuit, to perform amperometric electrochemical assays with an accuracy comparable to a laboratory analytical potentiostat. The miniaturization and low power consumption criteria for implantable sensors were easily met with the implementation in CMOS technology. High sensitivity, current-to-voltage conversion and differential measurement capability were demonstrated features of the design. The use of a simple two-stage operational amplifier and an output network with the minimum number of devices (two transistors, one resistor) resulted in a total die area, excluding bonding pads, of 0.53 mm^2 . This leaves ample real estate on a standard 5 mm by 5 mm die for the integration of additional signal processing and/or interface circuitry (or electrode structures). Flexibility for research applications was provided by the approach of taking the working electrode bias reference levels from the internal operational amplifier bias network. Thus, virtually any electrochemically significant working electrode bias voltage can be obtained simply by adjusting the symmetry between the power supply levels.

In respect of the second main objective of this project, the perfluorosulfonic acid polymer, Nafion, was investigated as an alternative to conventional dialysis membrane materials for glucose analysis in

biological media. Nafion dialysis membranes were characterized in whole blood and blood plasma samples *in vitro*, and were shown to substantially improve the stability, performance and reproducibility of amperometric glucose sensors in these media. The results of the first overview of the biocompatibility of Nafion polymer indicated the potential suitability of this material for long-term *in vivo* sensor applications. An attempt was made to further verify this potential in experiments with implantable versions of the Nafion encapsulated glucose electrodes developed previously, although these experiments were inconclusive. In order to properly evaluate the *in vivo* performance of Nafion polymer, extensive testing in laboratory animals will be required, involving both acute and chronic implantation. This scale of animal testing is beyond the scope of this project, however the experience gained from this first step should provide a useful starting point for subsequent investigations.

Research directed toward the development of an implantable glucose sensor for the artificial beta cell has been conducted in many laboratories throughout the world for more than fifteen years. Much of this effort has focused on exploring different analytical techniques and, through *in vivo* testing, on discovering the extent of stability and biocompatibility problems. The consensus which has emerged is that, in the long-term, some form of amperometric approach is most likely to succeed, and that the dialysis membrane component is crucial to implementing this approach *in vivo*. The instrumentation and Nafion encapsulation technology contributed by this project, addresses both of these aspects, if only in a modest way. Electrode fouling and biocompatibility problems clearly present enormous challenges and it seems likely that real progress will continue to be slow. Some new avenues have been opened up as a result of this research and some suggestions for further research are given in the following section.

It is also worth noting that, although the goal of an implantable artificial beta cell remains distant, a miniaturized glucose probe that would be stable even for a matter of hours *in vivo* could still be extremely useful. Other areas of diabetes research involving live animal studies would greatly benefit from the capability of continuously monitoring blood glucose levels in a subject over the duration of even a one-day experiment.

Presently, many projects are constrained to using large animals simply due to the necessity of withdrawing multiple blood samples for off-line analysis. If, for example, such projects could employ rats instead of dogs, the efficiency, both in terms of time and cost, of this research could improve considerably. For these types of research applications, it is usually important to perform the measurement in blood rather than interstitial fluids. It is therefore worthwhile to continue to pursue the goal of developing a whole blood compatible glucose sensor.

6.2 DIRECTIONS FOR FUTURE RESEARCH

The next obvious step to continue this project would be to carry out the recommendations presented at the end of the previous chapter, and to pursue further *in vivo* testing with a next-generation prototype of the implantable electrode. In addition to working in circulating blood, it would also be of interest to investigate the performance of Nafion encapsulated electrodes implanted in some of the other *in vivo* sites that have been suggested in the literature [1]. In particular, subcutaneous implantation should be considered, since most of the published literature involving *in vivo* studies pertains to this type of implant site [2-5]. In this case, a thin planar disc shaped electrode may be advantageous, and may also be less susceptible to membrane cracking and adhesion problems.

In regard to further *in vivo* testing, recall from Chapter 4 that the initial phase of the biological response is an acute reaction that eventually subsides, giving way to a chronic response involving fibrous encapsulation. The chemical and cellular species present at the site of implantation are quite different during each of these phases [6]. Thus, it may also be instructive, even at this stage, to perform some longer-term experiments (at least several days in duration) as an attempt to observe some of the dynamics of the biological response to an "active" sensor, through its effect on the sensor response (or drift). At present it is not known whether or not an implanted sensor could recover from the failure mode that was observed in Chapter 5, but this mode is reversible. That is, once the electrode is removed from the *in vivo* environment and washed with distilled water, it does regain its functional characteristics. The integrated potentiostat circuit presented in Chapter 2 could be useful in this type of investigation,

since it could easily be implanted with the electrodes. The electrodes could then be monitored periodically via external (percutaneous) lead wires, or an implanted telemetry system.

One direction in which to extend the kind of biocompatibility studies presented in Chapter 4 would be to perform the detailed time evolution studies (short-term) and investigation of geometric effects as suggested in that chapter. Another direction would be to consider the biological response to operating electrodes (perhaps in conjunction with the above), since working sensor electrodes interact chemically with the body and actually release chemical species into that environment (*e.g.* hydrogen peroxide and gluconic acid). The difficulty here is that the electrodes cannot, of course, be sectioned and stained for histochemical/microscopy examination as done with the polymer by itself. However, our experience indicates that the tissues surrounding a Nafion implant do not strongly adhere to the surface, and it is conceivable that one could remove the electrode from the fibrous capsule without damaging the surrounding tissue. The capsule tissues could then be examined histologically as before, and the electrode surface could be examined by scanning electron microscopy.

As noted in Chapter 4, the conditions under which Nafion films are cast and/or cured are known to affect the morphology of the resulting membranes [7]. The morphologies of commercially cast and solution processed Nafion films, cured at higher temperatures ($>200^{\circ}\text{C}$), have been well studied [8]. However, high temperature curing procedures are, in general, not feasible for biosensor applications. Little data are presently available on the morphology and properties of uncured or low temperature processed films cast from the soluble form of the polymer. Hence, it would be of interest to further investigate the morphology of uncured films of the type employed here in order to approach the optimization of the coating procedure. Transmission electron microscopy, for example, might be employed in order to study the effect of solvent composition and casting conditions on the gross morphology of solution cast films. These studies could serve to narrow the scope of subsequent investigations involving more sophisticated spectroscopic methods.

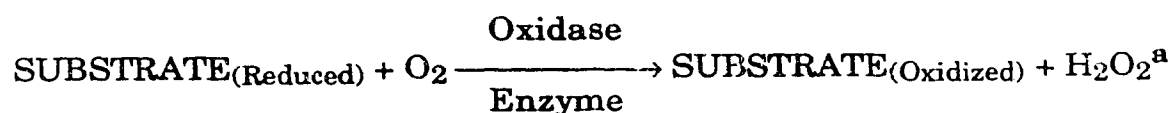
The integrated potentiostat circuitry presented here is the minimum instrumentation required to operate an amperometric sensor. It would be useful to expand on this design and to incorporate more advanced features such as variable sensitivity, analog-to-digital conversion facility and programmable control of the working electrode bias voltages. These additional capabilities would considerably improve the utility and flexibility of the instrument. For implantable applications, it would also be extremely useful to incorporate telemetry circuitry in order to eliminate the necessity of percutaneous lead wires for data acquisition and programming. The capability of implementing variable potential protocols could also lead to further improvements in the stability of implantable electrodes. An electrochemical cleaning cycle, for example, where the electrode is anodized for a period of time prior to a measurement cycle, has been shown to be effective in reversing some kinds of electrode poisoning [9].

6.3 OTHER APPLICATIONS

The body of work presented here was directed primarily toward medical applications. However, the closed-loop control of glucose concentrations in bioreactors is also an important application of glucose sensor technology [10,11]. Particularly with the current trend in the biotechnology industry toward higher cell density fermentation systems, the optimal control of glucose and other metabolites has become a critical factor in determining the economics of these processes [12]. There are similarities between the composition of some types of culture media used in fermentation systems, especially animal cell cultures, and that of blood plasma. Hence, many of the interfering species that complicate glucose assays in whole blood are also present in these culture media. The instrumentation and Nafion membrane technology described here may thus be applicable to the monitoring and control of bioreactor systems.

It was mentioned in Chapters 2 and 3 that the integrated potentiostat and Nafion encapsulation could also be applied to other biochemical assays. That is, several other useful oxidase enzymes also employ oxygen as a cosubstrate and produce hydrogen peroxide as a reaction product, and hence require the same basic instrumentation. The dialysis requirements

TABLE 6.1 Some other immobilized enzyme based biochemical assays that could be performed with the combined potentiostat/Nafion encapsulated electrode system presented here. (Source: Yellow Springs Instrument Co., Inc., Application Notes 13, 113 and Model 27 Industrial Analyzer Specification Sheets.)



SUBSTRATE (Reduced)	ENZYME CATALYST	SUBSTRATE (Oxidized)
β -D-Glucose ^b	Glucose Oxidase	D-Gluconic Acid
L-Lactate	L-Lactate Oxidase	Pyruvate
Ethyl Alcohol	Alcohol Oxidase	Acetaldehyde
Lactose	Galactose Oxidase	Galactose Dialdehyde
Glycerol	Galactose Oxidase	Glyceraldehyde

Starch ^c	Amyloglucosidase	β -D-Glucose
Sucrose ^c	Invertase + Mutarotase	β -D-Glucose

- (a) The hydrogen peroxide is subsequently determined electrochemically as previously described.
- (b) This is the principle assay for which the present system was designed and is included here since it is also involved in some multi-enzyme assays.
- (c) Analysis of these substrates requires the use of a bi-enzyme membrane system with the oxidase enzyme listed in the table, plus glucose oxidase which is used to determine the rate of glucose production.

for sensors based on these enzymes are also similar to those utilizing glucose oxidase, and the same methods of immobilization could also be applied to these systems. Specific examples of such alternative analytical applications are presented in Table 6.1. Note that many of these analyte species are of interest both clinically, and commercially in biotechnology and food processing industries.

6.4 REFERENCES

- [1] S.K. Wolfson, Jr., J.F. Tokarsky, S.J. Yao and M.A. Krupper, "Glucose concentration at possible sensor tissue implant sites", *Diabetes Care*, Vol. 5, pp. 162-165, 1982.
- [2] L.C. Clark, Jr. and C.A. Duggan, "Implanted electroenzymatic glucose sensors", *Diabetes Care*, Vol. 5, pp. 174-180, 1982.
- [3] Y. Yamasaki, "The development of a needle-type glucose sensor for wearable artificial endocrine pancreas", *Med. J. Osaka University*, Vol. 35, pp. 25-34, 1984.
- [4] K. Rebrin, U. Fischer, T. v. Woedtke, P. Abe and E. Brunstein, "Automated feedback control of subcutaneous glucose concentration in diabetic dogs", *Diabetologia*, Vol. 32, pp. 573-576, 1989.
- [5] M. Shichiri, N. Askawa, Y. Yamasaki, R. Kawamori and H. Abe, "Telemetry glucose monitoring device with needle-type glucose sensor: A useful tool for blood glucose monitoring in diabetic individuals", *Diabetes Care*, Vol. 9, pp. 298-301, 1986.
- [6] S.C. Woodward, "How fibroblasts and giant cells encapsulate implants: considerations in the design of glucose sensors", *Diabetes Care*, Vol. 5, pp. 278-281, 1982.
- [7] R.B. Moore, III and C.R. Martin, "Procedure for preparing solution-cast perfluorosulfonate ionomer films and membranes", *Anal. Chem.*, Vol. 58, pp. 2569-2570, 1986.

- [8] Eisenberg, A. and Yeager, H.L., Eds., Perfluorinated ionomer membranes, ACS symposium series 180 (M.J. Comstock, series ed.), American Chemical Society, Washington, D.C., 1982.
- [9] W. Preidel, G. Luft and K. Mund, "The electrocatalytic glucose sensor", in *Electrochemical Sensors for Biomedical Applications*, C. Li, Ed., Electrochemical Society, Pennington, N.J., pp. 26-34, 1986.
- [10] S-O. Enfors, "Oxygen stabilized electrode for D-Glucose analysis in fermentation broths", *Enz. Microb. Technol.*, Vol. 3, pp. 29-32, 1981.
- [11] N. Cleland and S-O. Enfors. "Control of glucose-fed batch cultivations of *E. coli* by means of an oxygen stabilized enzyme electrode", *European J. Appl. Microbiol. Biotechnol.*, Vol. 18, pp. 141-147, 1983.
- [12] W. Scheirer and O.W. Merten, "Instrumentation of Animal Cell Culture Reactors", in *Animal Cell Bioreactors*, M. Ho and D. Wang, Eds., Butterworths, London, in press.

APPENDIX

Integrated Potentiostat Circuit Implementation Data

TABLE A.1 Typical CMOS-1B process parameters. Data were obtained from measurements performed (by Northern Telecom) on wafers processed in the February 1988 fabrication run (MPC 8802). A total of 60 measurements were performed for each parameter, spread over 20 wafers. Capacitance data were not available. (Source: Canadian Microelectronics Corporation).

Parameter	Mean	Std. Dev.	Units
Threshold Voltage (p channel)	-1.016	0.02	V
Threshold Voltage (n channel)	0.890	0.01	V
Transconductance (p channel)	8.032	0.06	$\mu\text{A}/\text{V}^2$
Transconductance (n channel)	26.48	0.2	$\mu\text{A}/\text{V}^2$
Resistivity (p diffusion)	69.9	1.4	Ω/Square
Resistivity (n diffusion)	15.1	0.8	Ω/Square
Resistivity (polysilicon)	21.1	0.3	Ω/Square
Resistivity (capacitor polysilicon)	24.3	1.3	Ω/Square
Resistivity (p well)	4355.0	146.0	Ω/Square
Resistance (Contact + p Diffusion)	≥ 98.0	3.6	Ω
Resistance (Contact + n Diffusion)	≥ 30.9	2.1	Ω
Resistance (Contact + Polysilicon)	≥ 30.7	0.7	Ω

TABLE A.2 Pin assignments for CMOS potentiostat integrated circuits. All of the versions designated xxxL and xxxR are implemented on the same chip and the package is labeled IC5AAxxx. All versions listed here include internal connections between power supplies and gate protection circuitry (if applicable).

Node	PST ^c	PS2	PS3L	PS3R ^d	PS4L	PS4R	PS5L	PS5R
+V _{DD} ^a	21	NA	31,37	4,10	32,39	5,9	32,38	5,9
-V _{SS}	40	NA	32	9	33	8	33	8
GND ^b	9,32	NA	29,39	2,12	30,40	3,11	30,40	3,11
RE ₁	32	NA	29	2	30	3	30	3
WE ₁	31	NA	28	1	29	2	29	2
V ₀₁	30	NA	30	3	31	4	31	4
RE ₂	9	NA	33	12	40	11	40	11
WE ₂	10	NA	40	13	1	12	1	12
V ₀₂	11	NA	38	11	39	10	39	10

- (a) Connect all pins indicated to the external power supply (no internal connections exist between these points in the circuit).
- (b) Connect both pins indicated to the external circuit common (no internal common exists between Channel 1 and Channel 2 of the potentiostat).
- (c) This version (only) does not include gate protection circuitry.
- (d) This version includes several modifications to the output network including M14 (n channel device), current mirror (higher gain) and the output resistor (polysilicon, larger than PST version). NOTE: all tested chips of this design version were found to oscillate (or latch?).

TABLE A.3 Pin assignments for CMOS potentiostat integrated circuits. All of the versions designated xxxL and xxxR are implemented on the same chip and the package is labeled IC5AAxxx. All versions listed here require external connections between power supplies and gate protection circuitry.

Node	PS6L	PS6R	PS7L	PS7R ^c	PS8L	PS8R	PS9L	PS9R ^c
+V _{DD} ^a	31	3,5,11	32	5	32	3,5,11	31	5
-V _{SS}	22	19	22	19	22	18	22	19
GND ^b	29,39	2,12	30,39	2,10	30,39	2,12	29,39	2,11
RE ₁	29	2	30	2	30	2	29	2
WE ₁	28	1	29	1	29	1	28	1
V ₀₁	30	4	31	3	31	4	30	3
RE ₂	39	12	39	10	39	12	39	11
WE ₂	40	13	40	12	40	13	40	13
V ₀₂	38	10	38	9	38	10	38	10
+V _{PRO}	37	37	4	4	37	37	4	4
-V _{PRO}	21	21	21	21	21	21	21	21

- (a) Connect all pins indicated to the external power supply (no internal connections exist between these points in the circuit).
- (b) Connect both pins indicated to the external circuit common (no internal common exists between Channel 1 and Channel 2 of the potentiostat).
- (c) These versions include a metallization layout error and must be modified before use (*i.e.* the metal interconnect between the V₀₂ bonding pad and the +V_{PRO} supply rail must be severed).

CMC MULTIPROJECT BONDING DIAGRAM

RETICLE CODE V17M

BRAND ID LABEL IC5

OTHER IDENTIFICATION FEATURES _____

AA PS 3

WAFER NUMBERS _____

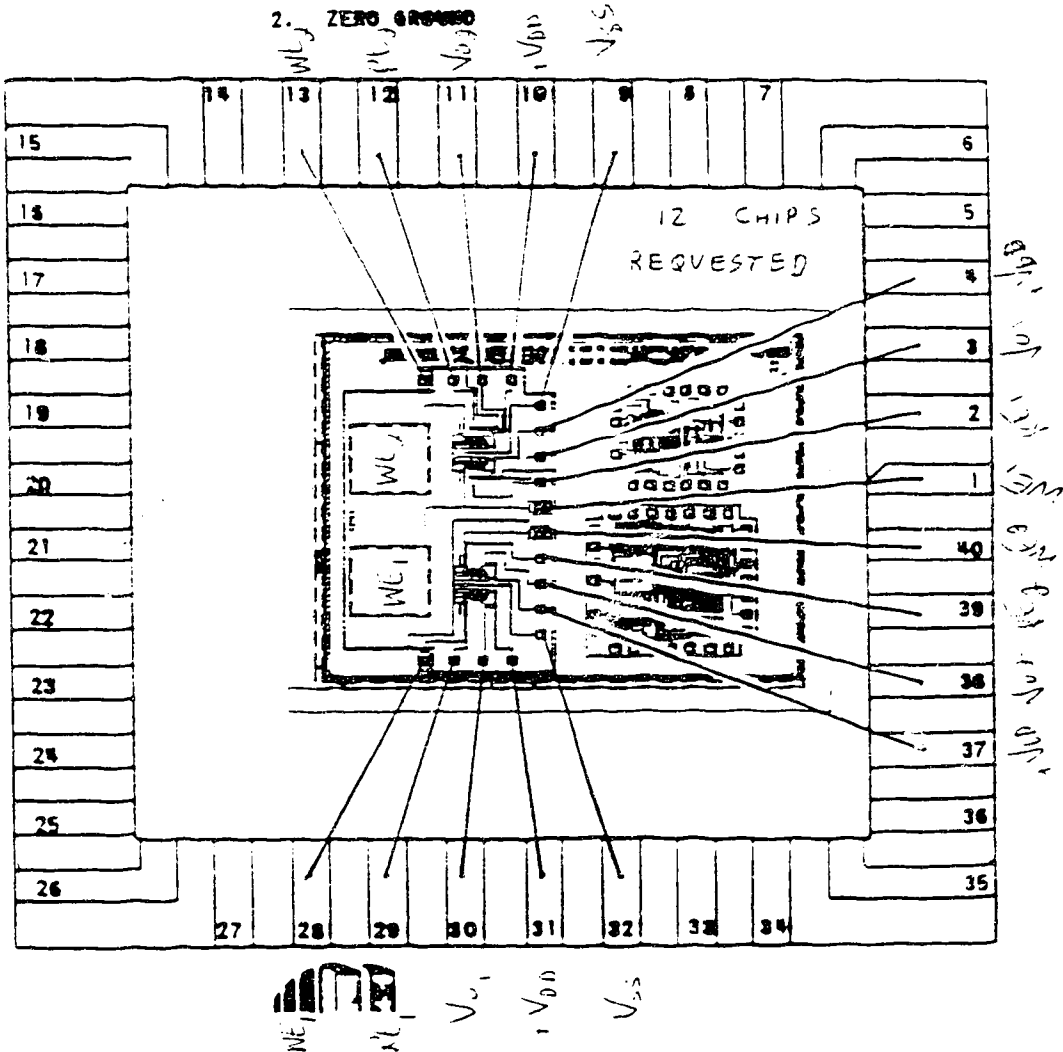
DESIGN FILE REFERENCE _____

PACKAGE	<u>IDK 4061-193G</u>	LID	<u>C-493-75-35M</u>
WIRE ALLOY	<u>99% Al/1% Si</u>	DIA.	<u>.001"</u>
	<u>99% Al/1% Si</u>		<u>.00125"</u>
		ELONG.	<u>1.5 - 4%</u>
			<u>1.5 - 4%</u>
		T.S.	<u>14-16 gms</u>
			<u>18-22 gms</u>
D/A PREFORM	ALLOY <u>99% Au/2% Si</u>	RECOMMENDED SIZE	<u>W/B METHOD U.S.</u>

BONDING DIAGRAM

NOTES: 1. DIE ATTACH PAD SIZE: .400 X .400

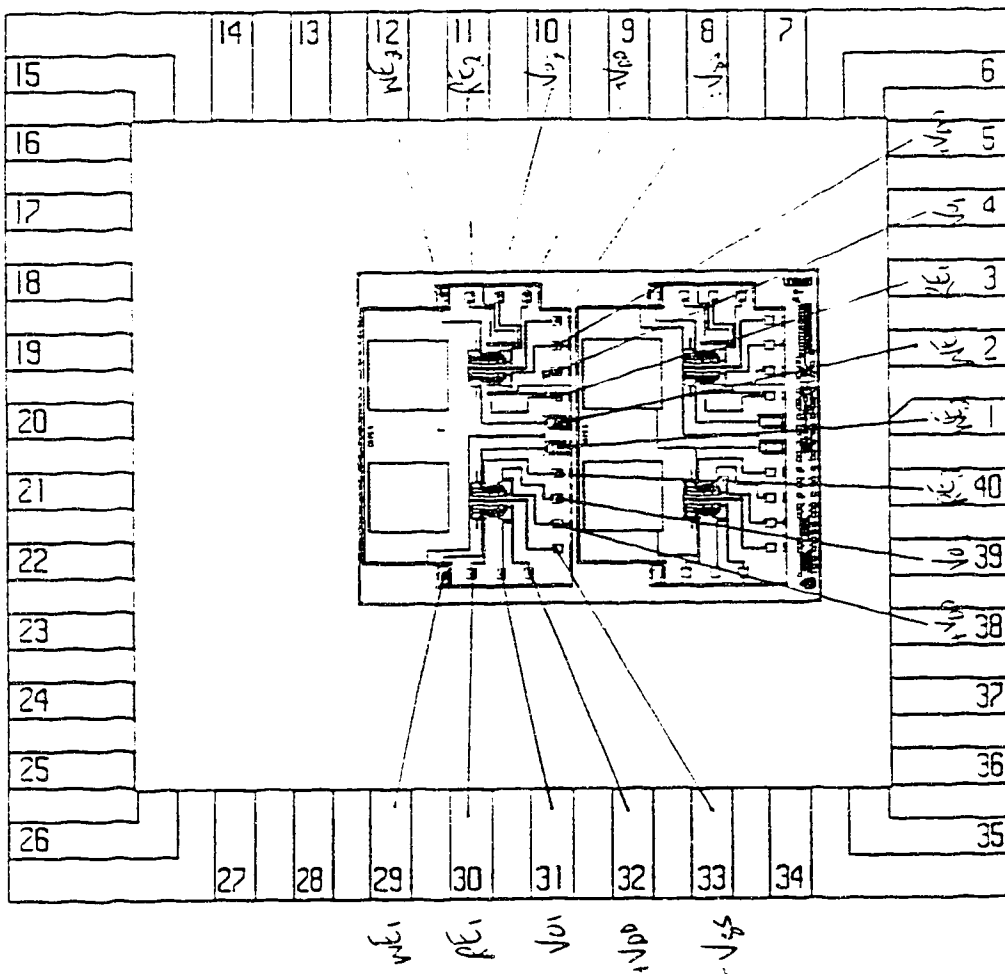
2. ZERO GROUPO



CMC MULTIPROJECT BONDING DIAGRAM
 RETICLE CODE 1177A BRAND ID LABEL 55
 OTHER IDENTIFICATION FEATURES HP54
 WAFER NUMBERS _____
 DESIGN FILE REFERENCE _____

PACKAGE	2DK40F1-192G	L10	C-493-175-35M
WIRE ALLOY	99% Al/1% Si	DIA. .001"	ELONG. 1.5 - 4%
	99% Al/1% Si	.00125"	T.S. 14-16 gms
			8-22 gms
D/A PREFORM	ALLOY 98% Au/2% Si	RECOMMENDED SIZE	W/B METHOD U.S.

BONDING DIAGRAM NOTES: 1. DIE ATTACH PAD SIZE: .400 X .400
 2. ZERO GROUND



QUANTITY 5 PACKAGES REQUIRED
 QUANTITY 12 (CASE DIE REQUIRED)

CMC MULTIPROJECT BONDING DIAGRAM

RETICLE CODE U27A

BRAND ID LABEL ICS

OTHER IDENTIFICATION FEATURES _____

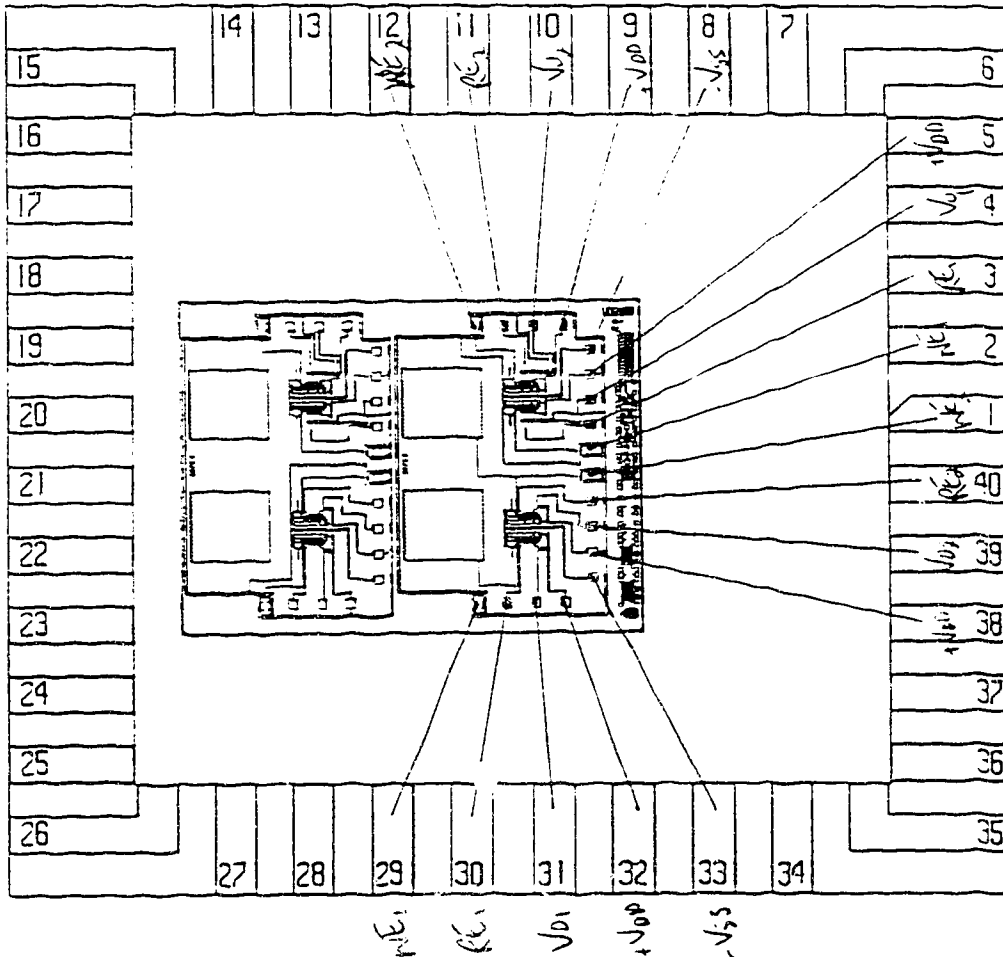
WAFER NUMBERS _____

DESIGN FILE REFERENCE _____

PACKAGE	2DK40F1-192G	LID	C-493-175-35M				
WIRE ALLOY	99% Al/1% Si	DIA.	.001"	ELONG.	1.5 - 4%	T.S.	14-16 gms
	99% Al/1% Si		.00125"		1.5 - 4%		8-22 gms
D/A PREFORM	ALLOY 98% Au/2% Si	RECOMMENDED SIZE		W/B METHOD	U.S.		

BONDING DIAGRAM

- NOTES: 1. DIE ATTACH PAD SIZE: .400 X .400
 2. ZERO GROUND



QUANTITY 5 PACKAGES REQUIRED
 QUANTITY 12 (LOSE DIE REQUIRED)

CMC MULTIPROJECT BONDING DIAGRAM

RETICLE CODE U27G

BRAND ID LABEL CS

OTHER IDENTIFICATION FEATURES _____

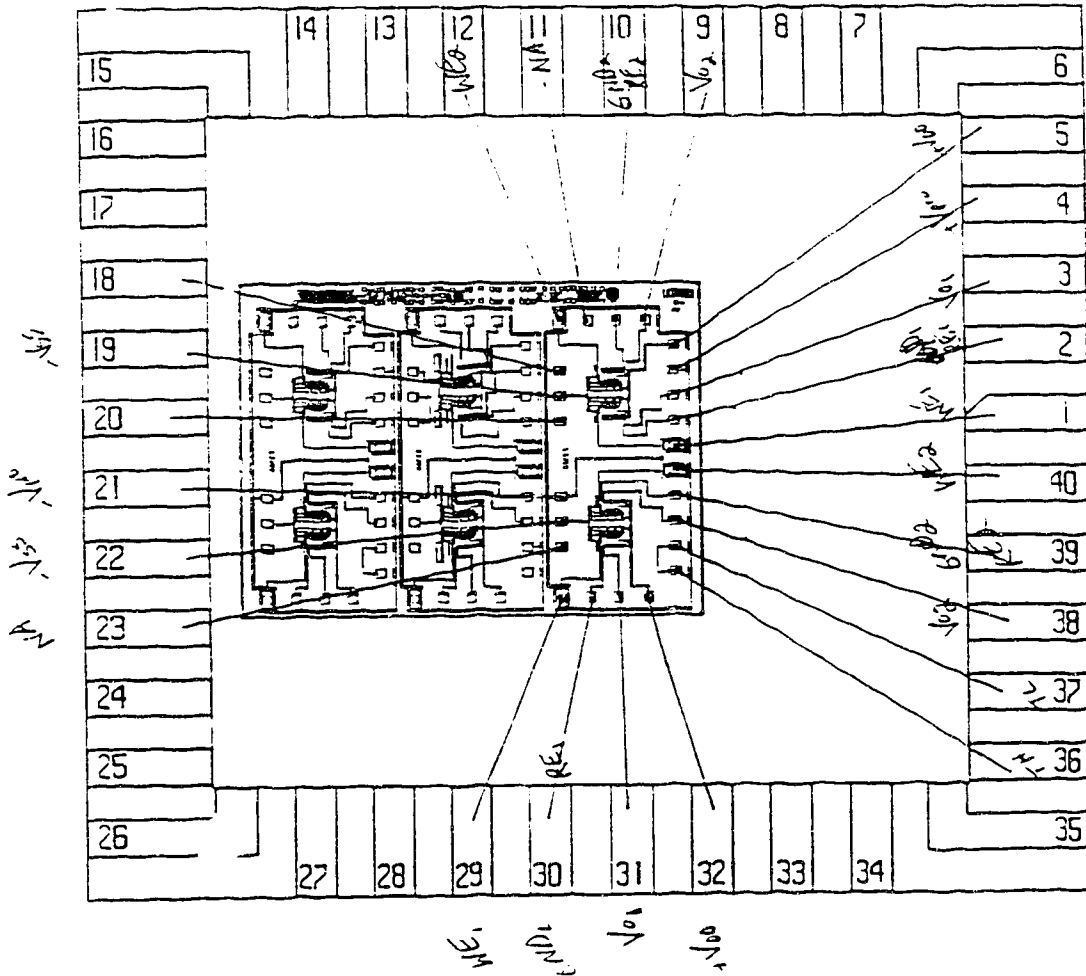
WAFER NUMBERS _____

DESIGN FILE REFERENCE _____

PACKAGE	IDK40F1-192G	LID	C-493-175-35M				
WIRE ALLOY	99% Al/1% Si	DIA.	.001"	ELONG.	1.5 - 4%	T.S.	14-16 gms
	99% Al/1% Si		.00125"		.5 - 4%		18-22 gms
D/A PREFORM	ALLOY 98% Au/2% Si	RECOMMENDED SIZE		W/B METHOD	U.S.		

BONDING DIAGRAM

- NOTES: 1. DIE ATTACH PAD SIZE: .400 X .400
 2. ZERO GROUND



QUANTITY 5 PACKAGES REQUIRED
 QUANTITY 12 LOOSE DIE REQUIRED

CMC MULTIPROJECT BONDING DIAGRAM

RETICLE CODE U27G

BRAND ID LABEL ICS
APP58

OTHER IDENTIFICATION FEATURES _____

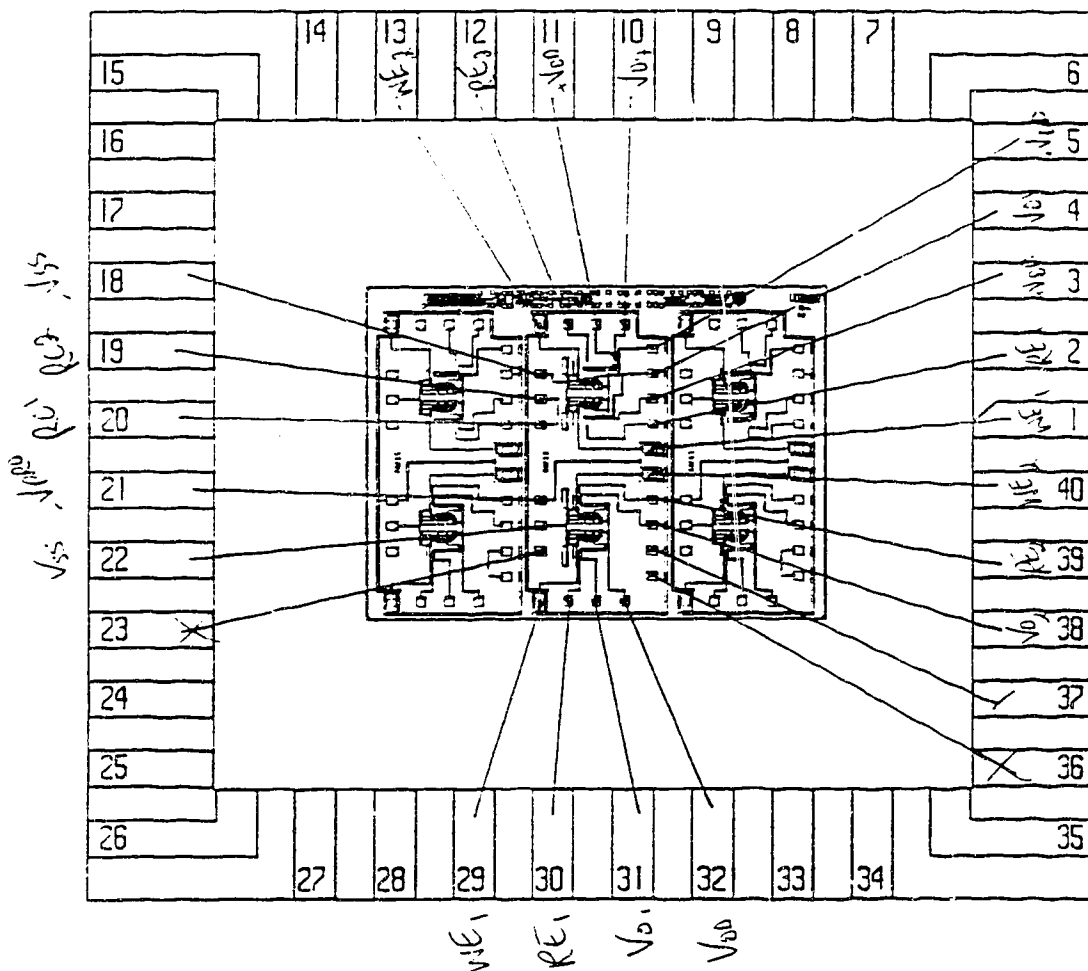
WAFER NUMBERS _____

DESIGN FILE REFERENCE _____

PACKAGE	IDK40F1-192G	LID	C-493-175-35M				
WIRE ALLOY	99% Al/1% Si	DIA.	.001"	ELONG.	1.5 - 4%	T.S.	14-16 gms
	99% Al/1% Si		.00125"		1.5 - 4%		9-22 gms
D/A PREFORM	ALLOY 98% Au/2% Si	RECOMMENDED SIZE		W/B METHOD	U.S.		

BONDING DIAGRAM

- NOTES: 1. DIE ATTACH PAD SIZE: .400 X .400
2. ZERO GROUND



QUANTITY 5 PACKAGES REQUIRED
QUANTITY 12 LOOSE DIE REQUIRED

CMC MULTIPROJECT BONDING DIAGRAM

RETICLE CODE U27G

BRAND ID LABEL 305

OTHER IDENTIFICATION FEATURES _____

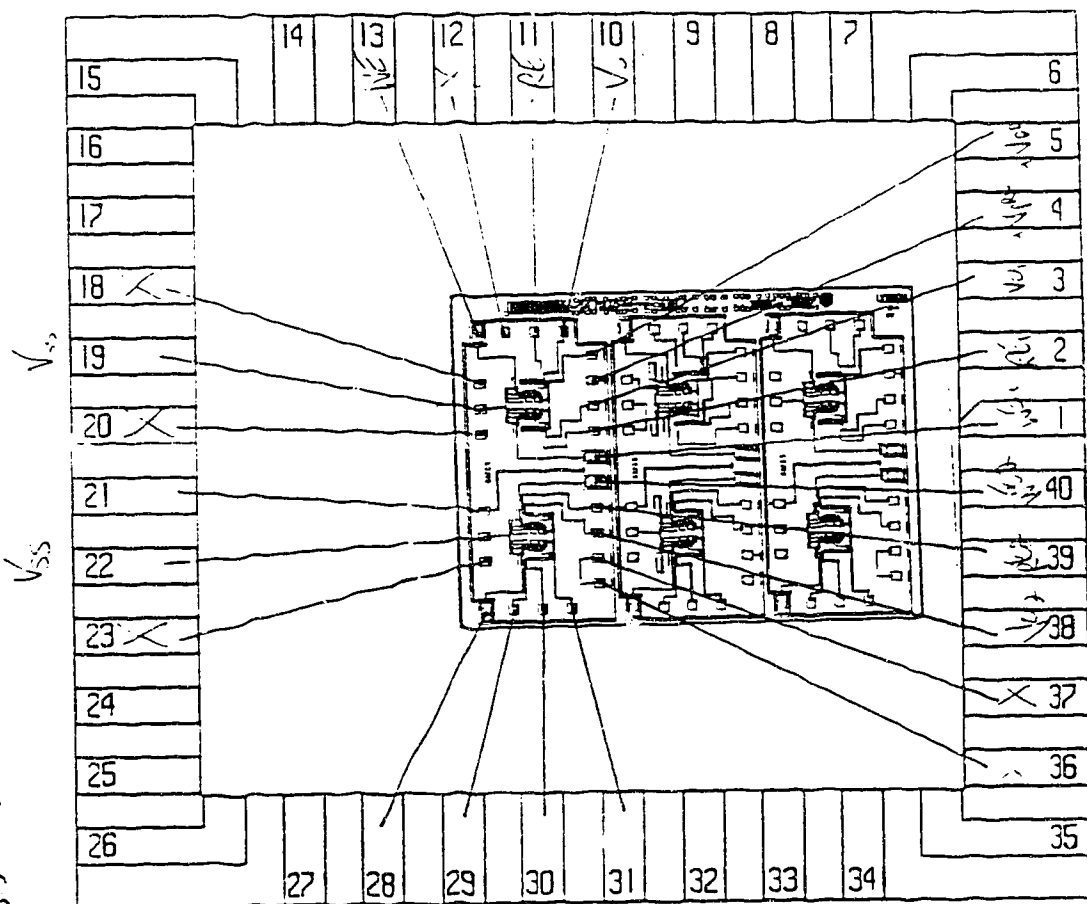
WAFER NUMBERS _____

DESIGN FILE REFERENCE _____

PACKAGE	IDK40F1-192G	LID	C-493-175-35M				
WIRE ALLOY	99% Al/1% Si	DIA.	.001"	ELONG.	1.5 - 4%	T.S.	14-16 gms
	99% Al/1% Si		.00125"		1.5 - 4%		18-22 gms
D/A PREFORM	ALLOY 98% Au/2% Si	RECOMMENDED SIZE		W/B METHOD	U.S.		

BONDING DIAGRAM

- NOTES: 1. DIE ATTACH PAD SIZE: .400 X .400
 2. ZERO GROUND



QUANTITY 5 PACKAGES REQUIRED
 QUANTITY 12 LOOSE DIE REQUIRED

$V_{DD} = 5.85 \pm .07$
 $V_{SS} = -5.5 \pm .55$

V_{E1} V_{E2} V_{S1} V_{S2}

END

22/04/91

FINI